APDA-144

CONCEPTUAL DESIGN OF AN IN-PILE PACKAGE LOOP FOR FAST REACTOR FUEL TESTING

AEC CONTRACT NO. AT(11-1)-865

July 28, 1961

CONCEPTUAL DESIGN OF AN IN-PILE PACKAGE LOOP FOR FAST REACTOR FUEL TESTING

W. G. Blessing, Project Engineer

Conceptual Design Group

R. R. Balsbaugh

W. G. Blessing

D. E. Bloomfield (Vitro Engineering Co.)

J. S. Busch

R. J. Hennig

W. H. Jens

E. C. Kovacic

A. C. Mansfield, Technical Editor

W. E. McHugh

J. B. Nims

E. M. Page (ASTRA, Inc.)

M. A. Silliman

SUMMARY

This report presents the results of a conceptual design study performed by APDA to adapt the Pratt & Whitney in-pile package loop (PW-19) for use as a fast reactor fuel test facility in the Advanced Test Reactor. The study was performed at the request of the AEC under Contract No. AT(11-1)-865, Project Agreement No. 4. The major design and performance objectives for this facility are listed on the attached table.

The in-pile package loop described in this report will permit the irradiation of fast reactor fuel assemblies to high burnups in a fast reactor environment. The neutron spectrum approximates that of a fast reactor, the geometry of the test fuel array is typical of fast reactors, and the test specimen coolant is a liquid metal.

A boron-loaded thermal neutron filter surrounding the loop provides the test fuel with a neutron spectrum approximating that of a fast reactor. The extensive physics calculations that were required to determine the proper boron loading showed that the filter caused a large reactivity decrease in the fast lobe of the ATR. This reactivity loss can be compensated by surrounding the thermal neutron filter with additional fuel elements.

A principal goal of this study was to utilize the PW-19 loop with only relatively minor modifications. This goal has been achieved by two design modifications to the lower end of the existing loop: (1) lengthening the test specimen section and (2) installing a removable closure. As a result of these modifications, fuel bundles can be irradiated to any convenient burnup, removed to an external hot cell for inspection, and reinserted into the same loop for additional irradiations. A conceptual design of a hot cell that provides all the necessary equipment for fuel sample insertion and removal and for loop maintenance was also made as part of this study.

Two concepts for removing the heat generated by the test fuel bundle were developed. In Concept 1, which is the preferred concept, helium is used as a secondary coolant. In Concept 2, demineralized light water is used as a secondary coolant. Of the two concepts, Concept 1 provides the greater range of thermal capacity and temperature control. However, more expensive equipment is required for circulating the secondary coolant than in Concept 2, and the loop is somewhat more difficult to install in and remove from the reactor. Concept 2, on the other hand, requires less expensive circulating equipment than Concept 1 and the loop is easier to handle. However, Concept 2 provides a smaller range of thermal capacity and temperature control. For this reason, APDA considers that the advantage of experimental flexibility provided by Concept 1 far outweighs the operational advantages of Concept 2.

The original Pratt & Whitney loop represents a notable achievement in the field of in-pile loop designs. The use of the APDA-modified loop in the ATR, together with a thermal neutron filter, will provide for the first time an acceptable fast neutron spectrum for testing fast reactor fuels in a circulating liquid metal coolant. From this study, it appears that there are no major problems in adapting the existing P&W loop for this purpose and that the cost of the research and development program can be kept to a minimum since the necessary research and development work on the major components of the loop has already been done. A list of recommended Title I design studies is provided in Appendix B to this report, and the P&W drawings and reports used by APDA in the conceptual design are listed in Appendix C.

TABLE 0.1

IN-PILE LOOP DESIGN AND PERFORMANCE OBJECTIVES

Materials of Construction

Liquid Metal Containment Vessel	Stainless Steel, Type 316
Helium Containment Vessel	Stainless Steel, Type 316
Secondary Coolant Containment Vessel	Stainless Steel, Type 316
Water Jacket (Not required for Concept No. 2)	Aluminum
Thermal Neutron Filter	Boron Stainless Steel
Extended Core	Same as ATR Core

Dimensions of Loop

Length, Excluding Extension Tube	ft	14
Outside Diameters		
In-Core Section	in.	2.875
Heat Exchanger Section (Concept 1)		6 in. sq.
" " " (Concept 2)	in.	5.526
Pump & Motor Section	in.	5.875
Weight of Loop	lb	700

Dimension of Thermal Neutron Filter

Length	ft	5
Inside Diameter	in.	3.000
Outside Diameter	in.	3.300

Dimensions of Extended Core

Length	ft	4
Inside Diameter	in.	3.300
Outside Diameter	in.	5.250
No. of Fuel Plates		7
Thickness of Fuel Plates		Same as ATR Core
Spacing of Fuel Plates		" " " "

Primary Coolant

Type	NaK - 44
Amount	1 Gallon

Design Conditions

Maximum NaK Temperature	F	1200
Maximum Motor Bearing Temperature	F	250
Maximum Internal Pressure	psi	585

Cover Gas

Type	Helium

Loop Operating Conditions, Concept 1

		18-inch Test Speciman
Heat Removed Through Heat Exchanger		
Test Specimen Power	kw	10-125
Gamma Heating and Pump Energy	kw	75
NaK-44 Flow Rate	gpm	5-22
Loop Pressure Loss (Exclusive of Test Samples)	psi	1-7
Maximum Total Pump Pressure	psi	53
NaK Temperature		
Entering Heat Exchanger	F	900-1200
Leaving Heat Exchanger	F	600-900
Helium Flow Rate (secondary coolant)	SCFM	580-5800
Static Pressure Entering Loop	psi	600
Maximum Pressure Loss	psi	300
Helium Temperature		
Entering Heat Exchanger	F	140
Leaving Heat Exchanger	F	300
Heat Removed Directly by ATR Coolant		
Gamma Heating in Loop	kw	104
Thermal Neutron Filter Heating	kw	300
Extended Core Region Power	kw	5600
ATR Primary Coolant Flow Through Lobe	gpm	738
ATR Primary Coolant Pressure Loss	psi	47
ATR Primary Coolant Temperature		
Entering Lobe	F	130
Leaving Lobe	F	187

Loop Operating Conditions, Concept 2

		18-inch Test Specimen
Heat Removed Through Heat Exchanger		
Test Specimen Power	kw	75-150
Gamma Heating and Pump Energy	kw	75
NaK-44 Flow Rate	gpm	10-30
Loop Pressure Loss (Exclusive of test samples)	psi	2-12
Maximum Total Pump Pressure	psi	53
NaK Temperature		
Entering Heat Exchanger	F	900-1200
Leaving Heat Exchanger	F	600-900
Water Flow Rate (secondary coolant)	gpm	15-60
Maximum Pressure Loss	psi	70
Water temperature		
Entering Heat Exchanger	F	140
Leaving Heat Exchanger	F	165
Heat Removed Directly by ATR Coolant		
Gamma Heating in Loop	kw	104
Thermal Neutron Filter Heating	kw	300
Extended Core Region Power	kw	5600
ATR Primary Coolant Flow Through Lobe	gpm	757
ATR Primary Coolant Pressure Loss	psi	47
ATR Primary Coolant Temperature		
Entering Lobe	F	130
Leaving Lobe	F	185

Utility Requirements - Failure-Free

In-Pile Loop Operation	
Electrical	480-volt, 3-phase 50-amp, 60-cycle
Instrument Air	100 psig
Helium (Concept No. 1, can be recycled)	5800 SCFM at 600 ps
Demineralized Water (Concept No. 2)	70 gpm at 400 psig
Hot Cell Operation	
Electrical	480-volt, 3-phase 50-amp, 60-cycle
Instrument Air	100 psig
Clean Process Air	800 SCFM @ 5 inche water
Process Water	Negligible
Helium	2 Cylinders per wee
Hot Liquid Waste Disposal	50 gal/month

Crane Requirements

Above Reactor Vessel		
Capacity	tons	40 and 2
Headroom	ft	30
Hook Travel	ft	30
Above Canal		
Capacity	tons	2
Headroom	ft	30
Hook Travel	ft	50
In Hot Cell Area		
Capacity	tons	40
Headroom	ft	30
Hook Travel	ft	30

TABLE OF CONTENTS

TABLE OF CONTENTS (Cont'd)

LIST OF ILLUSTRATIONS

LIST OF ILLUSTRATIONS (Cont'd)

LIST OF TABLES

1.0 INTRODUCTION

In January 1961, Atomic Power Development Associates, Inc. (APDA) was asked by the Atomic Energy Commission to review the design of the Advanced Test Reactor (ATR) to determine whether one of the lobes of this reactor could be used to test fast reactor fuel assemblies. APDA was also asked to review the design features of an in-pile package loop for testing fast reactor fuel assemblies in the ATR. After a brief but intensive study, APDA informed the AEC that the ATR could be used as a test facility for fast reactor fuel elements and recommended that the design of the Pratt & Whitney (P&W) loop which had been operated in the Engineering Test Reactor (ETR) be adapted for this purpose. Subsequently, the task of preparing a conceptual design of an in-pile package loop for testing fast reactor fuel elements and a conceptual design for the associated handling equipment and hot cell was assigned to APDA.

Fast reactor fuel elements have not been tested under their corresponding operating conditions because there are no reactor facilities that can be used to irradiate assemblies of fast reactor fuel elements to high burnups in a circulating liquid metal environment without large variations in burnup and power distribution within the assembly of elements and within the individual fuel elements. This deficiency exists because all existing testing reactors operate with a thermal neutron spectrum, and thermal neutrons have very short mean free paths in highly enriched fast reactor fuels. APDA had planned to irradiate a 49-pin fast reactor fuel assembly in the SRE; however, this program was abandoned because the resulting power depression would be too great.

In earlier studies of the problem of testing fast reactor fuel elements, the possibility of filtering out the thermal neutrons was recognized. However, the then existing reactors had such a low fast neutron flux component that it was impossible to obtain sufficient power generation in the fuel samples if the thermal neutrons were removed. The physical arrangement of the filter and the test specimens requires a large facility space within the reactor core. The ATR has a fast neutron flux component which is large enough to permit the use of a thermal neutron filter, and the facility space is large enough to accommodate the filter and test specimens. Thus, for the first time a reactor will be available which can be used to irradiate fast reactor fuel assemblies.

In developing the design for the ATR test loop, four requirements were considered essential to the design.

1. The use of a thermal neutron filter, as discussed above.

2. The use of a liquid metal for the primary coolant to provide the same nonthermalizing coolant environment found in fast reactors.

3. Modification of the existing loop design to permit removal, inspection, and reinsertion of test fuel specimens at various burnup increments.

4. Provision for a long in-pile residence, a minimum of 10,000 hours, because of the high burnup requirements for most fast reactor fuels and the high cost of loop fabrication.

It became apparent that a large research and development program could be avoided (1) if the existing loop design could be modified to permit removal, inspection, and reinsertion of test fuel specimens without changing the motor, pump, and heat exchanger portions of the loop and (2) if a loop operating life of 10,000 hours could be assured. An investigation of the durability of the loop components has indicated that the 10,000-hour operating life seems assured. Further, the internal working components of the original loop have been retained and the number of modifications needed for a reusable loop have been kept to a minimum. NaK alloy containing 44 per cent potassium has been retained as the primary coolant even though sodium is the accepted coolant for fast reactors. The use of NaK instead of sodium will not affect the experimental capabilities of the loop, and NaK has the advantage of being liquid at room temperatures.

2.0 DESIGN CRITERIA FOR FAST REACTOR FUEL TESTING

2.1 FAST REACTOR TEST FACILITY REQUIREMENTS

A comprehensive evaluation of the behavior and economics of a fast reactor fuel assembly requires information on hydraulics, heat transfer, and the effect of irradiation as a function of neutron spectrum, burnup rate, temperature, and other variables. Some of this information can be obtained out of pile by conventional methods. For example, hydraulic studies done outside a neutron flux field certainly can represent adequately the conditions within a fuel assembly if the coolant is in one phase. Similarly, if the effect of neutron flux on the materials in a structure is known, then the behavior of the structure may be determined without irradiation in a fast reactor. However, it would be extremely difficult to simulate out of pile the effects of the thermal gradients inherent in heterogeneous fast reactors. When thermal effects involve internal heat generation gradients, there is usually no way to mock up the problem without actually having internal heat generation. Internal heat may be generated either by fission or by resistance heating. Attempts to use resistance heating, however, have not been entirely successful.

In determining the effect of irradiation upon the fuel itself, a fast flux environment would be more truly representative of the actual operating conditions found in a fast reactor. Such an environment would provide valuable information regarding the effect of irradiation upon the support structure especially in regard to (1) materials of construction; (2) interaction between the structure and the thermal, hydraulic, and neutron environments; and (3) movement of the fuel, a problem of special interest in analyses of fast reactor fuel element behavior. In fast reactors, fuel movement, the primary contributor to the temperature coefficient, is produced by thermal gradients, which, as mentioned above, are hard to duplicate out of pile.

Fuel movement may also be produced by the migration of fuel within a fuel element. Determination of the effects of fuel migration requires that a fuel element be subjected to axial thermal gradients sufficient to duplicate the driving force that might cause fuel migration.

Coupled with the problem of fuel migration is the problem of gas accumulation within a fuel element. The amount of internal pressure generated in a fuel element because of fission gas production has not been established. This question, of course, is very important in sizing the cladding and is also very important in determining the economics of an element. Interaction between the fuel and the fission gases may

affect fuel expansion and, hence, reactivity. The reproducibility of axial thermal expansion when there are fission gases in the fuel element is of primary importance in reactor dynamics behavior.

A facility for testing fast reactor fuel assemblies must perform two functions: (1) materials testing, including testing of the fuel itself; and (2) gross assembly testing of the hydraulic, thermal, and materials characteristics of the entire structure.

The ideal test facility would provide for testing a structure which, if it were integral and had material properties within set limits, would move in an acceptable fashion. A fuel assembly would be fabricated and subjected to a prototype flux. After testing, the integral condition and the material properties of the assembly would be established. Such an approach places a minimum reliance on the designer and analyst, and a maximum burden on the test facility.

A minimum test facility would provide for testing some analyzable module of the fuel assembly in a prototype flux which would produce thermal gradients that could be reliably related to those in the proposed reactor. Such a facility would require extensive analytical work, first to develop a module, and then to interpret the test results. The specifications of the minimum facility must be specific for each fuel assembly and would involve much engineering judgment based on fast reactor design work. Such a test facility must be able to house enough fuel elements to make a module, and the environment must provide a prototype neutron flux and reasonable thermal gradients.

2.2 REFERENCE FUEL SPECIMEN

In establishing a reference fuel specimen design, several fast reactor designs were considered. Data on several fast reactor designs are presented in Table 2.1. Some of these will be recognized as designs now used for facilities that will become operational. As shown in Table 2.1, three fuel materials and two kinds of fuel elements are of interest. The fuel materials are alloys, such as uranium 10 w/o molybdenum; cermets, such as a dispersion of uranium oxide in a stainless-steel matrix; and ceramics, such as uranium oxide and uranium carbide.

Based on the above-mentioned data, the design criteria for fast reactor fuel specimens are given in Table 2.2. A PuO_2-UO_2 ceramic fuel was selected as the reference case for computational purposes since it represents one advanced fast reactor fuel design. A boron-loaded thermal neutron filter was selected to alter the flux in the existing reactor so that the fuel would experience a fast neutron spectrum and have a maximum internal heat generation of 2.8 kw/cc. A power depression (maximum to minimum value) of 1.3 was specified for the reference fuel specimen. This power depression is somewhat higher than expected (1.1) in a fast reactor, but it is thought to be within the range that can

TABLE 2.1 - CHARACTERISTICS OF FAST REACTOR FUELS

Reactor Core	A	B	C	D	E	F	G
Fuel Material	U-10 w/o Mo alloy	UO_2-SS Cermet	UO_2 Ceramic	PuO_2-UO_2 Ceramic	PuO_2-U-15 w/o Mo Cermet	Fissium Alloy	PuC-UC Ceramic
Cladding Material	Zr	SS	SS	SS	Zr	SS	High-Strength Alloy
Element Shape	Pin	Plate	Pin	Pin	Plate	Pin	Rod
Fabrication Method	Coextrusion	Picture Frame	Vibratory Compaction	Swaging	Pressure Bonding	Na Bonding	-
Element OD or thickness x width	0.158	0.115	0.212	0.122	0.132	0.136	0.620
Element Pitch (inches)	0.199 square	0.169	0.242 square	0.187 triangular	0.215	0.205 triangular	0.644 triangular
Elements/subassembly	140	14	100	397	16	331	-
Over-all Length (inches)	33	19 (1)	72 (2)	72 (2)	41.8	44	27
Cladding Thickness (inches)	0.005	0.005	0.015	0.009	0.005	0.008	0.031
Fuel Length (inches)	30.5	18 (1)	48	36	41.3	41.3	25
Initial Enrichment (% 235 or) (% 239+% 241)	25.6 U-235	93 U-235	~ 30 U-235	26 Pu	9.8 Pu	16.2 Pu	20 Pu
Average Burnup of Fuel	0.4 a/o total	20% U	10% U	13% U + Pu	6-2/3% Pu	3.0 a/o total	10% U + Pu
Average Fuel Power Density (kw/cc)	1.4	0.86	1.4	1.96	1.05	2.33	1.0
Coolant Inlet Temperature (F)	552	552	552	658	658	658	655
Average Coolant Outlet Temp (F)	824	802	852	1008 (3)	1008 (3)	1008 (3)	1009 (3)
Coolant Pressure Drop (psi)	40	75	90	50	65	60	100

(1) Core composed of two in-line bundles.

(2) Core, upper axial blanket, and gas-collecting region in one tube.

(3) Reactor outlet temperatures will probably increase as fast reactor technology becomes more advanced.

TABLE 2.2 - DESIGN CRITERIA FOR FAST REACTOR FUEL SPECIMENS

Type of Fuel		Ceramic
Fissile Material		Plutonium
Density of Fissile Material	g/cc	5.0
Type of Spectrum		Fast
Power Depression (initial)	Max/Min	1.30
Power Depression (final)	Max/Min	1.50
Maximum Fuel Burnup	Fissions/cc	2.5×10^{21} (10 a/o)
Fuel Burnup Increment	Fissions/cc	0.5×10^{21} (2 a/o)
Average Pin Power	kw/in.	1.2 (1.7 kw/cc)
Maximum Pin Power	kw/in.	2.0 (2.8 kw/cc)
Number of Pins		7
Specimen Length	inches	18
Pin OD	inches	0.282
Fuel OD	inches	0.236
Clad Thickness	inches	0.023
Geometry		Triangular Pitch, Spiral Spacers
Spacer OD	inches	0.023

be treated by an analyst in relating experimental fuel specimens to prototype fuel assemblies.

As stated previously, a major factor in the design of fast reactors is the accommodation of fuel movement, which may arise from gross movement of a fuel bundle or from migration of the fuel within a fuel element. To assay fuel migration properly, a representative fuel element about 2 feet long is needed, and this element should be subjected to an environment similar to that encountered in a fast reactor. The environment of a single fuel element can be simulated well if the test cell is arranged so that one fuel element is completely surrounded by other fuel elements in the same geometry that exists in a reactor. The reference 7-pin triangular-pitch geometry selected is shown in Figure 2.1. Alternate geometrics are shown in Figures 2.2 and 2.3. A fuel bundle and support structure representative of the type that might be tested in the ATR fast reactor fuel testing facility are illustrated in Figures 3.4 and 3.5.

2.3 ATR IN-PILE LOOP DESIGN CRITERIA

The design criteria for an in-pile loop facility for the testing of fast reactor fuels are listed in Table 2.3. The limitation on over-all dimensions of the loop is based on the existing ATR reactor vessel design dimensions. The diamter of the test section is fixed by the desire to use a design modification to the P&W in-pile loop, which is described in Section 3.0. The temperature and pressure-drop characteristics specified are necessary to provide the proper thermal and hydraulic characteristics for the reference fuel bundle.

2.4 FULFILLMENT OF DESIGN CRITERIA

The remaining sections of this report describe in detail the conceptual design of a facility for carrying out a fast reactor fuel testing program that will meet the design criteria specified above. The conceptual design of a specific loop is described together with loop-handling and service procedures and hot cell requirements. The conceptual design for a boron-loaded thermal neutron filter that will provide the proper neutron flux spectrum for fast reactor fuel testing has been included in the report. For the application described here, a boron filter is usable because a relatively low boron loading is required. The adequacy of the filter has been established by detailed physics, metallurgical, thermal, and stress calculations.

The fulfillment of design requirements is clearly illustrated in Figure 2.4 which shows average pin power as a function of fuel enrichment for the reference fuel specimen. These data are based on the use of a 1.2 w/o boron-loaded filter. This curve establishes the needed enrichment (47.5%) for the representative fuel specimen. The power

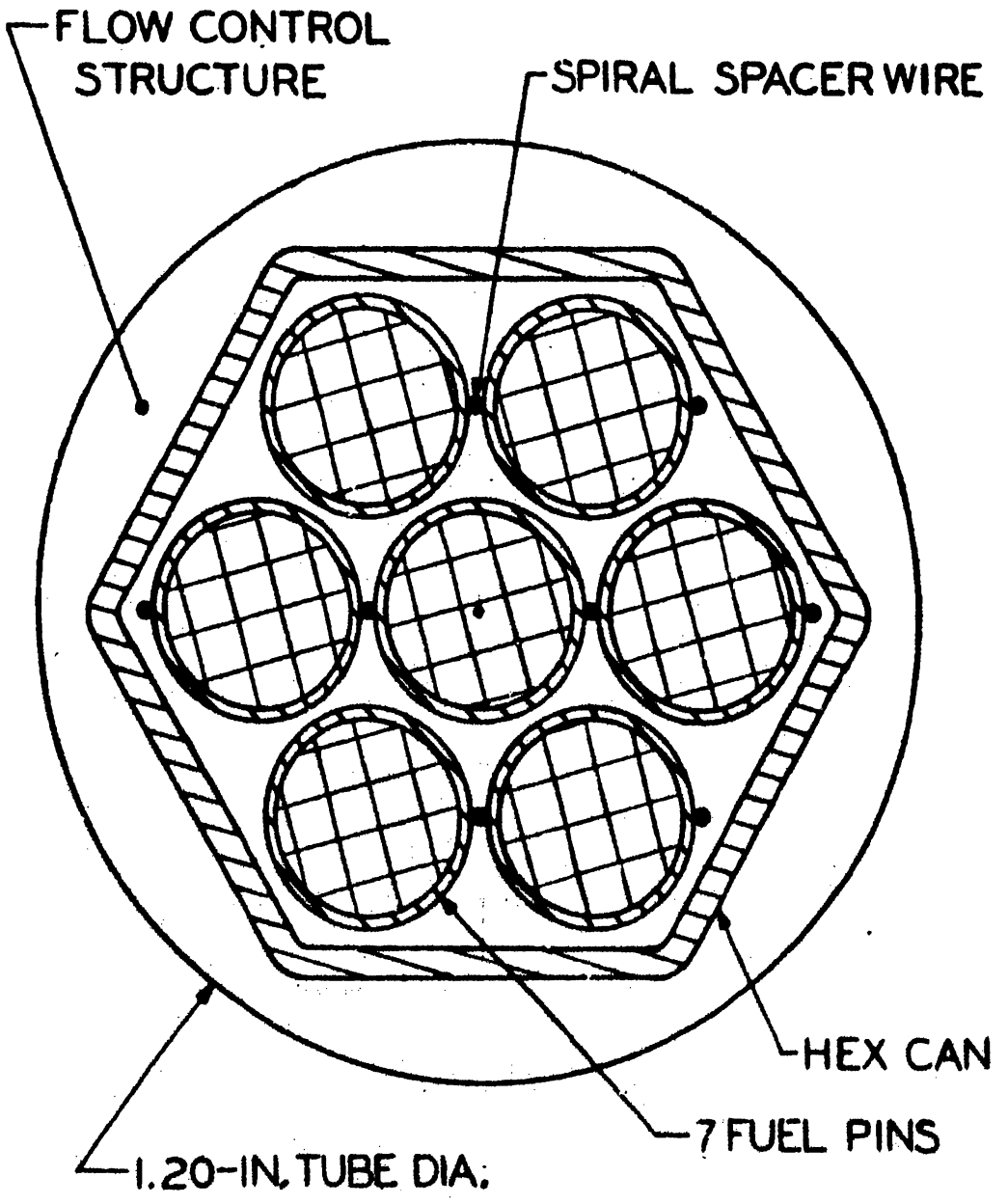

FIG. 2.1
REFERENCE TRIANGULAR-PITCH PIN SPECIMEN

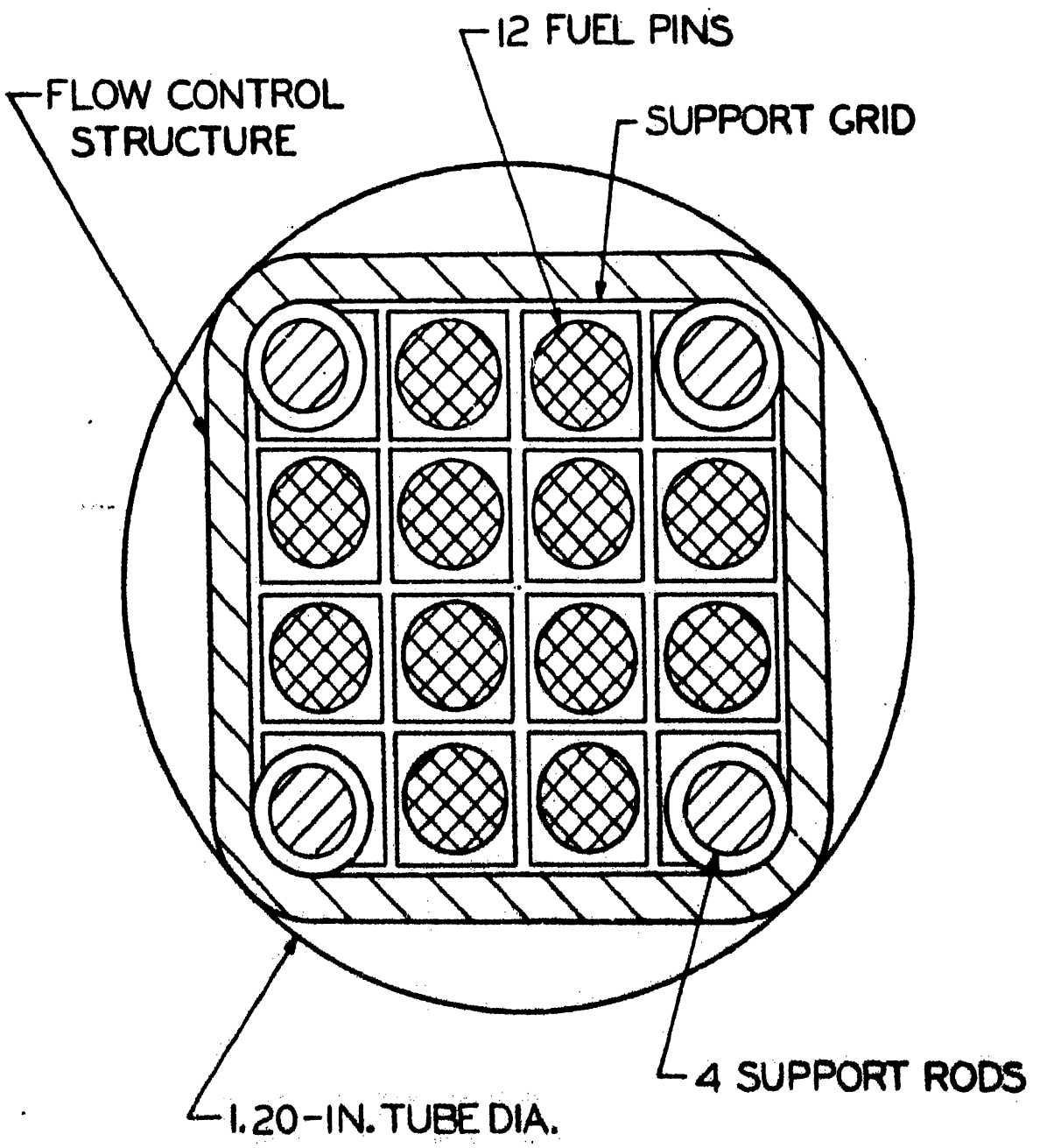

FIG. 2.2
ALTERNATE SQUARE-PITCH PIN SPECIMEN

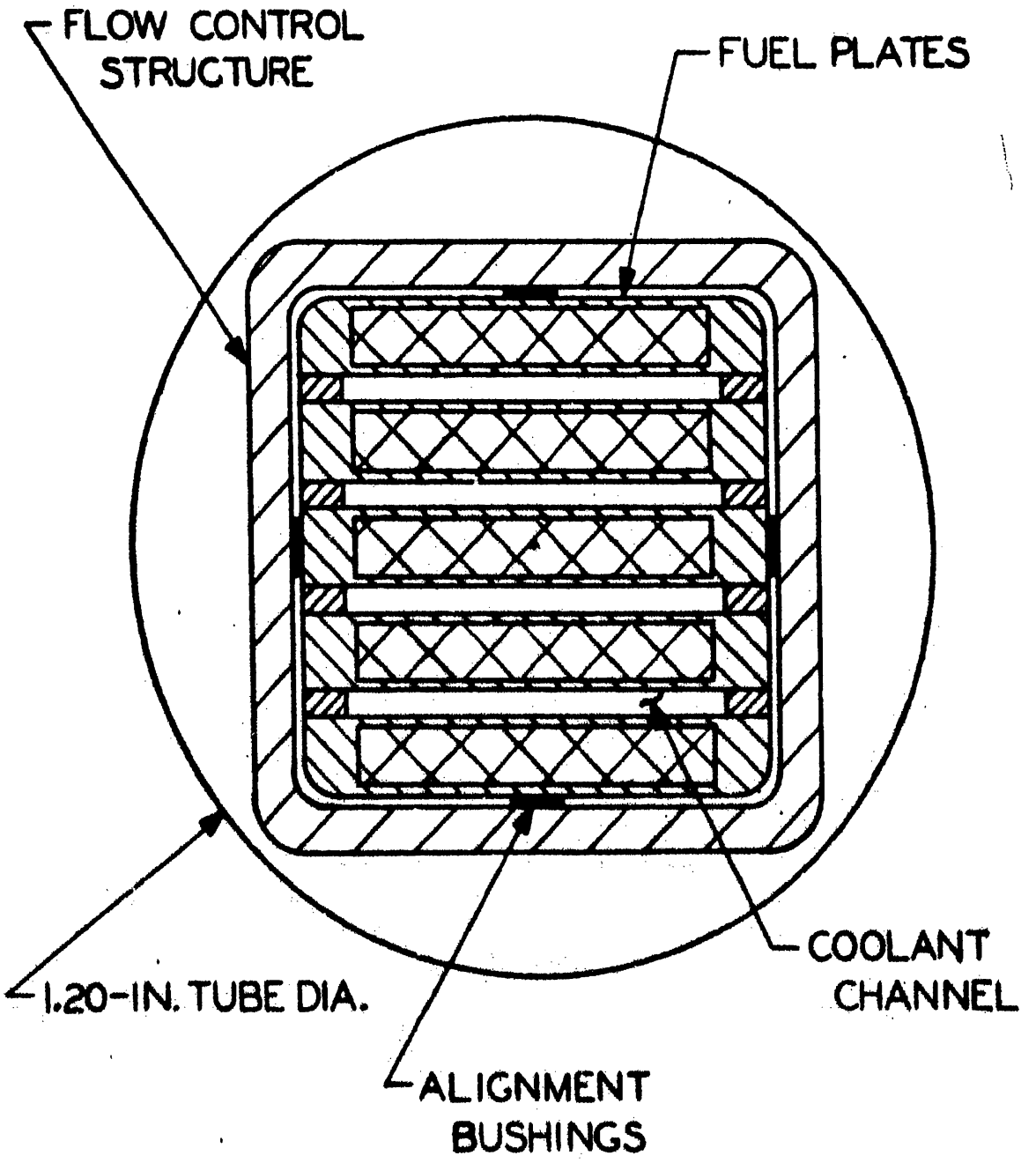

FIG. 2.3
ALTERNATE PLATE ELEMENT SPECIMEN

TABLE 2.3 - DESIGN CRITERIA FOR IN-PILE LOOP

Maximum Length	feet	15
Maximum Diameter	inches	6
Test Section Length	feet	4.5
Minimum Test Section Diameter	inches	1.2
Liquid Metal Coolant		NaK
Minimum Temperature Entering Test Section	F	600
Maximum Temperature Leaving Test Section	F	1200
Maximum Axial ΔT Across Test Section	F	300
Minimum Heat Exchanger Capacity	kw	200
Maximum Flow Rate	gpm	50
Maximum Pump Head	ft	140
Maximum Loop Pressure Drop (without test specimen)	ft	100

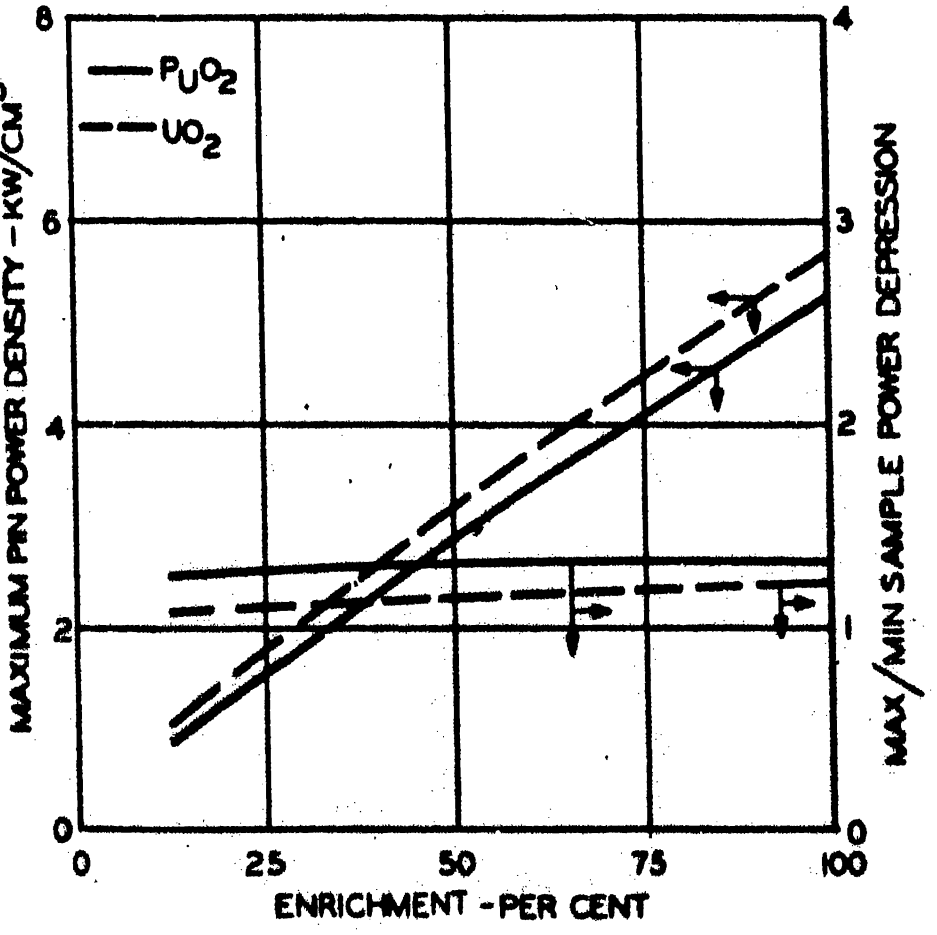

FIG. 2.4

HEAT GENERATION IN REFERENCE FAST REACTOR FUEL TEST SPECIMEN

depression factor is rather insensitive to enrichment since the absorption cross section of the plutonium oxide fuel and the uranium oxide diluent are approximately equal.

Note from Figure 2.4 that higher power and smaller power depression factors would result if a uranium oxide representative module were used instead of plutonium oxide-uranium oxide representative module. The reason for this variation is discussed in Section 4.0.

3.0 ENGINEERING DESCRIPTION OF THE ATR LOOP

3.1 GENERAL DESCRIPTION OF THE ATR LOOP

3.11 Physical Description

The ATR in-pile package loop for fast reactor fuel testing in the Advanced Test Reactor (ATR) is a design modification of the Pratt & Whitney (P&W) loop (PW-9) which was operated successfully in the Engineering Test Reactor (ETR). The dimensions of the loop and the materials of construction are shown in Table 0.1. The modified package loop system described in this report is cylindrical in shape and is made in two separate sections to facilitate handling during loop maintenance and transfer operations. The upper section, the loop extension tube, is approximately 10 feet long. The loop extension tube serves as a connection between the loop proper and the external operating equipment. The lower section, which contains the loop components, is approximately 14 feet long and weighs about 700 pounds. The design is based on the use of concentric annuli for flow passages to minimize the amount of structural material per unit flow area.

The complete package loop system consists of a totally enclosed test section and primary coolant system, a secondary coolant system, and an external electrical and instrumentation system.

A motor and pump located near the top of the lower section of the loop circulates the primary coolant through the test specimen and heat exchanger. The secondary coolant is circulated past the heat exchanger to remove heat from the primary coolant, and the flow is regulated to control the temperature of the test specimen. The electrical system provides power to operate the primary coolant pump and to operate the instruments and controls. The instrumentation system monitors temperatures and flow rates in the loop. Figure 3.1 illustrates the installation of the ATR in-pile package loop in the ATR vessel.

Since the ATR loop is to be used for the testing of fast reactor fuels, the proper neutron spectrum for the test specimens is provided by a thermal neutron filter that surrounds the loop in the ATR core region. The filter, made of stainless steel containing 1.2 w/o boron, is described in Section 5.0. An extended core section fills the space between the thermal neutron filter and the ATR flux trap moderator column. The extended core section which compensates for the reactivity loss caused by the thermal neutron filter, is described in Section 6.0.

3.12 In-pile Loop Modifications

In order to provide the proper facility for fast reactor fuel testing the following modifications were made to the P&W loop:

1. Because use of air as a secondary coolant limited the heat transfer capabilities of the loop, two new concepts using other

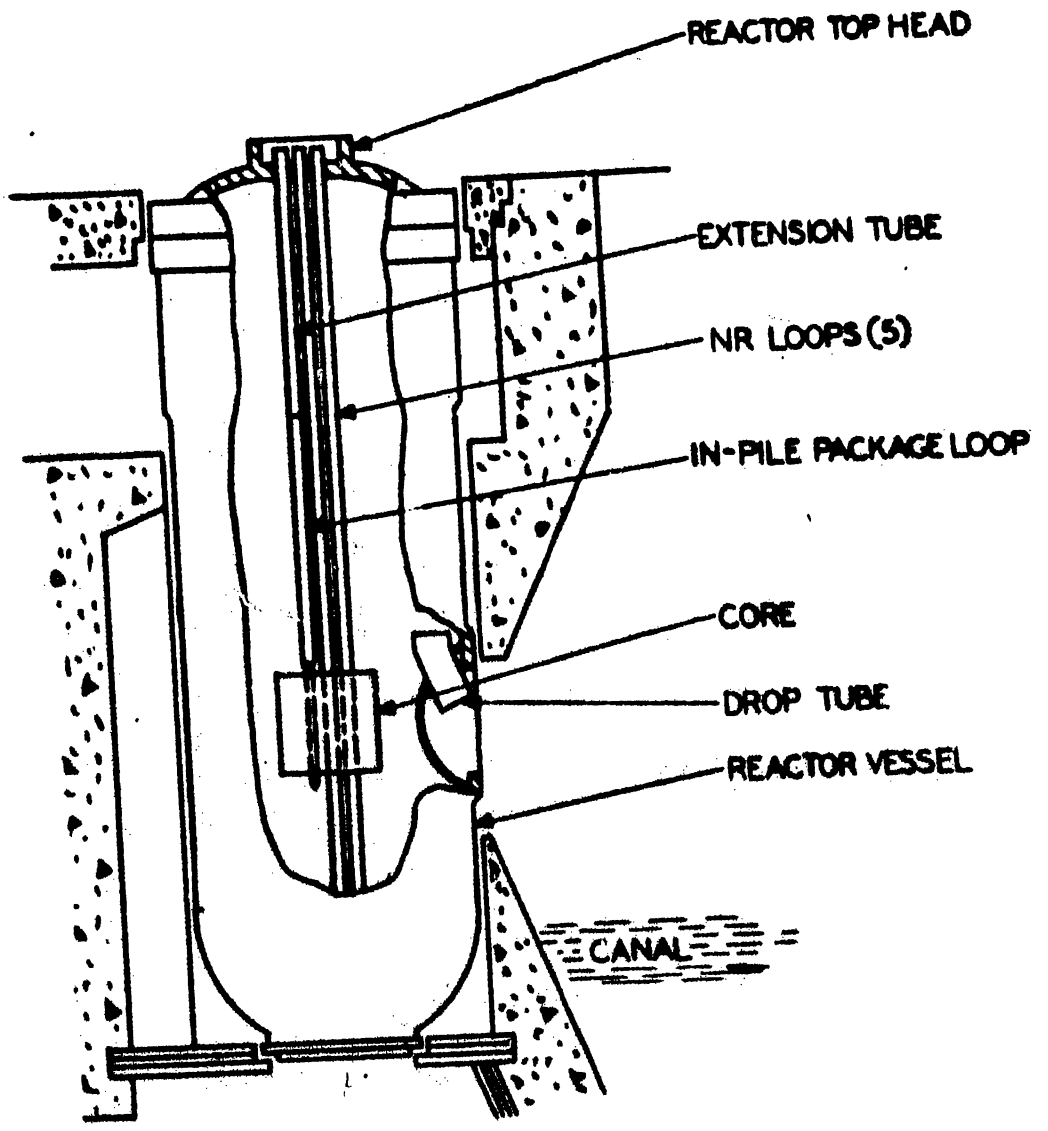

FIG. 3.1
EXPERIMENT INSTALLATION DIAGRAM

secondary coolants were developed. Concept 1, shown in Figure 3.2, uses helium as a secondary coolant. The use of helium as a secondary coolant allows the removal of more heat than the air coolant used by P&W, but less heat than is removed by the water coolant used in Concept 2. The use of Concept 1 requires the insertion and removal of the lower portion of the loop through the reactor vessel drop tube since the attached water jacket will not pass through the head of the reactor vessel. Section 8.3 describes the removal procedure for this concept. Concept 2 shown in Figure 3.3 uses water as a secondary coolant. The use of water increases the capacity of the heat exchanger and allows the removal of the secondary coolant return tubes and water jacket used in the original P&W design and in Concept 1. The removal of the return tubes reduces the size of lower portion of the loop to less than 6 inches in diameter, thus allowing the insertion and removal of the lower portion of the loop either through the reactor vessel head or the reactor vessel drop tube. Section 8.4 describes the removal procedure for Concept 2.

2. A removable closure device was added to the lower portion of the loop. This device allows the removal of the test specimen at various burnup increments and permits the insertion of a new test specimen without requiring fabrication of a new in-pile loop. Section 3.21 describes this device more fully.

3. The lower section of the loop was lengthened to allow the use of longer test specimens.

4. Approximately 12 inches of lead was added to the upper end of the in-pile loop to provide additional shielding.

5. The loop extension tube was lengthened to allow the tube to penetrate the reactor vessel head.

3.2 DESCRIPTION OF LOOP COMPONENTS

3.21 In-Core Section

As stated previously, the loop is constructed of a series of concentric cylinders. Figures 3.4 and 3.5 show the in-core portion of the in-pile loop with test specimens in place in the loop. (These specimens are not the reference specimens of Table 2.2). The innermost cylinder in the in-core section contains the test specimen. NaK flows down through the test specimen and reverses its flow at the end of the innermost cylinder. The innermost cylinder and the second cylinder form a helium-filled annulus, which separates the NaK flowing down through the test specimen from the NaK returning to the pump. The second and third cylinder form the NaK return annulus. The third cylinder and the outer loop wall form a helium annulus which separates the NaK from the ATR cooling water and provides double containment for the NaK. The thermal neutron filter and the

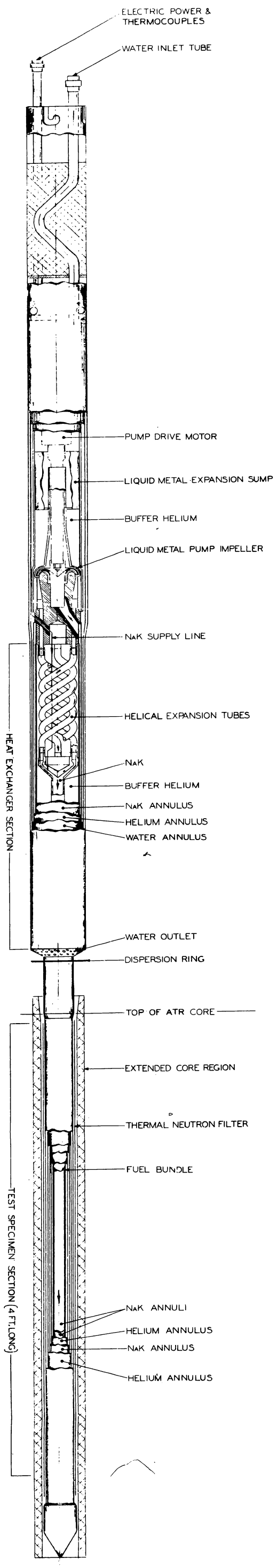

FIG. 3.3
IN-PILE PACKAGE LOOP FOR FAST REACTOR FUEL TESTING
CONCEPT 2

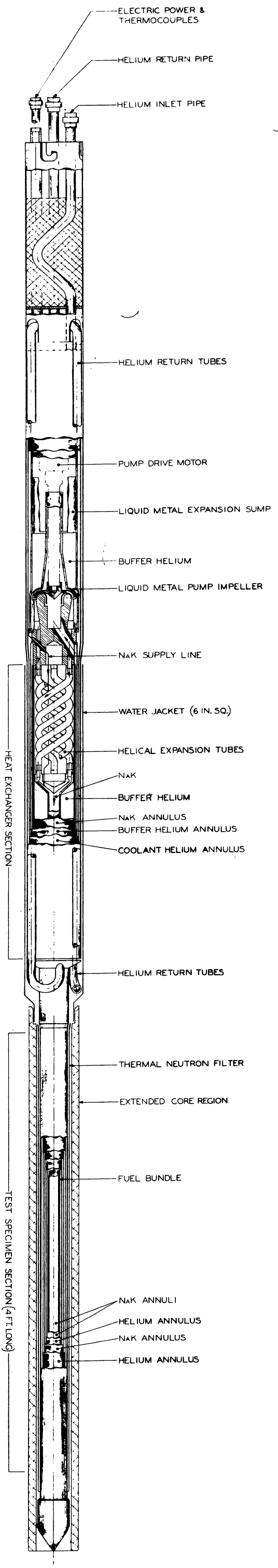

FIG. 3.2
IN-PILE PACKAGE LOOP FOR FAST REACTOR FUEL TESTING
CONCEPT 1

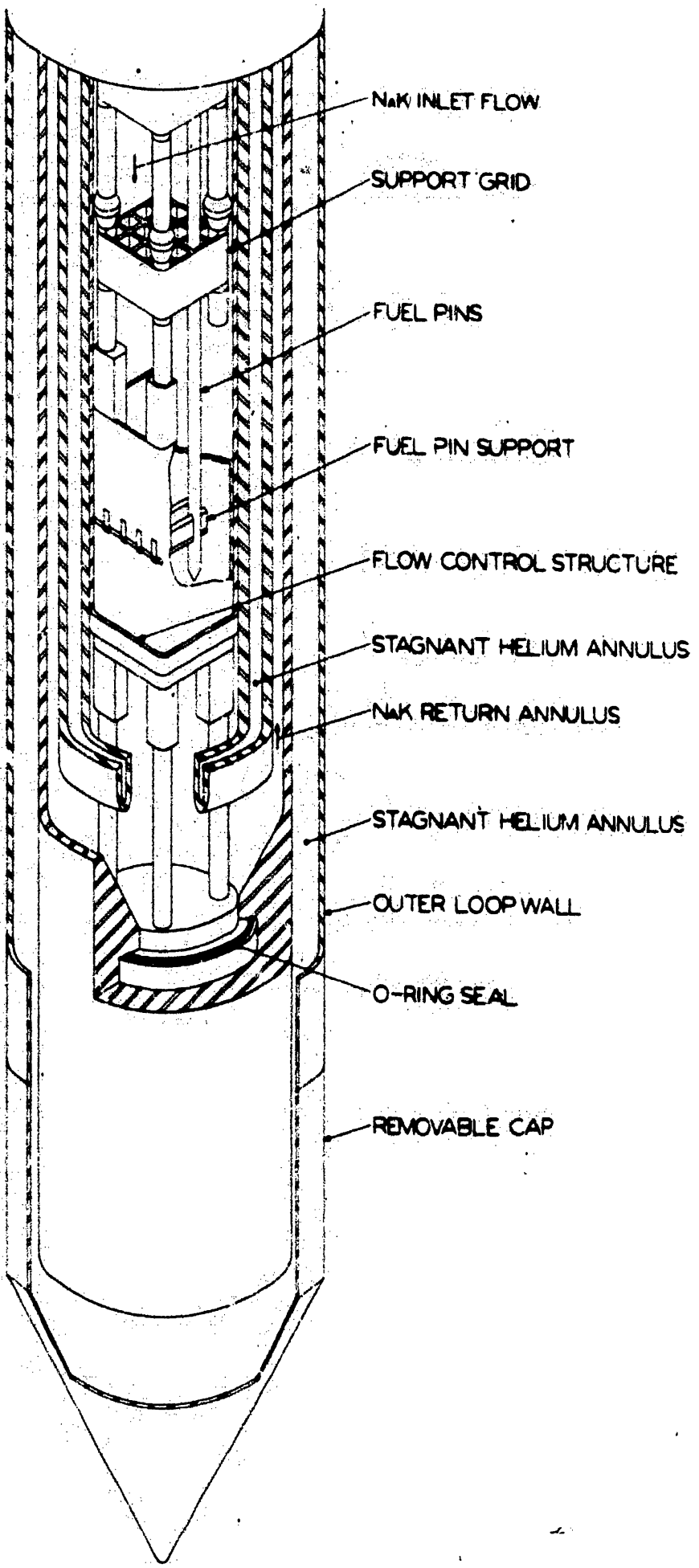

FIG. 3.4
IN-CORE PORTION OF IN-PILE LOOP
LOWER PORTION

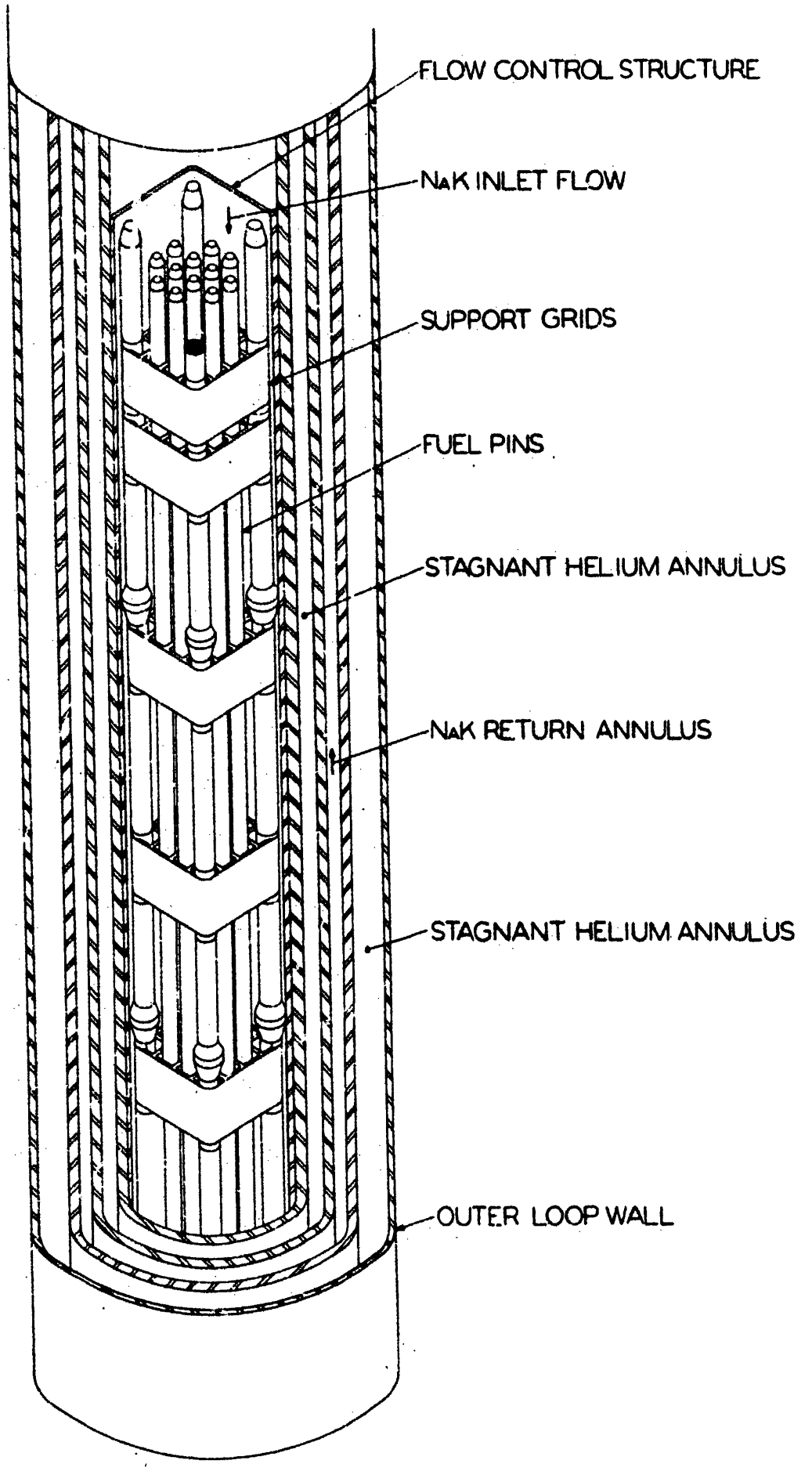

FIG. 3.5
IN-CORE PORTION OF IN-PILE LOOP
UPPER PORTION

extended core, described in Sections 5.0 and 6.0 respectively, are located outside of the loop.

The lower end of the loop contains a removable loop closure to permit the removal and reinstallation of test specimens in the loop. Figure 3.6 illustrates a conceptual design of the removable loop closure. The design is based on the following requirements:

1. Cylinder closures must be accomplished by welding to assure no leakage.

2. Welds should be easily formed by an automatic machine.

3. Provision must be made for sealing a NaK-filled container to the bottom of the loop and for removing a thermally hot assembly from the loop without at any time removing the assembly from a NaK bath.

4. Removal and reinsertion of a new fuel bundle and remaking of the welded seals must be a practical hot cell operation.

The removable closure consists of a test specimen support structure, attached to the test specimens and to the test specimen extracting plug; two lock screws; a seal plug; and the loop end cap. The Nak containment vessel is closed by an overhead seal weld between the lower lock screw and the extension of the NaK vessel. The weld is a fusion weld, made without the addition of filler metal. The threaded joint is used to minimize stresses in the seal weld. The portion of the NaK containment vessel that extends below the threads for the lower lock screw is long enough to permit repeated cut-off of the weld and rewelding of successively shorter lock screws. Metal O-rings permit cleaning the welding surfaces prior to welding without contamination of the loop and minimize NaK leakage when the seal weld is removed. The seal plug, which is attached to the lower lock screw by a shoulder screw, facilitates handling of these parts in the hot cell and allows the screw to be tightened without rotating the O-ring against the O-ring seal. The purpose of the upper lock screw is to compress the upper O-ring.

The outer cylinder of the loop is closed by butt-welding the end cap to the cylinder. If the required vacuum can be maintained in the dry box, all welding should be performed by the electron-beam method. Other methods may be used if the vacuum is unobtainable. The welds will be mocked up and exposed to in-pile temperatures to determine weld distortion and dimensional stability.

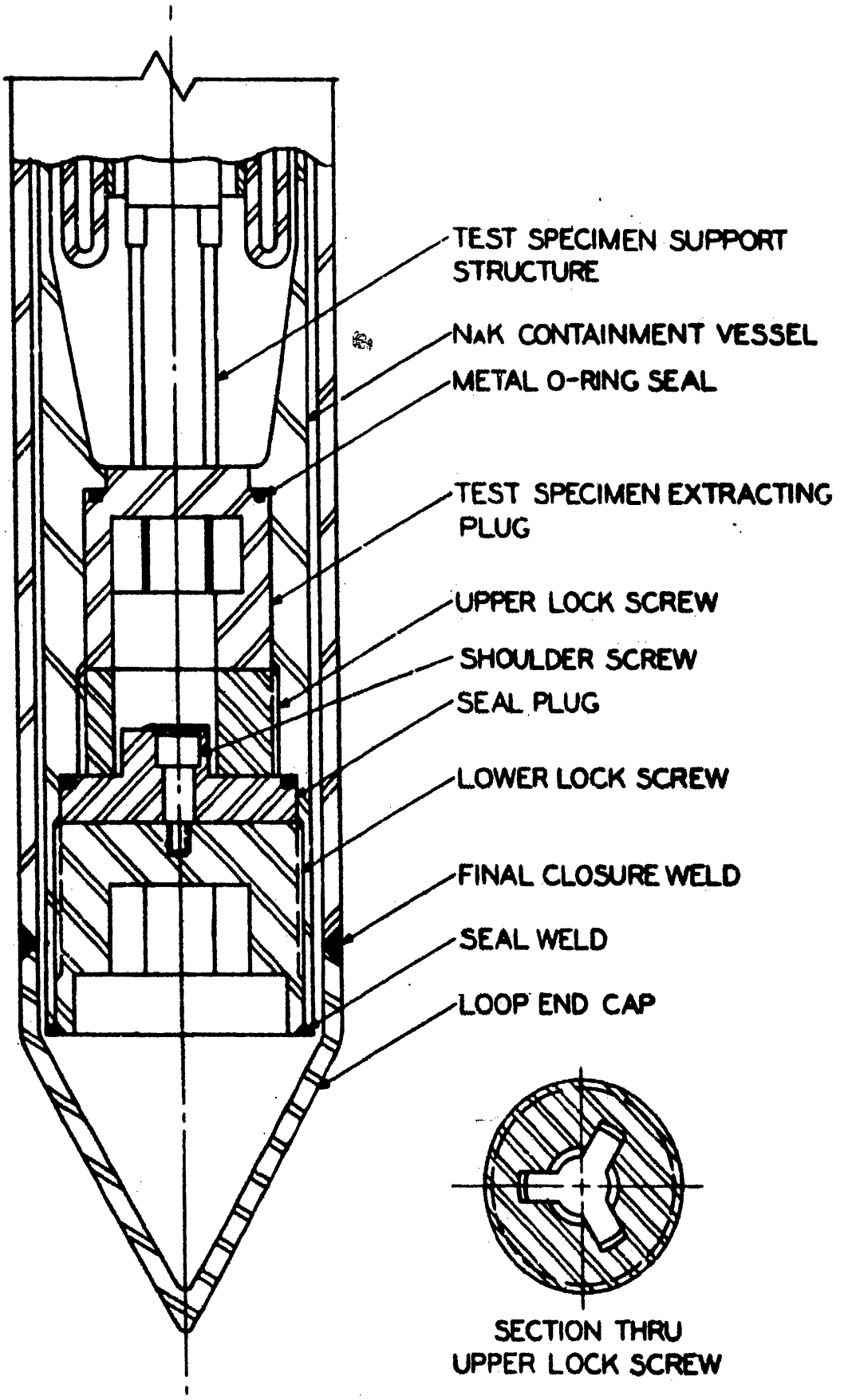

FIG. 3.6
REMOVABLE LOOP CLOSURE

The Nak temperatures in the in-core section will be measured by thermocouples attached to the walls of the NaK annuli. With one exception, the number of thermocouples and the method of installation will be identical to the original P&W design. The location and number of thermocouples is given in Report CNLM-1194(1) and in the P&W drawings listed in Appendix C. Because the fuel bundle is designed to be removable, it may not be possible to install a thermocouple on the fuel specimen. Therefore, this problem should be studied during the Title I effort. If it is impossible to install a thermocouple on the fuel specimen, the temperature of the fuel can be estimated by thermocouples installed in the NaK stream above and below the test specimen. In addition, provision should be made for either replacing or doubling the number of thermocouples used to monitor critical operating conditions that may affect reactor safety; e.g. the NaK outlet temperature from the test specimen. A leak detector will be installed in the outer helium space just above the end cap.

3.22 Heat Exchanger Section

Figure 3.7 illustrates a cross section of the heat exchanger. The diameter of this section, located above the in-core section, is larger than the in-core section to increase the heat transfer area. The innermost cylinder in this section is filled with helium and houses the four spiraled tubes which discharge the NaK into the test specimen. The innermost cylinder and the second cylinder form an annulus for the NaK returning to the pump. The second cylinder, the outside of which is grooved, and the third cylinder form a helium annulus to separate the returning NaK from the secondary coolant and thus provide double containment for the NaK. The instrumentation leads for the loop are carried out of the loop through this annulus. The third cylinder and the outside loop wall form an annulus for the secondary coolant. The reactor cooling water flows outside the loop wall.

3.23 Pump and Motor Section

The pump and motor section extends upward from the heat exchanger section to the end of the loop. The pump, a reversed, mixed-flow type with an axial diffuser, was designed and fabricated by Pratt & Whitney. Typical operating characteristics of the pump impeller are shown in Figure 3.8. The impeller is driven through a hollow overhung shaft, which passes through the liquid metal expansion tank. The NaK flows upward from the heat exchanger annulus to the inlet at the center of the impeller, reverses direction, and discharges into a spiral diffuser. From the diffuser, the NaK flows downward through four tubes, which are spiraled to accommodate differential expansion between the

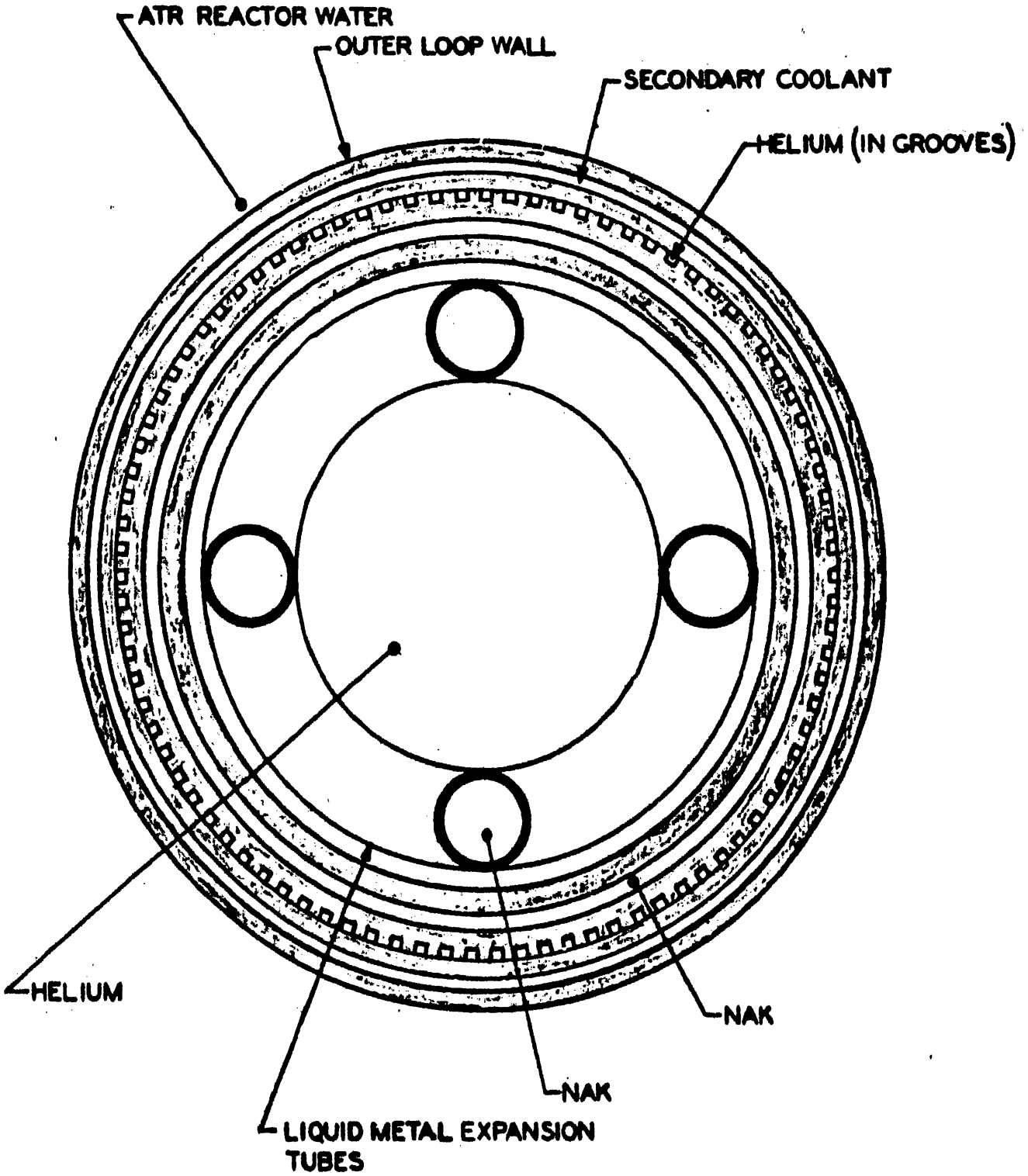

FIG. 3.7

HEAT EXCHANGER CROSS SECTION

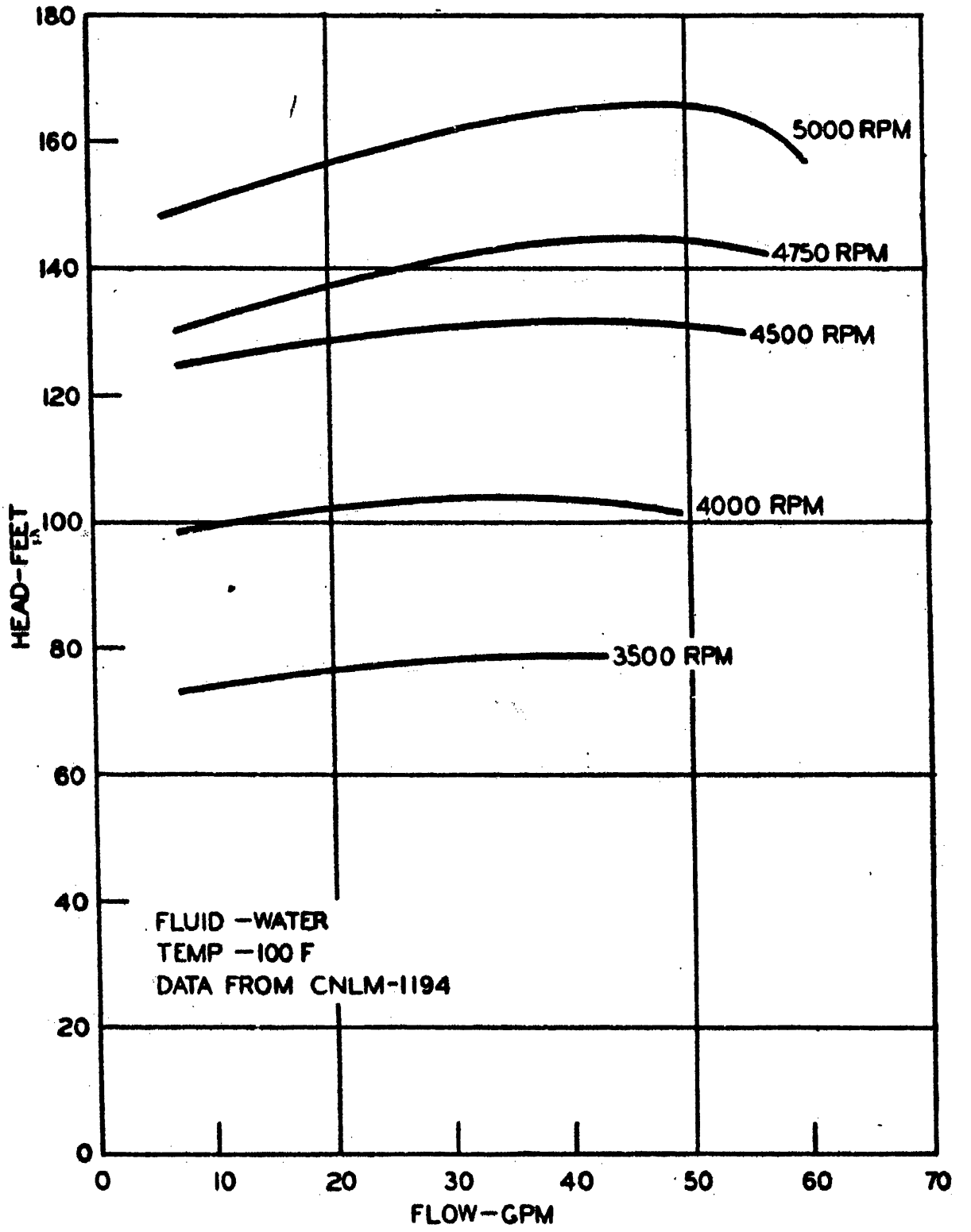

FIG. 3.8
TYPICAL OPERATING CHARACTERISTICS
PW-19 PUMP IMPELLER

hot and cold legs of the loop, to a header feeding the test section.

The drive motor is a three-phase, variable-frequency induction motor manufactured by the Bryant Chucking Grinder Company. The motor is enclosed in the helium cover gas over the primary coolant and thus operates in a helium-NaK vapor environment. No special seals are employed to prevent entry of NaK into the motor; thus the loop must be maintained in a vertical or near-vertical position when NaK is in the loop. The P&W loops have operated under similar conditions with no indication of motor damage by NaK vapor. The maximum motor-winding and motor-bearing temperatures have been tentatively set at 250 F. During Title I work, the manufacturers of the motors and bearings should be consulted to insure that the motors will operate without failure for 10,000 hours at this temperature. The bearing loads will have to be determined for this purpose.

The liquid metal expansion tank, located between the pump and the motor, accommodates the volumetric expansion of the NaK throughout the expected temperature range. It also serves as a heat sink to protect the motor and bearings from excessive temperatures. The heat is readily conducted by the NaK to the NaK containment vessel, where it is dissipated to the secondary coolant and the ATR cooling water. Broad, silver-plated, longitudinal fins on the cylinders comprising the NaK containment vessel and the stagnant helium containment vessel facilitate heat transfer from the motor and NaK expansion tank by insuring metal-to-metal contact between the cylinder walls. The motor and bearing temperatures are sensitive to variation in the NaK level in the expansion tank. For this reason, the desired NaK level will have to be determined in the study of the heat exchange system, the volumetric expansion of the NaK will have to be calculated, and the exact amount of NaK required will have to be introduced into the system.

The cylinders that constitute the loop are capped just above the motor. Motor and instrumentation leads penetrate the loop pressure vessles at this point only through hermetic seals. The outermost cylinder extends approximately 24 inches from its end cap to furnish the connection to the loop extension tube. A 12-inch lead-filled section of this extension provides a radiation shield for personnel making the connections to the motor leads, instrumentation leads, and secondary coolant tubing. Approximately 6 inches is allowed at each end of the section of lead to orient the loop connections in the desired positions. The connections will be spiraled through the lead to prevent a streaming path, and room for movement of the connections caused by thermal expansion will be provided. The motor and instrumentation leads and secondary coolant connections terminate about 5 inches above the end of the loop. The motor and instrumentation leads are housed in stainless-steel tubing to prevent water from contacting the leads.

3.24 Loop Extension Tube

The loop extension tube extends from the top of the in-pile loop out through the reactor vessel head. The loop extension tube houses the connections between the operating leads of the in-pile loop and the external operating equipment, including secondary coolant tubing, when the loop is in operating position in the reactor vessel. The loop extension tube also provides lateral support for the upper end of the ATR loop. The loop extension tube is a hollow cylinder and will be filled with ATR water when the ATR loop is in operating position. The electrical leads of the ATR loop are housed in stainless-steel tubing to prevent contact with the water and are spirally wound inside the loop extension tube to prevent radiation streaming. A plate of sufficient thickness to withstand the pressure of the reactor water is welded inside and near the top of the loop extension tube to prevent leakage of the reactor water out through the loop extension tube. The spirally wound operating leads penetrate this plate and are welded to it to complete the seal. The reactor head penetration by the loop extension tube is sealed by the use of a double-gland-type seal. Pure coolant water is injected between the gland at a pressure slightly higher than that of the reactor water to seal the outside of the loop extension tube to the reactor head. A spring-loaded hold-down device is attached to the loop extension tube above the reactor vessel head so that it will hold the loop firmly in the support plate and yet allow thermal expansion of the loop to take place. The lower end of the loop extension tube is attached to the upper end of the in-pile loop by means of a bayonet lock.

3.25 Loop Support

The loop is supported by the ATR support plate. The lower end of the loop rests in a conical socket in the support plate. The upper end of the loop is held down by the loop extension tube described in Section 3.24.

DESCRIPTION OF LOOP SYSTEMS

3.31 Primary Coolant System

Because liquid metals are the accepted coolants for fast reactors, the primary coolant system of the ATR in-pile loop will be identical to the one used in the P&W in-pile loop. An alloy of 56 per cent sodium and 44 per cent potassium, commonly referred to as NaK-44, is used in the loop since it remains liquid at room temperatures and thus obviates the need for auxiliary heating systems. Because liquid metals react chemically with water, a minimum of two walls, or pressure containers, is provided between the liquid metal and the ATR primary coolant to prevent contamination of the primary coolant. The NaK is circulated down through the test specimen, removing the heat generated there. It then flows up to the heat exchanger section, removing heat generated in the walls of the package loop by gamma absorp-

tion. It give up heat to the secondary coolant in the heat exchanger and flows to the pump.

The primary coolant system includes the test section, the liquid-metal coolant, a heat exchanger, a pump and motor, an expansion tank, and a cover gas (helium). The pump drive motor is located in the cover gas region above the surface of the liquid metal. The expansion tank above the pump fulfills the dual requirement of dissipating heat to the secondary coolant to keep the motor cool and of allowing the liquid metal to expand and contract as the temperature of the liquid metal changes. The primary coolant, pump drive motor, and cover gas are totally enclosed in the NaK containment vessel. The second containment vessel completely encloses the primary coolant pressure vessel. A buffer gas (helium) occupies the space between the two vessels. Helium is used because of its good thermal conductivity and inertness and because, in comparison with the other inert gases, it does not become radioactive. Liquid metal leak detectors are located in this gas region to detect the presence of a leak in the primary coolant system. The leads for the thermocouples used to detect the temperatures of the primary coolant and the test specimens are also located in this space.

3.32 Secondary Coolant System

As mentioned in Section 3.12, two concepts for the use of a secondary coolant are described. The secondary coolant system includes the external piping and equipment required to furnish a failure-free source of coolant to the loop.

Concept 1 requires a 5800 SCFM source of helium at approximately 600 psi. A flow diagram for this concept is shown in Figure 3.9. The helium, flowing in a closed circuit, enters the loop at the top and flows past the motor, cooling the motor. The helium then flows through the heat exchanger, removing heat from the NaK. At the end of the heat exchanger, the flow divides into four return tubes. The return tubes make a 180 degree bend just above the core and follow the outside of the package loop to the upper end of the loop. There they enter the support column and join in a header to discharge through the top head of the ATR in a common tube. As the helium flows up through the return tubes, it loses heat to the ATR cooling water. However, an external heat exchanger may be required to adequately cool the helium, and an external compressor will be required to circulate the helium. The helium flow will be regulated by a flow control valve actuated by the NaK temperature, leaving the heat exchanger to control the temperature of the primary coolant entering the test specimen.

A 6-inch-square water jacket is attached to the package loop in the heat exchanger section. The helium return lines are

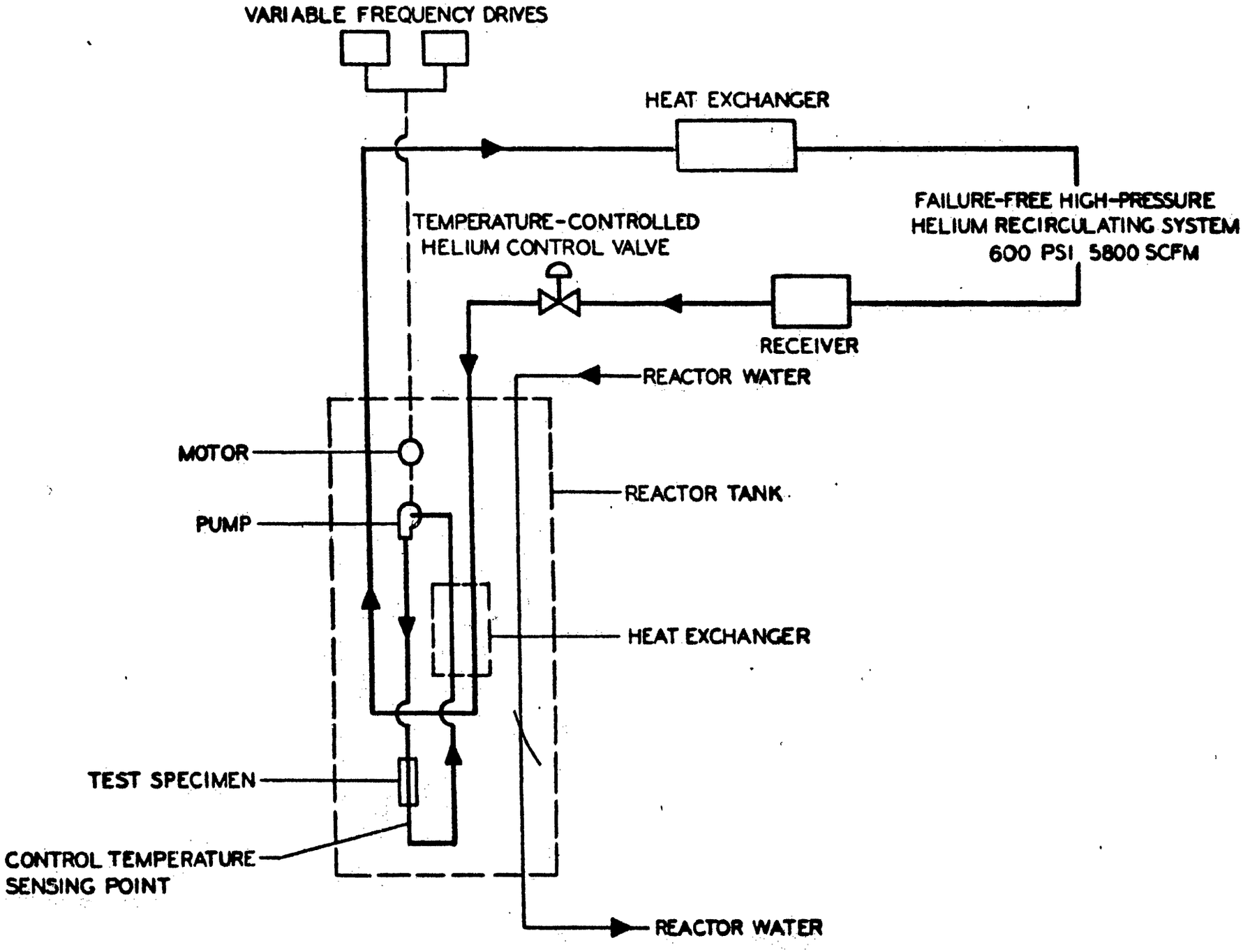

FIG. 3.9
IN-PILE LOOP FLOW DIAGRAM - CONCEPT I

located in the corners of the square. Filler pieces are placed in the corners and spaced away from the outside diameter of the loop to form a water annulus that is concentric with, and adjacent to, the heat exchanger. The water jacket mates with a socket in the top of the thermal neutron filter and the extended core so that water flow is maintained by the pressure differential across the ATR core. Reactor water enters the water jacket at the top and flows down past the heat exchanger, removing heat from the helium; the water then flows through the concentric annuli formed by the loop and the thermal neutron filter and the filter and the extended core, cooling these pieces as well. Figure 6.1 illustrates these annuli. The heat removal characteristics of Concept 1 are discussed in Section 3.5.

Concept 2 requires a 70-gallon-per-minute source of demineralized water at a pressure of approximately 400 psi, which is sufficiently larger than the ATR coolant pressure to overcome friction losses in the piping and the loop. A flow diagram for this concept is shown in Figure 3.10. The water should meet the following requirements:

Pressure	- 400 psi
pH	- 6.5 to 7.0
specific resistance	- 50,000 ohms/cu cm minimum
chloride ion concentration	- 1 ppm maximum

If the ATR primary coolant water meets these requirements, it may be used for the source. If the ATR primary coolant does not meet the requirements, a separate pump and demineralizer will be required.

The water enters the loop through a connection at the top and, flowing down past the motor, cools the motor; the water then flows through the heat exchanger, removing heat from the NaK. The water discharges into the ATR reactor water just above the core. The water flow will be regulated by a flow control valve actuated by the NaK temperature, leaving the heat exchanger to control the temperature of the primary coolant entering the test specimen. The heat removal characteristics of Concept 2 are discussed in Section 3.5.

As mentioned previously, the use of Concept 2 permits the insertion and removal of the ATR loop assembly through the reactor vessel head. This concept provides the most convenient method of loop handling as described in Section 8.4. However, the use of water limits the control of primary coolant temperatures, as discussed in Section 3.5.

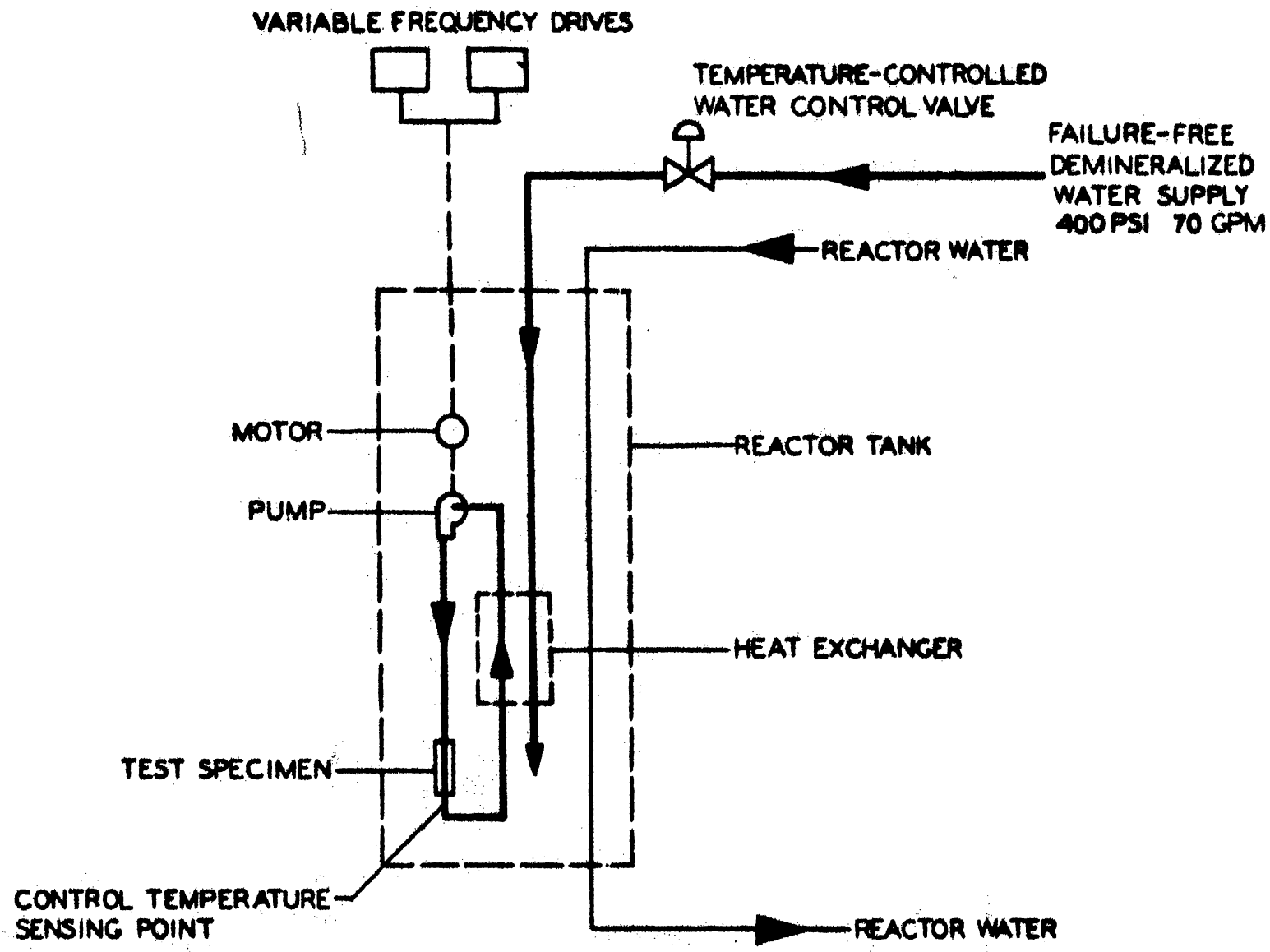

FIG. 3.10
IN-PILE LOOP FLOW DIAGRAM - CONCEPT 2

Since the square water jacket attached to the loop in Concept 1 will not pass through the head of the ATR vessel, the loop must be installed and removed through the reactor drop tube. This causes the handling of Concept 1 to be more difficult than the handling of Concept 2 as described in Section 8.3. Also the heat transfer capacity of Concept 1 is less than the capacity of Concept 2, as discussed in Section 3.5. However, it is considered that the increased control of the primary coolant and test specimen temperatures outweighs these difficulties. Therefore Concept 1 is the preferred concept.

3.33 Electrical System

A 480-volt, 3-phase, 50-amp, 60-cycle failure-free source of electrical power is required for this package loop. This provides sufficient power for the operation of the instrument and control console and for the pump drive motors. (NOTE: The power for pumps or compressors in the secondary coolant system is not included.) The existing PW-19 electrical console power circuits are shown in Figure 3.11* It is expected that this control console could be used with only minor modifications.

The variable-frequency pump drive motor receives its power from two 9.4 kva variable-frequency M-G units. The units are operated simultaneously at synchronous speed, one unit supplying power and the other unit on standby. The units are equipped with an automatic transfer device to provide uninterrupted power to the loop pump motor if the normal drive unit fails. These drive units could be used "as is" for the modified loops.

3.34 Instrumentation System

This section describes the PW-19 control console and discusses the function of the instrumentation and control system of the experiment as abstracted from CNLM-1194[1].** It also summarizes pertinent information concerning the components in the instrumentation and control system. The existing control console can be readily modified for use with the ATR loop described in this report.

The control console consists of two L-shaped sections that contain a total of nine panels, numbered consecutively from left to right. The layout and component locations for the control console are shown in Figure 3.12. A relay cabinet containing the majority of the control panel relays is located at the intersection of the two sections. A transformer rack containing three delta-connected 5-kva 240-120 step-down transformers is located against the left-hand side of panel No. 1. Power for the control

---

* Reproduced by permission of Pratt & Whitney Aircraft.

** Literature references are listed in Appendix C.

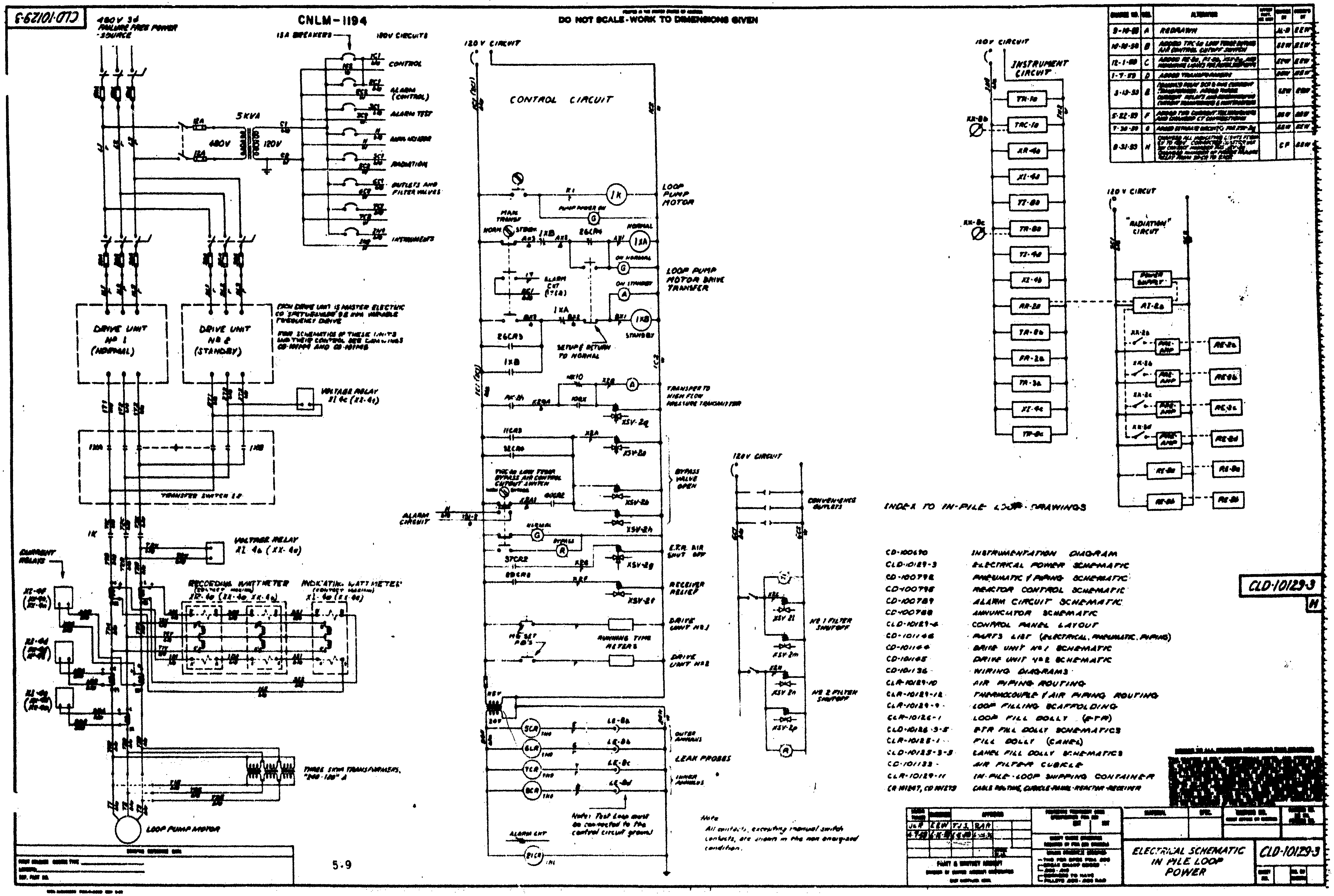
CLD-10129-3
480V 3φ FAILURE FREE POWER SOURCE
CNLM-1194
DO NOT SCALE - WORK TO DIMENSIONS GIVEN
15A BREAKERS
120V CIRCUITS
CONTROL
ALARM (CONTROL)
ALARM TEST
ALARM HOLDERS
RADIATION
OUTLETS AND FILTER VALVES
INSTRUMENTS
5KVA
480V
120V
120V CIRCUIT
CONTROL CIRCUIT
LOOP PUMP MOTOR
LOOP PUMP MOTOR DRIVE TRANSFER
NORMAL
STANDBY
SETUP RETURN TO NORMAL
DRIVE UNIT Nº 1 (NORMAL)
DRIVE UNIT Nº 2 (STANDBY)
VOLTAGE RELAY
TRANSFER SWITCH
CURRENT RELAYS
VOLTAGE RELAY
RECORDING WATTMETER
INDICATING WATTMETER
THREE 5KVA TRANSFORMERS
LOOP PUMP MOTOR
TRANSFER TO HIGH FLOW PRESSURE TRANSMITTER
BYPASS VALVE OPEN
ALARM CIRCUIT
RECEIVER RELIEF
DRIVE UNIT NO 1
DRIVE UNIT NO 2
RUNNING TIME METERS
LEAK PROBES
OUTER ANNULUS
INNER ANNULUS
ALARM CKT
Note: Test Loop must be connected to the control circuit ground
Note: All contacts, excepting manual switch contacts, are shown in the non energized condition.
CONVENIENCE OUTLETS
NO 1 FILTER SHUTOFF
NO 2 FILTER SHUTOFF
INSTRUMENT CIRCUIT
"RADIATION" CIRCUIT
POWER SUPPLY
INDEX TO IN-PILE LOOP DRAWINGS
CD-100690 INSTRUMENTATION DIAGRAM
CLD-10129-3 ELECTRICAL POWER SCHEMATIC
CD-100792 PNEUMATIC PIPING SCHEMATIC
CD-100795 REACTOR CONTROL SCHEMATIC
CD-100789 ALARM CIRCUIT SCHEMATIC
CD-100788 ANNUNCIATOR SCHEMATIC
CLD-10129-4 CONTROL PANEL LAYOUT
CD-101146 PARTS LIST (ELECTRICAL, PNEUMATIC, PIPING)
CD-101164 DRIVE UNIT NO1 SCHEMATIC
CD-101165 DRIVE UNIT NO2 SCHEMATIC
CD-101136 WIRING DIAGRAMS
CLR-10129-10 AIR PIPING ROUTING
CLR-10129-12 THERMOCOUPLE & AIR PIPING ROUTING
CLR-10129-9 LOOP FILLING SCAFFOLDING
CLR-10126-1 LOOP FILL DOLLY (ETR)
CLD-10126-3-5 ETR FILL DOLLY SCHEMATICS
CLR-10128-1 FILL DOLLY (CANEL)
CLD-10128-3-3 CANEL FILL DOLLY SCHEMATICS
CD-101133 AIR FILTER CUBICLE
CLR-10129-11 IN-PILE LOOP SHIPPING CONTAINER
CR 101247, CD 101275 CABLE ROUTING, CUBICLE-PANEL-REACTOR-RECEIVER
REDRAWN
ELECTRICAL SCHEMATIC IN PILE LOOP POWER
CLD-10129-3
H

FIG 3.11

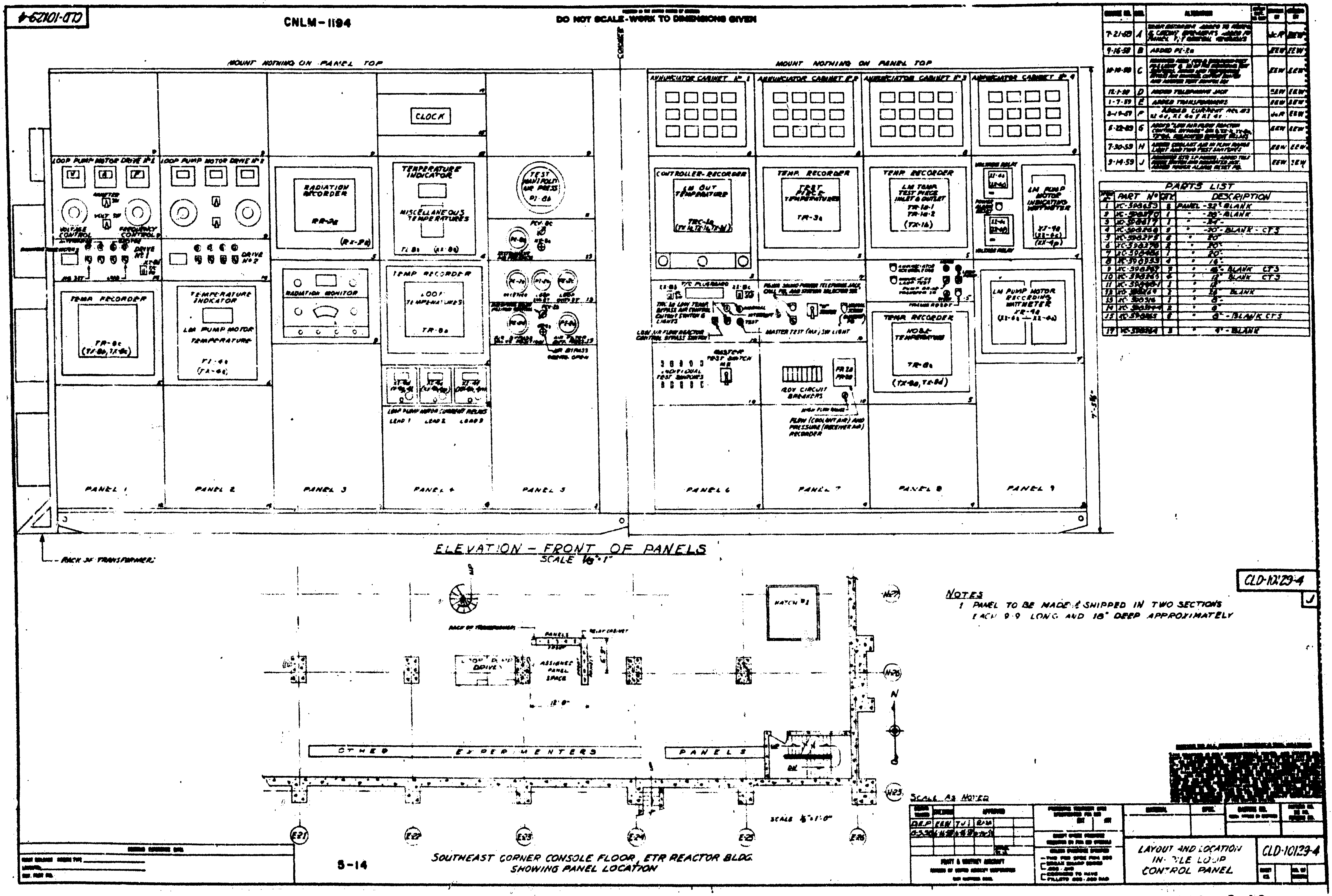
CLD-10129-4
CNLM-1194
DO NOT SCALE-WORK TO DIMENSIONS GIVEN
MOUNT NOTHING ON PANEL TOP
ANNUNCIATOR CABINET
CLOCK
LOOP PUMP MOTOR DRIVE Nº 1
LOOP PUMP MOTOR DRIVE Nº 2
RADIATION RECORDER
TEMPERATURE INDICATOR
MISCELLANEOUS TEMPERATURES
TEST MANIFOLD AIR PRESS
CONTROLLER-RECORDER
TEMP. RECORDER
LM PUMP MOTOR INDICATING WATTMETER
TEMP RECORDER
TEMPERATURE INDICATOR
LM PUMP MOTOR TEMPERATURE
RADIATION MONITOR
LOOP TEMPERATURES
NOSE TEMPERATURE
LM PUMP MOTOR RECORDING WATTMETER
MASTER TEST (IND.) SW LIGHT
RDY CIRCUIT BREAKERS
PANEL 1
PANEL 2
PANEL 3
PANEL 4
PANEL 5
PANEL 6
PANEL 7
PANEL 8
PANEL 9
PARTS LIST
PART Nº
QTY.
DESCRIPTION
ELEVATION - FRONT OF PANELS
RACK OF TRANSFORMERS
HATCH #1
ASSIGNED PANEL SPACE
OTHER EXPERIMENTERS PANELS
NOTES
1 PANEL TO BE MADE & SHIPPED IN TWO SECTIONS EACH 9'-9" LONG AND 18" DEEP APPROXIMATELY
SCALE AS NOTED
5-14
SOUTHEAST CORNER CONSOLE FLOOR, ETR REACTOR BLDG. SHOWING PANEL LOCATION
LAYOUT AND LOCATION IN-PILE LOOP CONTROL PANEL
CLD-10129-4

FIG. 3.12

console will be supplied from a failure-free, 480-volt, 3-phase, a-c source. This supply power will be fed through the control console to the two loop pump motor drive units. A 480-120 5-kva transformer located in panel No. 1 will supply 120-volt, single-phase, a-c control power. The control console will also require 100-psig instrument air to actuate the pneumatic control system.

Panel No. 1 contains the No. 1 or "Normal" loop pump motor drive unit controls; a Brown recorder, designated TR-8c; and a thermocouple selector switch. The loop pump motor drive unit controls include a 0- to 300-volt voltmeter and a 0- to 30-ampere ammeter, each with a 3-phase switch; a 0-to 200-cps frequency meter and frequency controller; a voltage controller; and four drive unit on-off control switches with green indicating lights. The TR-8c recorder is a Brown single-point strip chart recorder that will monitor the outer helium annulus temperature. This instrument will energize a high-temperature annunciator and slow scram circuit. Panel No. 1 also contains a running time meter that is connected across the "Normal" drive unit "M-G Set" on-off switch to provide measurement of the total accumulated hours of "Normal" drive unit operation.

Panel No. 2 contains the No. 2 or "Stand-by" loop pump motor drive unit controls and a running time meter. These controls and time meter duplicate the "Normal" drive unit controls previously described. This panel also contains a 0- to 500-F Brown precision indicator, designated TI-4a, which will monitor the stator temperature of the loop pump motor. This instrument will energize a high-temperature alarm annunciator circuit.

Panel No. 3 contains a 0-to 50-MV Brown Electronic Recorder, designated RR-2a; a Technical Measurements Corporation RM-1b radiation count rate meter; four channel selector switches; and an Atomic 312 power supply. The RR-2a recorder will record the total radiation level sensed by any or all the four channels selected and will energize a high-radiation-level annunciator. This equipment was used by P&W to monitor the radiation level of the exit air from the loop heat exchanger and could be used with Concept 1.

Panel No. 4 contains a temperature indictaor, designated TI-8a; a temperature recorder, designated TR-8b; three current-monitoring relays, designated XI-4d, XI-43, and XI-4f; and a clock. Indicator TI-8a is a 0-to 2000-F Brown precision indicator equipped with 24 pushbutton thermocouple selector switches. This instrument will indicate miscellaneous loop temperatures. Recorder TR-8b is a 0-to 2000-F, 12-point Brown strip chart recorder which will record the temperatures of the liquid metal in the pump inlet, pump outlet, pump sump, and heat exchanger, as well as the air temperatures in the heat exchanger inlet and outlet.

Panel No. 5 contains the test manifold pressure gauge PI-8b (Heise 3 to 15 psig, graduated 0 to 100 per cent); instrument air pressure gauge PI-8a (0 to 200 psig); test manifold pressure

regulator PCV-8c; test manifold shutoff valve HV-8a; reactor inlet and discharge air pressure indicators PI-2b and PI-2c (0-to 300 psig); receiver air pressure indicator PI-2a (0 to 300 psig); inlet filter pressure differential indicator PI-2e (0 to 100 per cent); emergency air bypass valve control valve PCV-2b; position indicator PI-2d; and emergency open valve HV-2a. All of this equipment except the instrument air equipment was required by the air cooling system used by P&W and would not be needed with Concept 2.

Panel No. 6 contains Annunciator Cabinet No. 1; a recorder controller, designated TRC-1a; a thermocouple plugboard with two 3-position switches; a master test switch with a red test position light; 10 pneumatic test switches; the TRC-1a low-temperature bypass air control cutout switch, with red and green indicating lights; and the low-air-flow reactor-control bypass switch. Annunciator Cabinet No. 1 contains seven alarm circuit annunciators, none of which have any reactor control function.

Panel No. 7 contains Annunciator Cabinet No. 2; temperature recorder TR-3a; a sound-powered telephone jack and buzzer; a "W" switch; a push-button switch, designated "Manual Scram"; eight 120-volt, 15-ampere circuit breakers; flow and pressure recorder FR-2a--PR-2a; and a high-flow-range light. Annunciator Cabinet No. 2 contains 10 alarm circuit annunciators that do not have reactor control functions.

Recorder TR-3a is a 16-point 0- to 2000-F Brown strip chart recorder, which will record test piece temperatures. The "Scram" button is protected by a guard to prevent an inadvertent reactor power reduction.

Panel No. 8 contains Annunciator Cabinet No. 3, temperature recorders TR-1a-1, 1a-2, and TR-8a, the console annunciator acknowledge and lamp test push-button switches, and the loop pump and pump drive transfer switches. Annunciator Cabinet No. 3 contains 12 alarm circuit annunciators, each of which (with the exception of the "Activity Heat Exchanger Air" annunciator) has a reactor control function. Recorder TR-1a-1, 1a-2 is a two-pen 0-to 2000-F Brown strip chart recorder, which records the test piece inlet and outlet temperatures. Recorder TR-8a is a 0- to 2000-F Brown single-point strip chart recorder, which records the liquid metal temperature in the loop nose section downstream of the test piece. This instrument energizes a high-temperature annunciator and slow scram circuit. The loop pump switch is a two-position rotating turn switch, which is provided with a green "on" position-indicating light. The pump drive manual transfer is controlled by two switches. One switch has a "Normal" and a "Stand-by" position with green and amber indicating lights, and the other is a push-button transfer reset switch.

Panel No. 9 contains Annunciator Cabinet No. 4, under-voltage relays XI-4B and XI-4C, wattmeters XI-4a and XR-4a, and the wattmeter alarm contact reset switch. Annunciator Cabinet No. 4 contains five reactor control alarm circuit annunciators, one alarm annunciator, and the reactor power reduction alarm

circuit annunciators. The undervoltage relays are Assembly Products Co. 0-to 300-volt instruments, which are equipped with low-voltage alarm contacts. Relay XI-4B monitors the pump motor lead line voltage and energizes the automatic transfer to the "Stand-by" drive unit circuit and the "Auto Transfer Loop Pump Drive" annunciator. Relay XI-4C monitors the "Stand-by" drive unit output voltage and energizes the "Failure Stand-by Loop Pump Drive" annunciator. A slow scram circuit is energized when both undervoltage relays sense low voltage. Both relays are equipped with reset switches that release the alarm contact holding coils. The wattmeters are Esterline Angus Model AW, three-phase power-measuring instruments. Meter XR-2a is a 0-to 10-kw dual instrument containing a power recorder and indicator with high-and low-power annunciator alarm circuit contacts. The low-power annunciator contact also energizes a slow scram circuit. Meter XI-4a is a 0-to 10-kw indicating instrument with a "Stall Power" annunciator and slow scram circuit contact. All four wattmeter alarm contacts are wired to lock in on contact and are provided with a single reset switch, which releases the alarm contact holding circuits.

3.4 OPERATING PROCEDURE

The location of the package loop when installed in the ATR is shown diagrammatically in Figure 3.1. The loop will be inserted into the test reactor during scheduled shutdowns, either through the top head of the ATR pressure vessel, or through the ATR canal. Before insertion, the test specimen will have been installed, the system charged with NaK and helium, and the connections for the external auxiliary systems will have been capped to prevent water or dirt from entering these connections.

The loop will be inserted into the ATR pressure vessel, either through the top head or through the drop tube, and positioned through the top head sealing gland so that the connections for the external auxiliaries are accessible above the top head. The loop extension tube will be positioned over the loop, and the connections of the external auxiliary systems to the loop will be made. The loop extension tube will then be attached to the loop. The sealing gland will be loosened, and the loop will be lowered by an overhead crane until the spring-loaded collar on the loop meets with the socket in the top of the thermal neutron filter. The loop will then be pushed down until it rests in the support plate socket. (See Section 5.1). The loop hold-down device will then be attached and the sealing gland tightened.

Circulation of the primary coolant will be started by adjustment of the pump speed so that the designated flow rate of the coolant is main-

tained. This coolant flow rate is a function of the pump speed and, thereby, a function of the input power, which will be continuously monitored and controlled. The reactor will then be brought up to operating power in suitable small increments. During this period, the primary coolant temperature will increase at a rate dependent on the power developed in the test specimen and the gamma heating developed in the loop structure. When the desired NaK temperature is attained, the secondary coolant control valve will begin to open. The position of this control valve will be controlled automatically by the primary coolant temperature. After the reactor has reached scheduled power, the pump speed will be varied as required to maintain the desired temperature differential across the test specimen. The experiment will then operate automatically throughout the duration of the test. In the event of unscheduled reactor shutdowns, the experiment will automatically return to isothermal operation at a temperature slightly above that of the reactor process water. The experiment will continue to operate in that manner until the reactor returns to power. CNLM-1194[1] may be used as a guide to writing detailed operating procedures.

Upon completion of the scheduled test, the overhead crane will be attached to the loop support tube and the hold-down device removed. The sealing gland in the top head of the ATR pressure vessel will be loosened and the loop withdrawn until the connection between the loop support tube and the loop proper is accessible above the top head of the ATR pressure vessel. The loop support tube will then be detached from the loop proper, the connections to the removal equipment power and cooling sources will be made, and the connections between the auxiliary system and the loop will be disconnected. The loop will then be removed from the ATR as described in Section 8.0.

3.5 HEAT TRANSFER AND HYDRAULICS

The results of heat transfer calculations to establish the feasibility of the concepts are summarized in Table 0.1 and Figures 3.13 and 3.14. In these calculations, it was assumed that the heat loss from the motor was gained by the secondary coolant before entering the heat exchanger. The heat exchanger must remove all the heat generated in the structural materials in the in-core section, except for the heat generated in the outermost cylinder, as well as that generated in the test specimen. Axial conduction of heat along the loop walls on either end of the heat exchanger has been ignored as was conduction along the pump shaft. It has been assumed also that the third cylinder expanded sufficiently to establish metal-to-metal contact with the fourth cylinder through the fins. No heat transfer resistance across this interface was included in calculating the over-all heat transfer coefficient. Radiation and conduction across the helium space between the fins was ignored as it was considered to be negligible. The NaK heat transfer coefficient was computed from the Lubarsky-Kaufman equation:

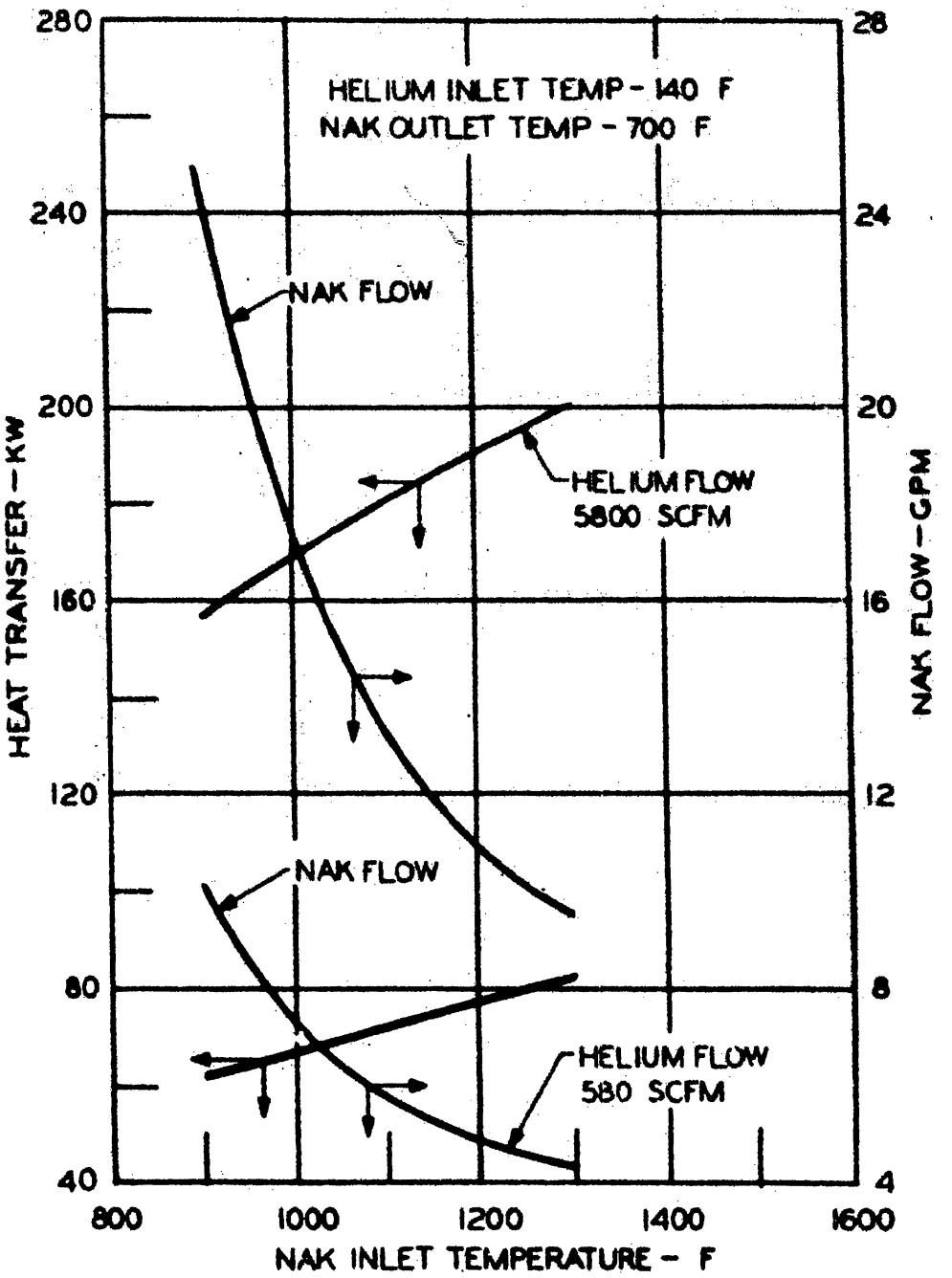

FIG. 3.13
TYPICAL HEAT EXCHANGER CHARACTERISTICS
[HELIUM-COOLED]

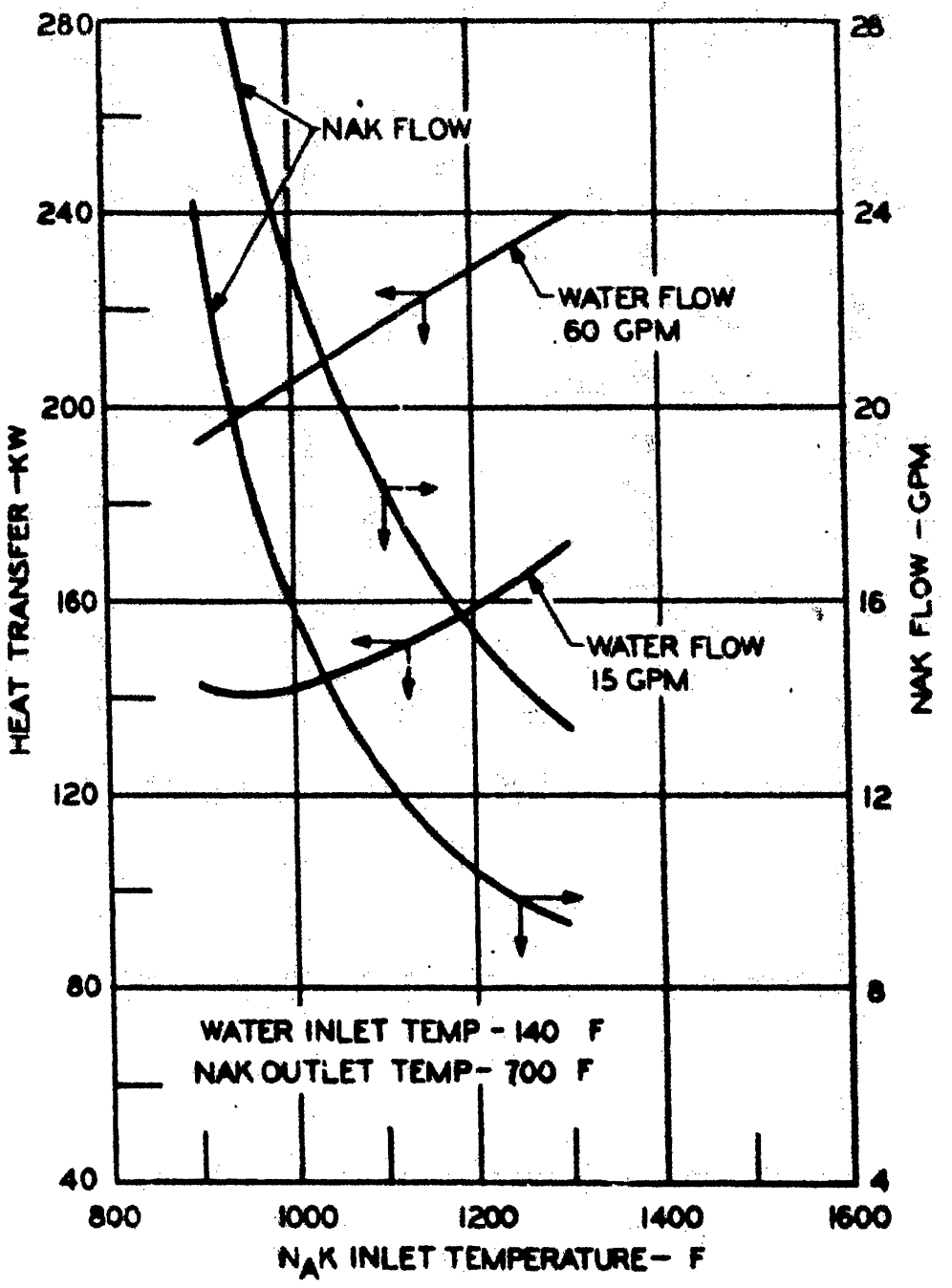

FIG. 3.14
TYPICAL HEAT EXCHANGER CHARACTERISTICS
[WATER-COOLED]

$$Nu = 0.625\ Pe^{0.4} \quad (2)$$

The modified Colburn equation

$$\frac{hD}{k} = 0.023\ Re^{0.8} Pr^{0.3} \quad (3)$$

with all physical properties evaluated at the film temperatures, was used to calculate the water film coefficient. The helium film coefficient was calculated from the equation:

$$\frac{h}{c_p G} Pr^{2/3} \left(\frac{\mu_w}{\mu_b}\right)^{0.14} = \frac{0.023}{Re^{0.2}} \quad (4)$$

with all physical properties evalutated at the bulk temperature except μ_w in the viscosity ratio term.

The nomenclature for the preceding equations is

c_p = specific heat at constant pressure, Btu/(lb) (F)

D = hydraulic diameter, feet

G = mass velocity, lb/(hr) (sq. ft. of cross section)

h = heat transfer coefficient, Btu/(hr) (sq ft) (F)

k = thermal conductivity, Btu/(hr) (sq ft) (F/ft)

Nu = Nusselt number, dimensionless

Pe = Peclet number, dimensionless

Pr = Prandtl number, dimensionless

Re = Reynolds number, dimensionless

Greek:

μ = Viscosity of fluid, lb/(hr) (ft)

Subscripts:

b = bulk

w = wall

Figure 3.13 shows the heat transfer capability of the heat exchanger and the associated NaK flow rate when 5800 SCFM and 580 SCFM enters the heat exchanger at 140 F. The temperature of the NaK leaving the heat exchanger is held constant at 700 F. A similar set of curves for water coolant is shown in Figure 3.14. The maximum allowable temperature limit is pri-

marily due to the stress caused by the radial temperature gradient in the exchanger walls.

Table 3.1 shows the heat load on the heat exchanger caused by the combined gamma heating in the loop structural materials and the test specimen fissions as a function of the length of the test specimen. It is assumed that the length of the inner cylinders of the in-pile portion of the loop is no longer than the length required for the particular test specimen length; it is further assumed that the top of the test specimen is level with the top of the ATR core. The outer cylinder of the loop and the thermal neutron filter extend the full length of the ATR core. The gamma heating load of the upper loop is assumed to be a constant 25kw and the gamma heating in the in-pile portion is 11 watts per gram of structural material.

A comprehensive study of the heat transfer system will be required in the Title I effort to determine the optimum heat transfer system and the optimum operating conditions. As previously noted, some of the mechanisms of heat transfer were deliberately neglected to give the most conservative heat exchanger capability. Thus, it is expected that the capacity of the heat exchanger will be greater than that shown in Figures 3.13 and 3.14. For this reason a nominal heat capacity of 225 kw is given in Table 3.1. The comprehensive study will also determine the NaK flow rate to be used. Figure 3.15 shows the test specimen Nak flow requirements as a function of test specimen power. It appears that a portion of the NaK flow must be allowed to bypass the test specimen if the desired temperatures into and out of the test specimen are to be held, and if the maximum allowable primary coolant temperature is not to be exceeded. The study also may indicate that the use of air as a secondary coolant is preferable to the use of either helium or water. The use of gas for the secondary coolant increases the temperature control and reduces the minimum test specimen power but exacts a penalty in the form of reduced capacity, increased circulation costs, and the inability to remove the loop through the top head of the ATR pressure vessel. The use of water increases the heat transfer capability of the unit for given temperatures but also limits the amount of control of loop temperatures that may be attained without boiling in the secondary coolant channel. It also establishes a relatively high minimum test specimen power.

The heat transfer from the loop outer cylinder and thermal neutron filter to the ATR primary coolant in the in-core region must be checked in the Title I effort to be certain that the stresses caused by temperature gradients are not excessive. The work performed indicates that no serious problems are involved.

Figure 3.16 shows the nominal head-flow relationship of the NaK pump impeller, the nominal pressure drop characteristic of the loop

TABLE 3.1 - ALLOWABLE TEST SPECIMEN POWER GENERATION

Test Specimen Length (ft)	Nominal Heat Exchanger Capacity (kw)	Lower Loop Gamma Heating Load (kw)	Upper Loop Gamma Heating Load (kw)	Maximum Total Specimen Power (kw)
4	225	132	25	68
3	225	99	25	101
2	225	66	25	134
1	225	33	25	167

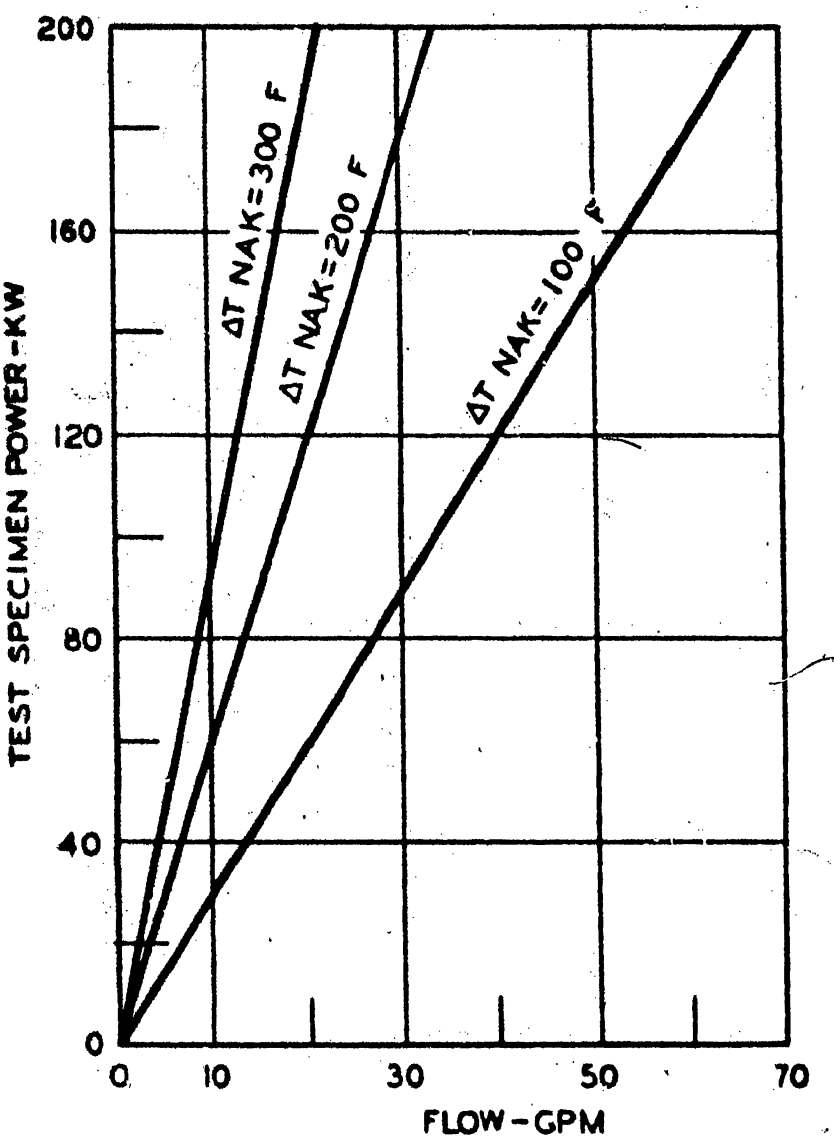

FIG. 3.15
TEST SPECIMEN NaK FLOW REQUIREMENTS

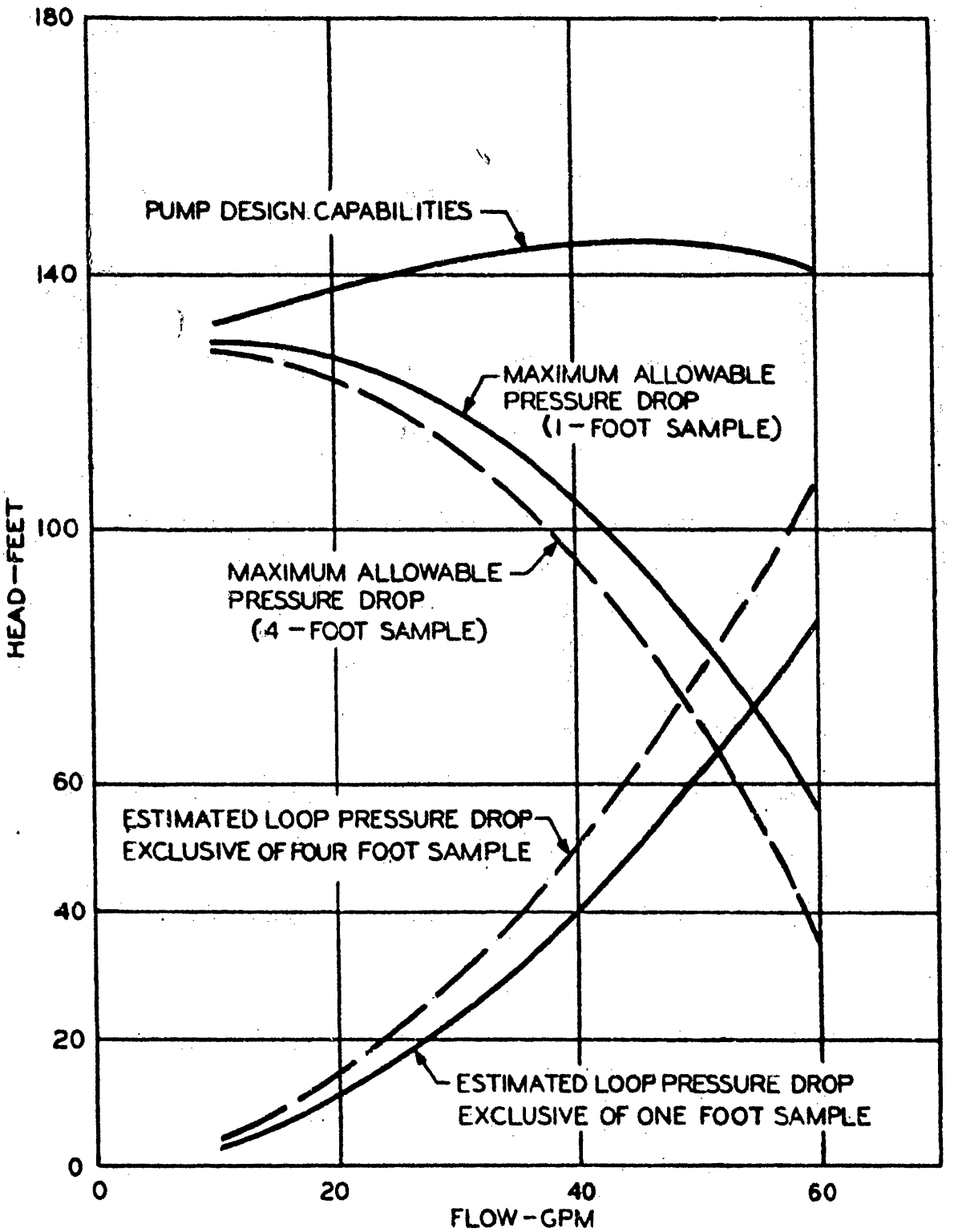

FIG.3.16
PRIMARY SYSTEM HYDRAULIC
CHARACTERISTICS

primary coolant circuit exclusive of test specimens, and the maximum permissible test specimen pressure drop. The NaK pressure drop characteristics curve was taken from TIM-483, "Forced Convection Liquid Metal In-Pile Loop Liquid Metal Pressure Drop Calculations."[5]

The secondary coolant pressure drop for Concept I was calculated for transition losses using the formula

$$\Delta P = \frac{KV^2}{2g} \frac{P}{144}$$

where ΔP = pressure loss, lb/sq in.

K = resistance coefficient

V = mean velocity in channel, ft/sec

g = acceleration of gravity, ft/(sec) (sec)

p = density, lb/cu ft

The friction losses in pipe, channels, and annuli were calculated from the Darcy-Weisback formula

$$\Delta P = \frac{f}{2g} \frac{L}{D} \frac{PV^2}{2g}$$

where f = friction factor

L = channel length, ft

D = diameter or equivalent diameter, ft

other symbols same as above.

The values of K and f were taken from IDO-16368, "Hydraulic Flow Calculations for MTR-ETR Experiments Standard Practices Manual."[6]

The secondary coolant pressure drop for Concept 2 was calculated from the formula

$$\Delta P = \frac{0.0001\, K\, \bar{V}\, w^2}{A^2\, Y^2}$$

which was derived from the formula

$$w = 0.525\, Y\, d^2 \frac{\Delta P}{K\bar{V}}$$

from "Flow of Fluids" pp. 3-4, Crane Company[7]

where P = pressure loss, psi

K = resistance coefficient, ($f\frac{L}{D}$ for pipe friction losses)

V = specific volume, cu ft/lb

w = rate of flow, lb/sec

A = cross sectional area of channel, sq. ft

Y = net expansion factor for compressible flow.

The flow path was broken down into lengths of constant cross section and transition sections and the pressure drop was calculated for each section. The specific volume was calculated for each section, taking into account pressure changes due to flow losses and temperature changes due to heat flow.

The ATR primary coolant pressure drop through the water jacket used in Concept I is shown in Figure 3.17. ATR coolant flows through the water jacket around the heat exchanger and then through the annular spaces on both sides of the thermal neutron filter. The flow path geometry for this concept is such that the pressure drop will be greater than that of Concept 2. The ATR coolant pressure drop through the extended core region is not included in this figure. Since the heat generation per unit volume in the extended core is less than the heat generation per unit volume in the ATR core, the required coolant flow and pressure drop will be less than that of the ATR core for the same temperature rise.

3.6 ESTIMATE OF PRATT & WHITNEY LOOP LIFE

The Pratt & Whitney loop for the ETR was overdesigned for 1600F operation and was based on ASME allowable codes for Type 316 stainless steel. Strain cycling was also factored into the design where the thermal stresses exceeded the yield under transient conditions. For 1200 F operation the stresses are less, and there should be no problem in obtaining 10,000-hour life from a stress-rupture standpoint.

The radiation stability of the pump motor was confirmed by irradiating smaller motors in the VG facility of the MTR. The motors have been irradiated to a calculated exposure of 10^9 rads while operating to 2900 hours maximum. This dosage is about an order of magnitude higher than the expected life that was planned for the ETR loop. Radiation did not significantly affect the properties of the insulating materials of the pump electrical system, and there was little deterioration of the bearing lubricants. Therefore, the motors should be workable to an exposure of

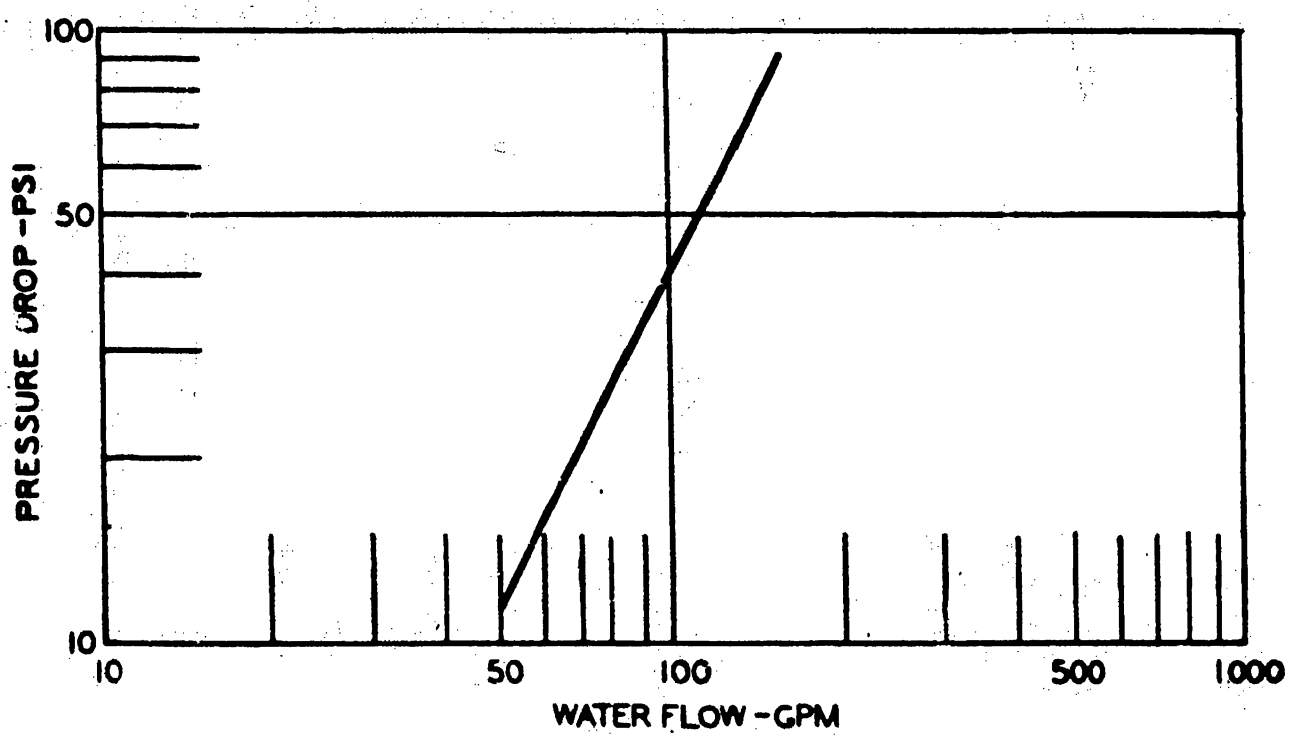

FIG. 3.17
PRESSURE LOSS THROUGH
LOOP WATER JACKET

10^9 rads. Although out-of-pile life tests on actual loop motors were not run for the complete 10,000 hours required, irradiation effects are not the limiting factor if the total dose is less than 10^9 rads. To allow a 10,000-hour life, it will be necessary to shield the motor in the ATR if the amount of radiation is greater than 10^5 rads per hour.

High-pressure piping is commonly made by Type 316 stainless steel for operation to 1200 F in conventional systems. Postirradiation examination of the microstructure of the Type 316 stainless steel from the first P&W in-pile loop indicated that, as in unirradiated stainless steel, there was sigma phase formation and some indication of carbide precipitation at the higher temperatures (1300 to 1600 F). At these temperatures there was evidence of intergranular corrosion to a depth of about 2 mils. At temperatures between 1000 F and 1200 F carbide precipitation was noted as it would be in unirradiated material. Although this precipitate would decrease the ductility slightly, P&W examinations showed no corrosion at this temperature, confirming APDA experimental results in flowing sodium at 1000 F. With the existing design conditions at a temperature of 1200 F, it is considered that no difficulties would occur in allowing the loop to operate for 10,000 hours.

Examination of the pump impeller of the loop that operated in the ETR for 200 hours indicated the possibility of some erosion at the "V" section, and it was postulated that this erosion may have been caused by (a) the forming of a hard compound by the intergranular corrosion of the Type 316 stainless steel at elevated temperatures (1300 to 1600 F) and subsequent spalling of this compound, (b) a possible reaction of impurities in the coolant with the fuel cladding, and (c) undetected surface defects in the original material. Examination of the impeller which operated for 700 hours in the ETR indicated that rather than erosion, original machining defects were found. Based on all experimental data from P&W it is concluded that there should be no erosion problem if the fuel is clad with stainless steel and the loop is operated at 1200F.

3.7 STRESS ANALYSIS REQUIREMENTS

A comprehensive stress analysis will be required in the Title I work. Much of the work done by Pratt & Whitney should be applicable to the proposed modifications to the Pratt & Whitney Loops. It is expected that the major stress components will be due to temperature effects as the internal helium pressures can be chosen to minimize the stress components due to pressure. Some difficulty may be experienced in balancing these pressures in Concept I because the preliminary calculation of the secondary coolant pressure drop through the loop is approximately 300 psi for an inlet pressure of 600 psig.

Since the major stresses will be thermal, the stress analysis will require a comprehensive heat transfer analysis. The spiraled pump discharge tubes must be checked to be certain they will accommodate the differential expansion between the hot and cold legs of the NaK circuit. The preliminary work indicates they will be sufficiently flexible for this service. In Concept 2, a temperature difference of 1000 F exists between the primary and secondary coolants where the primary coolant enters the heat exchanger. This temperature difference is divided between two stainless-steel walls and two film resistances. Thus the maximum strain across any one wall is less than 0.004 inch/inch and is acceptable. The acceptable strain of 0.004 inch/inch is based on a conservative extrapolation of strain-fatigue data for Type 304 stainless steel[22]. The discontinuity stresses at junctions between adjacent parts as well as the stresses due to the axial and radial temperature must be accounted for. Thus, a strain fatigue criteria similar to a modified Goodman Diagram must be established based on metal temperatures and expected number of cycles.

4.0 PHYSICS ANALYSIS

4.1 SCOPE

The primary aim of this physics analysis is to determine whether or not a flux environment suitable for testing fast reactor fuel subassemblies can be established in an ATR lobe. The analysis first investigates the utilization of an outer lobe in the ATR as a fast reactor fuel in-pile test loop. The analysis then determines the physics design values that will meet the criteria discussed in Section 2.0. This determination of design values is based on a 7-pin fuel bundle as specified in the conceptual design discussed in Section 4.6.

Since the ATR is nominally a thermal reactor, provisions must be made to keep low-energy neutrons from entering the fast fuel element test sample. This requirement is met through the use of a neutron filter. Nominally, such a filter is in the form of a sleeve containing a high thermal cross-section material, which is located exterior to the test loop, i.e., between the fast test sample and the reactor core (Figure 4.1), and which captures almost all low-energy neutrons and allows the fast neutrons to be transmitted into the fuel sample.

The initial concern of the physics analysis is to determine the power levels attainable within the fast fuel element test sample and the corresponding power depressions* across the sample. These quantities relate directly to the basic feasibility of the test loop for use with fast fuel elements. Some minimum sample power is required and some maximum power depression can be tolerated to obtain useful information from the testing of fast fuel elements in such a loop. Such feasibility criteria are discussed in Section 4.2. In the basic feasibility studies, started before the design criteria were established, a 19-pin fuel bundle was assumed although, as mentioned above, the conceptual design specifies a 7-pin fuel bundle. As far as feasibility is concerned, however, the conclusions reached from the physics analysis of the 19-pin bundle are equally valid for the 7-pin bundle, discussed in Section 4.6.

The effect of the proposed test loop on the rest of the system also has been determined by this analysis. The presence of such a filtered loop will affect the reactivity contribution of the lobe and will affect the power distribution within the core region of the ATR. Further, the high-cross-section neutron filter will generate a large amount of

---

*Power depression is defined at the ratio of maximum-to-minimum power density.

heat. All of the above-mentioned effects have been considered in this analysis.

The power spectrum within the sample and the flux spectra throughout the entire lobe have been determined. Though actually not necessary for a determination of basic feasibility, this information helps present a comprehensive picture of the entire filtered test lobe concept.

Kinetics and static constants relating directly to kinetics have not been analyzed in this preliminary study. The effects of filter and test sample burnup on loop performance are considered in Section 5.0.

The power spectrum within the sample and the flux spectra throughout the entire lobe have been determined. Though actually not necessary for a determination of basic feasibility, this information helps present a comprehensive picture of the entire filtered test lobe concept.

Kinetics and static constants relating directly to kinetics have not been analyzed in this preliminary study. The effects of filter and test sample burnup on loop performance are considered in Section 5.0.

PART I - BASIC FEASIBILITY STUDIES

4.2 FEASIBILITY CRITERIA

Criteria to satisfy basic feasibility will be discussed briefly here since a more detailed discussion is given in Section 2.0. For power levels to be of interest in the testing of advanced-type fast reactor fuel assemblies, they must be about (in the case of pins) 1.7 kw/in. per pin at the central plane. Such a value results from a review of power densities expected in the fast power reactors now existing.

Establishing criteria concerning power shapes across the sample in question is not quite so straightforward. Ideally, the power shape should be almost flat across a fuel assembly and slightly peaked across an individual element so as to correspond to shapes experienced within a fast reactor. Such ideal power distributions are impossible to obtain with any practical system within a non-fast reactor. Therefore, practical limits must be set that will still allow the obtaining of useful information from fuel bundle irradiation in the proposed test loop. For single pins, the upper limit for radial maximum-to-minimum power ratio (referred to as power depression in this study) is set at 1.25. This ratio should not be exceeded for any pin in the bundle. The value, while not ideal, will still allow useful information to be obtained concerning irradiation damage following a test irradiation. The upper limit for acceptable power depression across a bundle has been set at 1.50. Although this value is definitely greater than that found over the equivalent dis-

tance at the core edge of a typical fast reactor (approximately 1.10), it still represents a limit within which useful information may be obtained from irradiation of pin bundles.

The criteria set above are not the result of any physical threshold phenomena; they are simply based on judgment. Neither do they represent design goals; every effort should be made to improve the flux environment so as to surpass the limits set above, particularly in the area of power depression.

4.3 RESULTS OF FEASIBILITY STUDY

4.31 Sample Power and Power Depression

The analysis for determining basic feasibility considers three physical cases described in detail in Appendix A1. Briefly, the cases assume 19-pins, 0.212 inch in diameter, of solid PuO_2 (Pu-239) cooled by liquid sodium in a test loop 1.5 inches in inside diameter. The neutron filter consists of a 1/8-inch ring of boron at a radius of 1.5 inches. The model is pictured schematically in Figure 4.1. The parameter varied among the cases was the number density of B-10 in the filter. Results of these studies in terms of sample power and radial power depression across the entire sample are given in Table 4.1 for both maximum and minimum Pu-239 cross sections in the resolved resonance regions. (Refer to Appendix A2 for a discussion of Pu-239 cross-section options.) Hence, six computational cases are considered. Power levels are normalized so that there is a maximum power density of 2.5 mw/liter in the core.

Examination of Table 4.1 reveals that all the power levels for the cases examined meet the criteria set forth in Section 4.2. In the consideration of power depression, the Pu-239 resonance cross section option becomes important. For the "maximum" and "minimum" options the limiting cases become Case 3 and Case 5, respectively. If the boron concentration for these cases is lowered, the criteria for sample power depressions will not be met. For reasons discussed in Appendix A2, the minimum value option on the Pu-239 cross sections has been chosen as the more appropriate option. Therefore, Case 5 becomes the limiting case. To complete the examination of basic feasibility, power depressions through single pins for this case must be determined. An analysis of single pin power depression is discussed in Section 4.32.

4.32 Single-Pin Power Depression

To determine basic feasibility, the power depression through a single pin in the 19-pin bundle must be determined. Reference

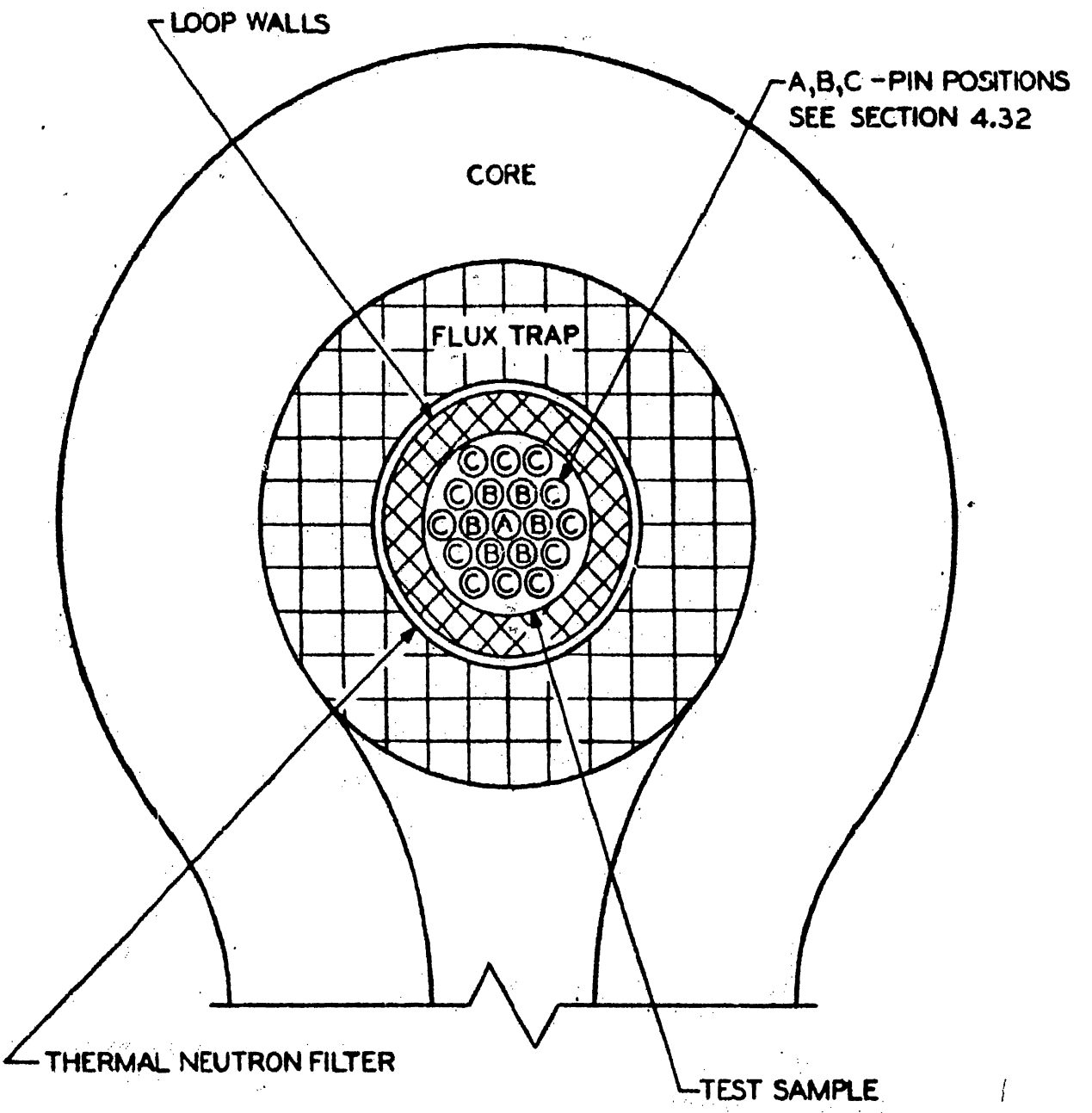

FIG. 4.1
SCHEMATIC DIAGRAM OF ATR OUTER LOBE
FOR FAST REACTOR
FUEL TESTING

TABLE 4.1 - BASIC FEASIBILITY RESULTS 19 HIGH-DENSITY PuO_2 PINS

Case	B-10 Concentration (atoms/$cm^3 \times 10^{-24}$)	Pu-239 Cross Section Option	Sample Power Depression	Central Plane Power for Average Pin(kw/in.)
1	0.00261	maximum	1.91	3.7
2	0.00523	maximum	1.50	3.1
3	0.01046	maximum	1.29	2.6
4	0.00261	minimum	1.72	3.0
5	0.00523	minimum	1.29	2.5
6	0.01046	minimum	1.11	2.2

to Table 4.1 indicates that Case 5 represents a practical limiting case from the point of view of sample power and power depression across the bundle. Lower concentrations of boron in the filter result in too great a power depression across the pin bundle. High concentrations correspondingly decrease the system reactivity and increase engineering problems such as heat transfer and thermal stress. Therefore, the single-pin power depression for Case 5 has been investigated.

Exact analysis of the power depressions through a single pin in a 19-pin bundle is quite complex for the geometry involved. There is lack of symmetry, and the incident flux is highly anisotropic. However, limits on the power depression may be established. These limits are given in Table 4.2 for three types of pin positions (A, B, and C) in a 19-pin bundle. The positions are shown in Figure 4.1.

The maximum and minimum power depression values were obtained in the following manner. To obtain a minimum value, each pin was considered to be isolated and located in an infinite medium of isotropic flux. If the problem is now treated as a transmission problem, the attenuation of a given flux may be determined. This determination was made for each of the 16 group fluxes resulting from the multigroup computation, and the resulting power distribution was determined. The incident spectrum is assumed to be that resulting from the multigroup computation of the homogeneous sample taken in the vicinity of the pin in question. Now, the actual incident flux for pins B and C (Figure 4.1) is quite nonuniform; the incident flux on the side of the pin toward the center of the lobe is severly reduced. Therefore, the previous determination of power distribution will underestimate the power density variation. Hence, the resulting power depressions for pins B and C will be considered minimum. For position A the incident flux is uniform around the pin so that the resulting value should be farily good and hence, cannot be assumed to be a minimum. Unity, therefore, is taken at the minimum for power depression in pin type A.

The maximum values are based on simple exponential attenuation of the group fluxes using the same source of incident spectrum mentioned above. The straight line attenuation distance for pins B and C is taken as the mean chord length (twice the thickness) of a slab the thickness of which is equal to the diameter of the pin. For pin A the thickness of the slab is taken as the radius of the pin. The power depressions resulting from such flux attenuation will represent an extreme upper limit.

Examination of the single pin power depression results of Table 4.2 indicate that pin C has a marginal value; i.e., the limit set in the basic feasibility criteria lies between the minimum and maximum values given. Power depression values for the other pins are quite acceptable. Since the other criteria of power level and bundle power depression have been met, Case 5 will be accepted as a limiting case for solid PuO_2 pins.

TABLE 4.2 - SINGLE-PIN RADIAL POWER DEPRESSIONS IN A 19-PIN BUNDLE *

(B-10 number density in filter = 0.00523×10^{24} atoms/cm^3)

Position **	Maximum	Minimum
A	1.12	1.00
B	1.25	1.04
C	1.49	1.14

* Power depression is defined as the ratio of maximum-to-minimum power density.

** Position letter refers to Figure 4.1.

4.33 Conclusions Regarding Basic Feasibility

The criteria for basic feasibility have been met. In particular, Case 5 represents a limiting case for these criteria. The addition of more boron to the filter will, of course, improve the power density distribution, but will decrease the power output. For the 19-pin configuration considered here, extrapolation of the results of Table 4.1 indicate that the upper limit of B-10 concentration (i.e., to give average pin power of 1.7 kw/in.) is greater than 0.0105×10^{24} atoms/cm^3. However, since minimizing the amount of boron also minimizes other design problems associated with both the lobe and total reactor, Case 5 will be taken as the reference.

Since, for Case 5 there appears to be a fairly good power margin (2.5 kw/in. compared to a minimum design objective of 1.7 kw/in.,) it is possible that oxide pins diluted with fertile material may be used and still meet the basic feasibility requirements. This possibility with accompanying analysis is presented in Section 4.42.

Sample power spectra resulting from the use of various B-10 concentrations (including no B-10) in the basic feasibility model are plotted in Figures 4.2 through 4.5. A typical fast power spectrum (dotted line) is included for comparison. The suppression of the power contributions in the low energy groups as the B-10 concentration increases is quite evident. The flux spectrum at sample edge for one B-10 concentration (reference case) is given in Figure 4.6. Comparison of this spectrum with the corresponding power spectrum (Figure 4.4) reveals that the relatively small low energy tail of the flux spectrum is responsible for a great deal of the edge power. It is this power component that is responsible for the sample power depressions. Examination of the power spectrum for the reference case at the center of the sample (Figure 4.7) will disclose the reduction in the low energy power component as compared to the edge power spectrum (Figure 4.4). If sufficient power can be obtained, the outer sample fuel used in the sense of a filter could produce very attractive fast spectra for small fuel bundles located at the center of the loop. Based on the sample powers achieved thus far, such a scheme would appear quite plausible. (Sufficient heat removal capacity for the loop is assumed.)

A multigroup flux distribution (reduced to eight groups) across the cylindrical model of the lobe is given in Figure 4.8 for the reference case. Note the negligible effect of the filter on all but flux groups 6 through 8.

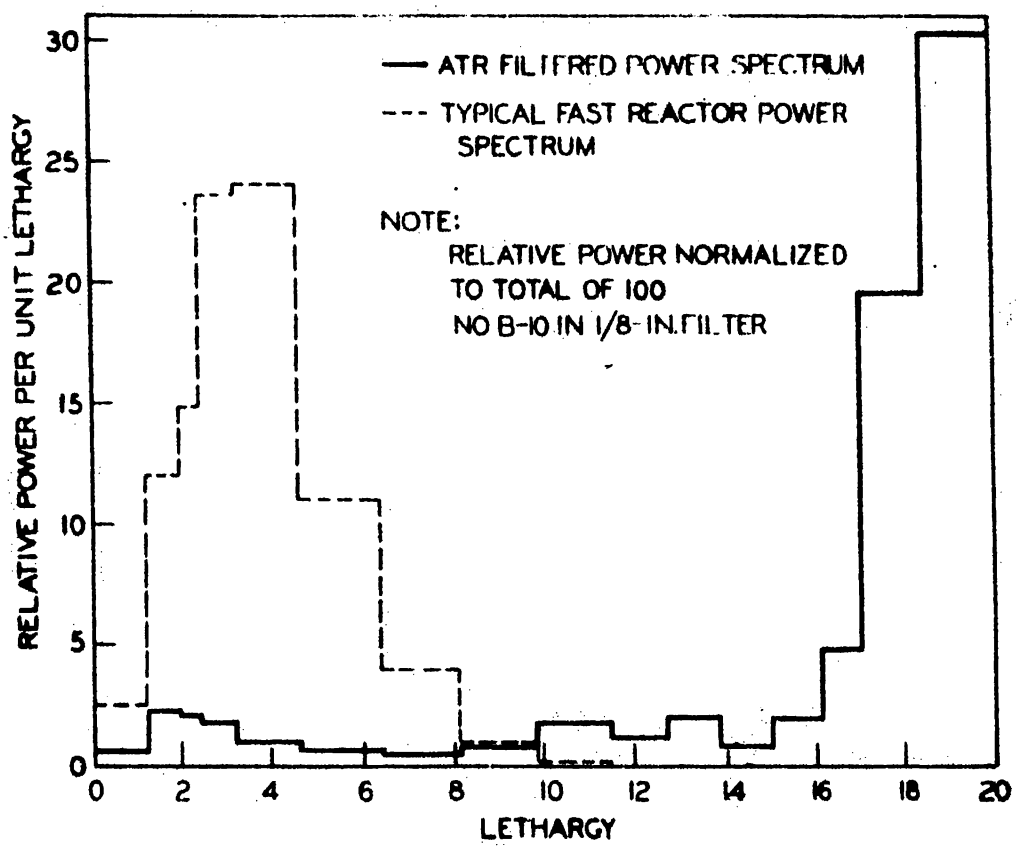

FIG. 4.2
POWER SPECTRUM AT OUTER EDGE
OF 19-PIN PuO_2 BUNDLE

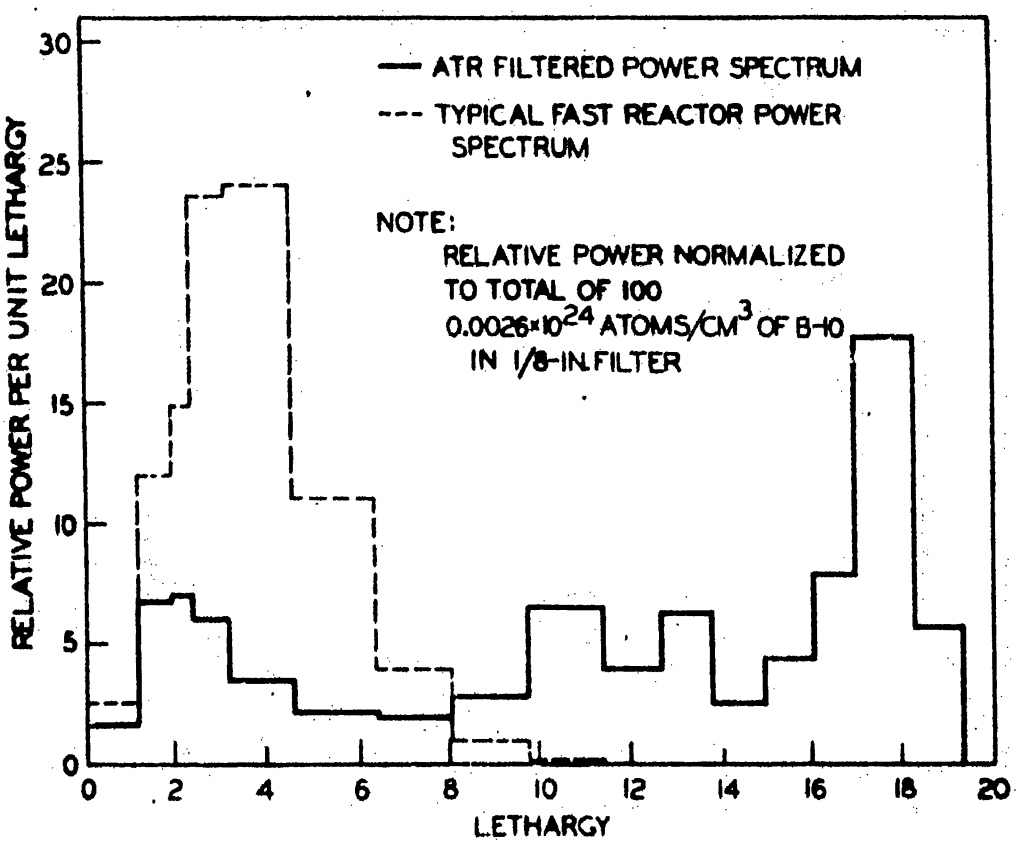

FIG. 4.3
POWER SPECTRUM AT OUTER EDGE
OF 19-PIN PuO_2 BUNDLE

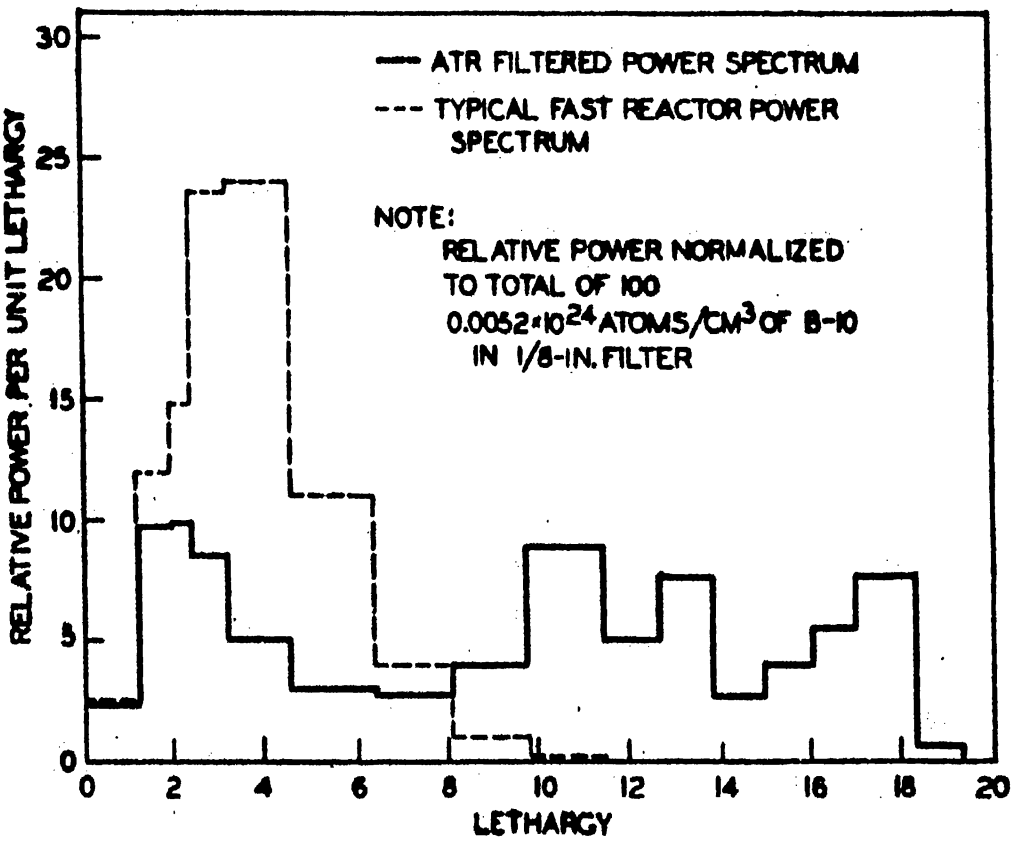

FIG. 4.4
POWER SPECTRUM AT OUTER EDGE OF 19-PIN PuO_2 BUNDLE

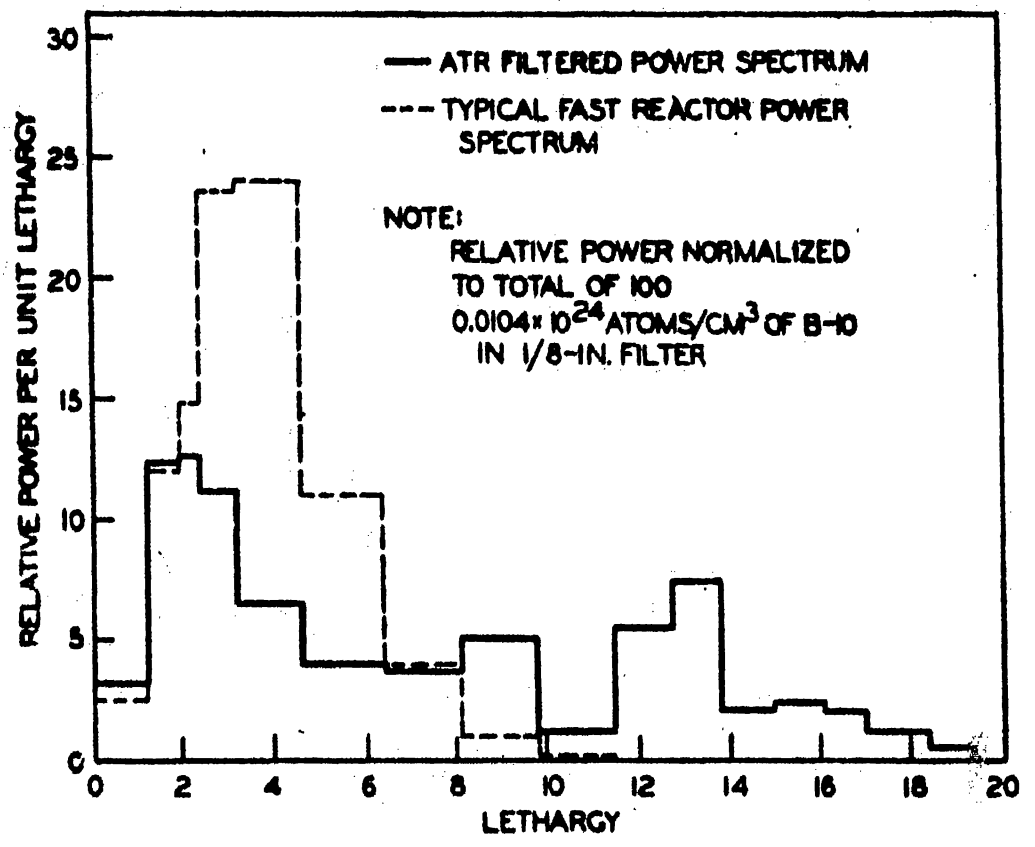

FIG. 4.5
POWER SPECTRUM AT OUTER EDGE OF 19-PIN PuO_2 BUNDLE

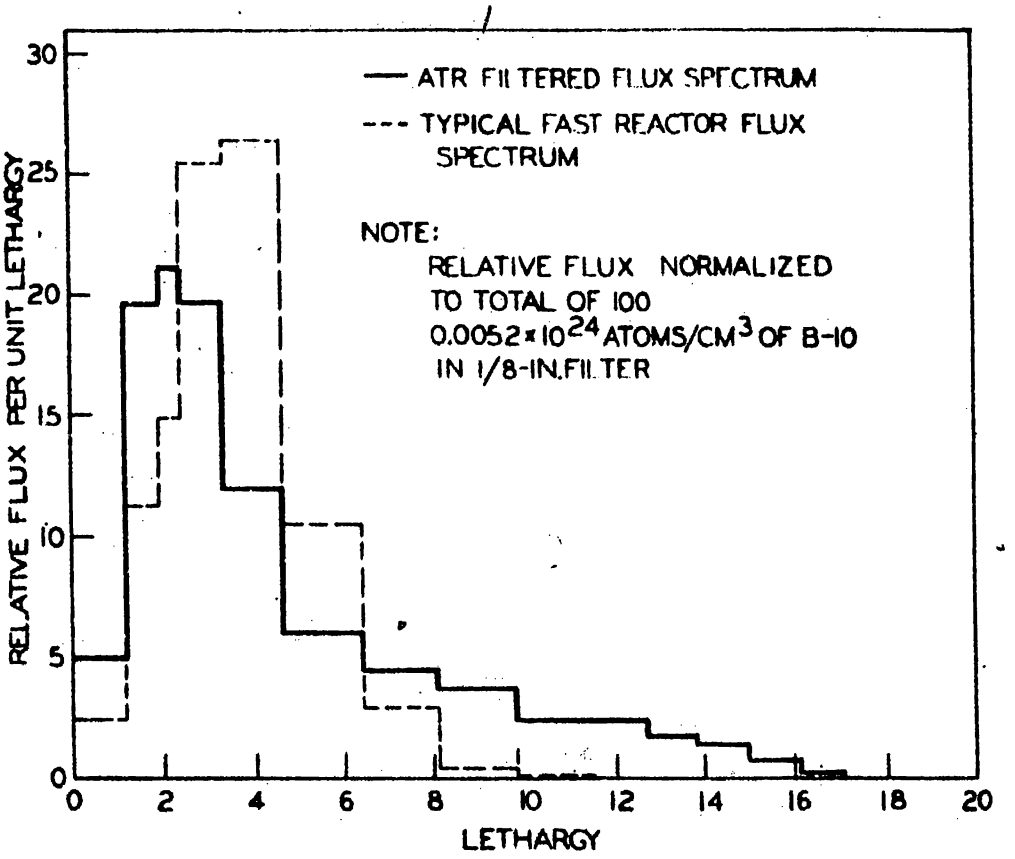

FIG. 4.6
FLUX SPECTRUM AT OUTER EDGE
OF 19-PIN PuO_2 BUNDLE

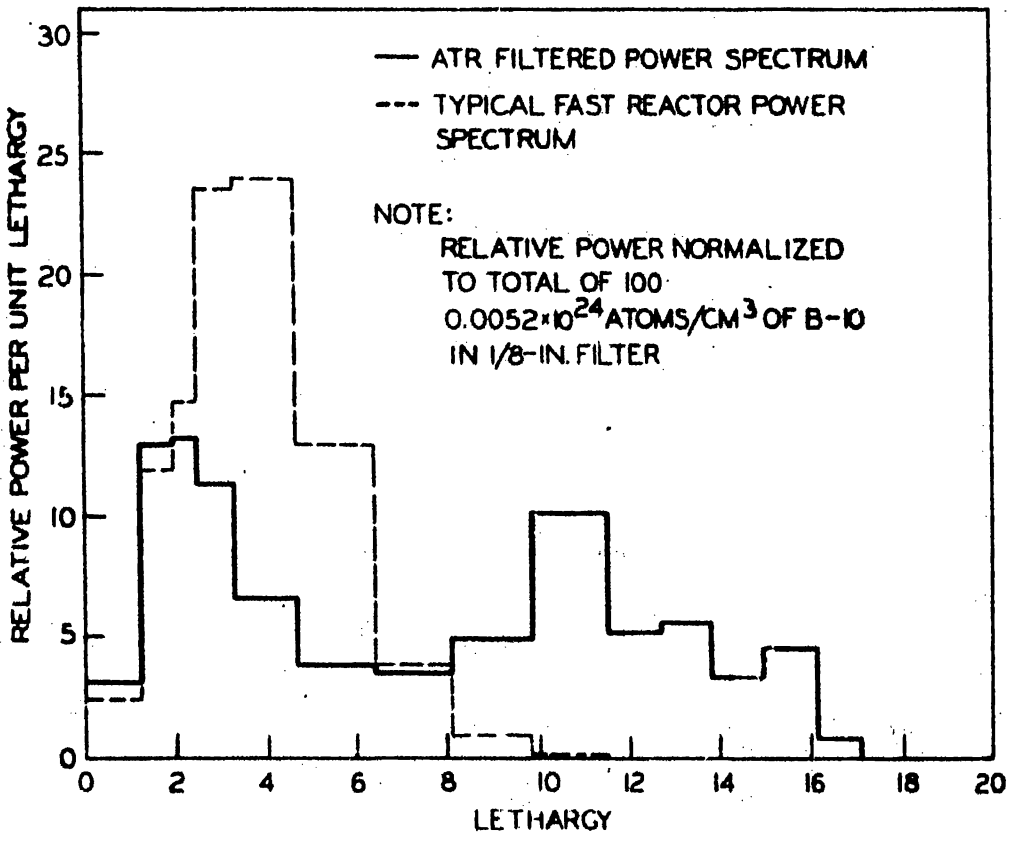

FIG. 4.7
POWER SPECTRUM AT CENTER OF
19-PIN PuO_2 BUNDLE

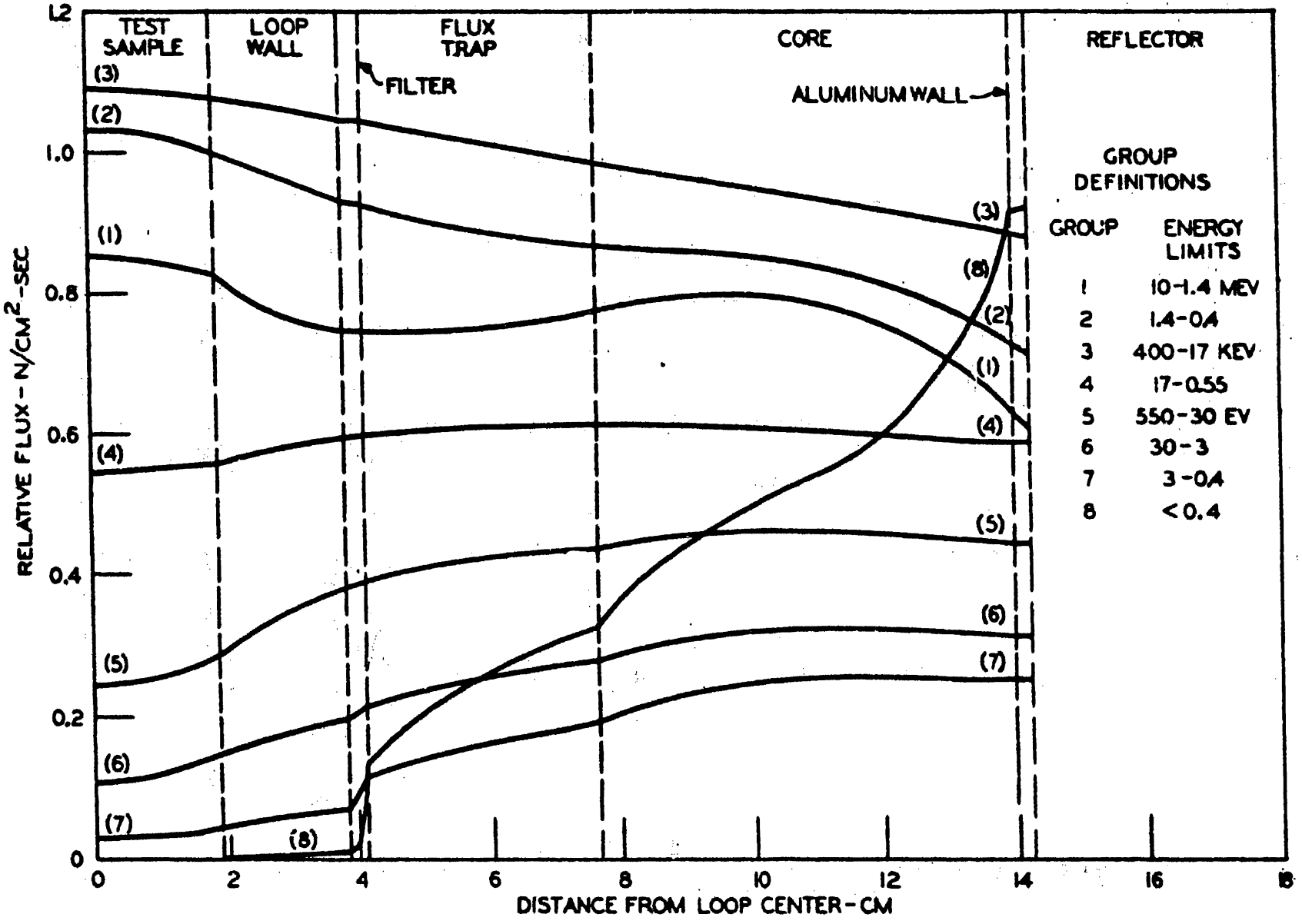

FIG. 4.8
ATR LOBE FLUX DISTRIBUTION

It should be noted that the satisfying of the basic feasibility criteria does not necessarily mean that all the design requirements of the loop and reactor have been met. The introduction of boron raises many design problems, particularly in the realm of heat transfer and lobe reactivity. The satisfying of the basic feasibility criteria with the model used establishes what might be called a feasibility potential. Any design alterations which clearly enhance the basic feasibility may proceed without the re-examination of such basic feasibility. Those necessary alterations that clearly detract from basic feasibility will be closely examined and compensated for if necessary. Such necessary design alterations are discussed in later sections.

Uncertainties involved in the analysis presented thus far are difficult to determine in a preliminary study. The validity of diffusion theory for certain portions of the problem is questionable. Determination of the proper cross sections is also difficult. However, a brief analysis of uncertainty and the philosophy regarding it is discussed in Appendix A5.

4.4 RESULTS OF BASIC FEASIBILITY DESIGN PERTURBATIONS

As mentioned earlier, engineering design considerations may necessitate some deviation from the model chosen for the basic feasibility study. Two such deviations are considered here. The first is the addition of a 1/16-inch cooling water annulus interior to the filter; the second is dilution of the sample enrichment. The effects of such changes are determined.

Due to reactivity considerations, further modifications have been made. However, because of the basic nature of the reactivity problem, it and the resulting design changes are considered in a separate section (Section 4.5).

4.41 Effect of Interior Moderator

To achieve the most desirable flux spectrum within the sample, it is necessary to keep moderating material between the filter and the sample at a minimum. Such an interior moderator reduces the magnitude of the desired high-energy flux and increases the level of the unwanted low-energy flux. Cases 1 through 6 considered in the basic feasibility study contain only sodium and stainless steel in such an interior position. However, because of the farily large amount of heat generated within the boron filter used in these cases, it will be necessary to provide some cooling on the inside surface. If, because of mechanical and heat transfer considerations, it is necessary to use water as the coolant, the deleterious effect described above

is introduced. Such a water gap is incorporated in the conceptual design for the neutron filter described in Section 5.0. Therefore, an estimate of the spectrum softening due to the addition of water has been made for the 19-pin samples used in the basic feasibility study.

A 1/16-inch cooling annulus on the interior surface of the filter is necessary if water is to be used as the coolant. A multi-group problem (Case 7) has been run with such a water gap replacing a portion of the tube wall adjacent to the filter. The remainder of the problem is identical to the reference problem, Case 5. The results of the addition of this interior moderator are given in Table 4.3.

It can be seen that the effect on power depression of this small amount of moderator is quite severe. This severity is due to the fact that a large portion of the sample power is caused by the large resolved absorption resonances in plutonium. Hence, small changes in spectrum cause rather large changes in reaction rates. In fact, a large portion of the additional power depression is due to the increased absorption rate in the single large resonance at 0.297 ev. The total sample power increase due to the water annulus is quite small, however, since the increased reaction rates are an edge effect and hence occur over only a small portion of the sample volume. Note the effect of the Group 15 contribution as given in Table A7 (Appendix A2) for Case 5 (No water annulus) and Case 7 (1/16-inch water annulus).

The increased depression factor problem discussed above may be alleviated by one of two basic courses of action. The first is to remove the problem by using a nonmoderator-type coolant; the expected power depression will then be that indicated in Table 4.1.

The second is to increase the effectiveness of the filter. An obvious step in this direction is to increase the boron concentration. For example, increasing the B-10 concentration by 50% gives power depressions almost idential with those of the reference case (Case 5). The results are included in Table 4.5 in the section dealing with the extended core concept (Section 4.54).

An additional method of increasing the effectiveness of the filter is to use a more effective poison than boron. The possibilities of such a filter are discussed in Appendix A4.

4.42 Effect of Sample Dilution

All the 19-pin cases analyzed have assumed 100% enriched PuO_2 fuel. Fuels of most interest for fast power reactors will be diluted by some fertile material, e.g., U-238. Such dilution for samples in the fast ATR loop appears feasible since the pin powers for fully enriched material are quite high. The effects of dilution on power performance of PuO_2 fuel in a 19-pin bundle are given in Table 4.4. Here results for 100% PuO_2 are compared with those for 50% enriched PuO_2 with U-238 as the diluent. As expected, the sample power is almost proportional to enrichment since only a very small power contribution is made by the diluent. Unfortunately, power depression is not decreased very greatly by dilution.

Additional samples of the effect of U-238 dilution for 7-pin bundles with both U-235 and Pu-239 as the fissionable material are included in Table 4.6 (Section 4.61).

4.5 LOBE REACTIVITY

Basic feasibility criteria have been established by assuming a maximum allowable power density in the core based on heat transfer considerations. As yet, no specific mention has been made of lobe reactivity corresponding to the various configurations discussed thus far. Since the power balance among the various ATR lobes is quite sensitive to the relative reactivity among the lobes, it is necessary to discuss the question of lobe reactivity as it pertains to the fast test lobe.

Specific computation of reactivity for the entire reactor for the various configurations considered is beyond the scope of this analysis. However, since optimum power balance is obviously attained when lobe reactivities are equal, it will be necessary only to establish a suitable standard reactivity in one lobe and compare reactivity values for single-lobe configurations of interest to this reference value. The standard value is based on what is taken to be the typical thermal flux experiment found in the lobes other than the fast test lobe in question. Geometric and material specifications for this typical experiment are taken to be identical to those presented on pages 3 and 4 of "Single-Lobe Be-Reflected Reference Core" (21). This case will be named "reactivity standard" and designated as Case 8. An effective multiplication factor for the reactivity standard was computed by the multigroup code AIM 6 to be 1.026.

Any lobe configuration with an identical value of effective multiplication is assumed to present no initial power balance problem, and hence it is further assumed that the maximum core power density of 2.5 mw/liter is attainable. Deviations from this value are expected to affect the initial lobe power in a manner consistent with the values given in Table 3.5A of Ref. (8).

TABLE 4.3 EFFECT OF INTERIOR MODERATOR

(1/16-inch Cooling Water Annulus)

Case	Description	B-10 Concentration (atoms/cm^3 x 10^{-24}	Sample Power Depression	Central Plane Power for Average Pin
5	no water	0.00523	1.29	2.5
7	water	0.00523	1.43	2.6

TABLE 4.4 - EFFECT OF SAMPLE DILUTION BY U-238

(19-Pin PuO_2 Sample Fuel)

Case	Fuel Enrichment (%)	Central Plane Power Average Pin (kw/in.)	Power Depression
7	100	2.60	1.43
12	50	1.38	1.12

Consideration should be given in the Title I effort to the problem of lobe reactivity as a function of time. Here, too, the standard situation is taken to be the time dependence of reactivity implicit in the configuration chosen as the reactivity standard.

Lobe reactivity for various fast lobe configurations is discussed below in the framework of the philosophy outlined above.

4.51 Basic Feasibility Cases

The effective multiplication of the basic feasibility cases (Cases 1 through 6) are much lower than the reactivity standard. The reference case (Case 5) and its counterpart with the cooling water annulus (Case 7) possess effective multiplication factors lower than the standard value by approximately 5%. Note that this reduction applies only to the particular lobe and not to the reactor. This would correspond to approximately a 35% drop in initial lobe power and hence would not permit satisfactory operation.

Two basic alternatives would tend to relieve this reactivity deficit. The first is to change the nature of the filter so that it becomes less of a system poison. The second is to accept the reactivity loss as an intrinsic feature of the lobe and adjust the core composition or geometry to compensate for the loss. Such adjustment must remain within the outside dimensions set for the core, must have a negligible effect on reactor operation, and must not introduce severe engineering problems. These core alterations are discussed in Sections 4.53 and 4.54.

4.52 Converter Plate

One approach to altering the filter would be to select a poison (other than B-10) that would have the desirable effect on the sample spectrum and yet have less effect on lobe reactivity. Possibly cadmium would produce results that would tend toward this goal; a brief discussion of its use is contained in Section A4. However, it is quite doubtful that any method that relied solely on poison could satisfy the basic feasibility criteria and at the same time allow suitable lobe reactivities.

To solve the reactivity problem by revision of the filter alone necessitates the incorporation of a converter plate consisting of a rather large concentration of fissionable material, e.g., U-235. Complete replacement of B-10 with U-235 is not feasible because of the high heat generation accompanying the necessary U-235. Hence, a combination of converter plate and poison is

required to produce the desired effect. A preliminary investigation has indicated that there may still be heat generation problems connected with the use of a high-density converter plate.

A moderator-type coolant would probably have to be used interior to the plate so that the converter plate with coolant would become more of a source of additional thermal neutrons rather than fast neutrons. Hence, the major portion of the thermal neutron filtering must still be done by a pure poison. This idea carried to the extreme becomes the basis of the extended core concept discussed in Section 4.54. While a converter plate system (in the normal sense) has not been proven unfeasible, the extended core concept appears more attractive.

4.53 Deletion of Core Poison

An obvious way to achieve a boost in initial reactivity is to delete the burnable poison from the core. The result of removing all poison from the core of Case 7 has been analyzed. It is found that the initial reactivity increases by 7% and hence adequately makes up for the 5% deficit discussed in Section 4.51. The burnable poison effect is now left entirely up to the burnout of the B-10 in the filter. The initial total reactivity worth of the filter (approximately 12%) is greater than that of the burnable poison in the core. However, both the thermal flux and reactivity worth per B-10 atom is significantly less for the filter than for the core. Correspondingly, the rate of change of reactivity with time due to B-10 in the filter is much less than for B-10 in the core. Therefore, complete removal of B-10 from the core cannot be compensated by B-10 in the filter because of its ineffectiveness as a burnable poison.

The effect of removing only a portion of the burnable poison from the core may be of some advantage. However, the necessary analysis must be made in conjunction with the control system for the entire reactor.

4.54 Extended Core Concept

The most attractive way of achieving sufficient reactivity and maintaining suitable sample power is through the use of an extended core. The entire flux trap region, with the exception of an aluminum wall at the inside of the nominal core, is replaced by core-type fuel plates with an associated water coolant. Burnable poison is maintained in this extended core region. The resulting multiplication factors, as well as sample powers and power depression, are given in Table 4.5 for various fuel

TABLE 4.5 - EFFECT OF EXTENDED CORE

Case	Extended Core Fuel Concentration (fraction of core value)	Filter B-10 Concentration (atoms/cm^3 x 10^{-24})	Effective Multiplication	Sample Power Depression	Central Plane Power-Average Pin (kw/in.)	Radial Maximum to Average Core Power Density
7	(No extended core)	0.00523	0.975	1.43	2.60	1.72
8	0.33	0.00523	1.010	1.42	2.48	1.63
9	0.67	0.00523	1.029	1.41	2.54	1.64
10	1.0	0.00523	1.043	1.39	2.56	1.65
11	1.0	0.00693	1.034	1.28	2.42	1.66

concentrations in the extended core. Results for Case 7 (no extended core) are included to aid in interpretation of the results. All cases presented include the 1/16-inch water annulus interior to the boron.

Several pertinent observations should be made from the results presented in Table 4.5. First, note that fuel concentrations in the extended core equal to less than 0.67 of that used in the nominal core, and using the reference concentration of B-10, yield reactivity values greater than the standard value of 1.026. Further, the reactivity is maintained above the standard when the B-10 concentration in the filter is increased over 30% by using a fuel concentration in the extended core equal to that in the normal core (Case 11). Such a concentration of B-10 results in sample power behavior almost identical to the reference case (Case 5). It is interesting to note that the presence of an extended core has little effect on sample performance. The extended core also leads to more favorable maximum-to-average core power densities. The values appear quite insensitive to extended core fuel concentrations. Further, it appears that the presence of an extended core tends to decouple the core fluxes from the effects of the B-10 filter so that the core maximum-to-average power density ratio changes little with B-10 loading (Refer to Cases 10 and 11).

4.55 Minimum Length Filters

All analyses regarding the effect of the B-10 filter on reactivity has assumed a filter extending the entire length of the core, i.e., 48 inches. However, it is very probable that test samples will be shorter than this length. Hence, it would be necessary that the filter be only slightly longer than the sample. The corresponding effect on reactivity of such a shortened filter would then be less than that for the full-length filter. However, rather than base a conceptual design on such a shortened filter, it is preferred to keep this source of reactivity gain as margin.

4.56 Conclusions Regarding Lobe Reactivity

Sufficient values of lobe reactivity may be established by the use of an extended core. The necessary fuel concentrations are easily obtainable, since they do not exceed those of the nominal core. No heat transfer problems should occur in the extended core since the cooling annuli of the same thickness as in the nominal core are used, and since the power densities at every point are lower than the minimum value in the nominal core. Power depressions in both the core and the extended core

are quite acceptable. The important relation between sample power depression and sample power that establishes basic feasibility is not affected by the extended core.

In view of the above, the fast test lobe should pose no power balance problem because of a reactivity deficit. Hence, a maximum power density in the core of 2.5 mw/liter is attainable if an extended core is used. Sample powers that were normalized to this power density are realizable values. Power depressions corresponding to a given sample power as presented in the basic feasibility study apply also in the case of the extended core concept.

PART II - REFERENCE FUEL SPECIMEN DESIGN

4.6 REFERENCE FUEL SPECIMEN

4.61 Physics Design Values

This part of the analysis is concerned with determining the physics design values for the fuel specimen that will meet the criteria specified in Section 2.0. The detailed specifications for the reference design physics calculations are given in Tables A5 and A6 of Appendix A3. The calculations are similar to those used in Part I of this section but incorporating the following revisions.

The sample loop inside diameter (now accommodating 7 fuel pins of diameter 0.236-inches) is reduced to 1.2-inches; the tube wall composition is altered slightly; a 1/16-inch water gap interior to the neutron filter has been included for cooling purposes; the neutron filter is taken as boron steel with thickness increased to 0.15-inches; the flux trap has been replaced by an extended core idential in composition to the nominal core in order to enhance the effective multiplication of the lobe; the inner aluminum wall of the core has been included as a separate region. Varying enrichments of PuO_2 and UO_2 have been considered as sample fuels. Detailed values of region radii and material concentrations also are given in Appendix A3.

Concentrations of B-10 in the filter and of fuel in the extended core have been based on the results of the basic feasibility study (Section 4.3) and on the results of the additional parametric analysis of this report. Varying enrichments of PuO_2 and UO_2 have been considered as sample fuels. Since there is no severe resonance in U-235 that corresponds to the 0.297 ev resonance in Pu-239, comparable power depressions may be obtained in U-235 with less B-10 concentration in the filter. The resulting lobe characteristics for a range of enrichments are presented in Table 4.6. Design values for both a PuO_2 and a UO_2 sample are given in Table 4.7.

The non-design values of Table 4.6 themselves are quite important since they illustrate the sensitivity of various lobe characteristics to a design parameter over which the experimenter has some control, i.e., sample enrichment. The effect on design sample performance of possible alternatives in lobe design may be partially compensated for by alteration of the sample enrichment.

4.62 Reactivity Worth of Specimen

The effect on lobe reactivity of completely removing a 48-inch-long 7-pin bundle from the tube has been computed. For 100%-enriched PuO_2 or UO_2 pins (Cases 12 or 15, respectively) such removal results in a reactivity decrease of 1%. Pins of lower enrichment have correspondingly less effect, as indicated by the effective multiplication values given in Table 4.6. Obviously, if the sample length is less than that of the full core (e.g., 18 inches as specified in the loop conceptual design), the reactivity contribution is reduced still further. No analysis has been performed concerning the worth of shortened samples.

TABLE 4.6 - LOBE CHARACTERISTICS FOR 7-PIN FUEL BUNDLE

Case	Filter B-10 Concentration (atoms/cm^3 x 10^{-24})	Sample Composition *	Lobe Reactivity **	Central Plane Power for Average Pin (kw/in.)	Maximum Pin Power Density (kw/cm^3 of fuel)	Maximum/Minimum Sample Power Depression
12	0.0052	100% PuO_2	1.028	3.09	5.24	1.32
13	0.0052	75% PuO_2	1.026	2.42	4.08	1.32
14	0.0052	25% PuO_2	1.021	0.96	1.55	1.27
15	0.0052	100% UO_2	1.026	3.74	5.69	1.22
16	0.0052	75% UO_2	1.024	2.99	4.48	1.19
17	0.0052	25% UO_2	1.020	1.23	1.77	1.10

Quantities Insensitive to Sample Enrichment

Lobe Core Power (1/5 of Reactor)	56 mw
Extended Core Power	160 kw/in.
Radial Maximum to Average Core Power	1.66
Average Central Sample Flux	1.8 x 10^{15} neutrons/cm^2-sec

* Percentage values refer to enrichment. Diluent is U-238.

** Reactivity for other lobes is assumed to be 1.026. (See Section 4.5.)

TABLE 4.7 - REFERENCE DESIGN VALUES FOR 7-PIN FUEL BUNDLE

(Sample Power Fixed at 150 kw)

Fuel Type	Enrichment (%)	Lobe Reactivity	Central Plane Power For Average Pin (kw/in.)	Maximum Pin Power Density (kw/cm^3 of fuel)	Sample Power Depression
PuO_2	47.5	1.024	1.67	2.69	1.29
UO_2	34.5	1.021	1.67	2.30	1.12

5.0 THERMAL NEUTRON FILTER

5.1 GENERAL REQUIREMENTS

The thermal neutron filter provides a neutron spectrum similar to that available in a fast reactor. The filter is designed to absorb the low-energy (thermal) neutrons before they reach the test specimen. Since the neutron absorption rate varies inversely with the neutron energy, the filter will be nearly opaque to low-energy neutrons and transparent to high-energy neutrons.

The design and fabrication requirements for the filter are stringent. The filter must be uniform in dimensions, and the material must be homogeneous and free of cracks and voids. If the filter contained a region transparent to thermal neutrons, these low-energy neutrons would stream through the filter and cause unacceptable local overheating of the test specimens.

5.2 FILTER DESIGN

5.21 Reference Design

A conceptual design of the thermal neutron filter, intended for use with loop Concept 1 (Section 3.32), is shown in Figure 5.1. This design is for a separate filter that is not attached to either the loop or the extended core. A similar arrangement would be used with loop Concept 2.

The filter consists of a single, hollow cylinder of a boron-stainless steel alloy. This cylinder, 3.3 inches in outside diameter by 0.15 inches thick, extends the full length of the ATR core. Flow passages, to provide adequate cooling of the filter by ATR coolant, are supplied at both ends of the filter. The loop water jacket mates with the top of the thermal neutron filter so that water flow is maintained by the pressure difference across the ATR core.

In the design shown in Figure 5.1, the bottom of the loop rests in a hole in the ATR core support plate. The lower end of the filter rests on the ATR core support plate. A spring, attached to the outside of the loop above the filter, pushes the cone-shaped retaining ring into the fitting on the top of the filter to restrain

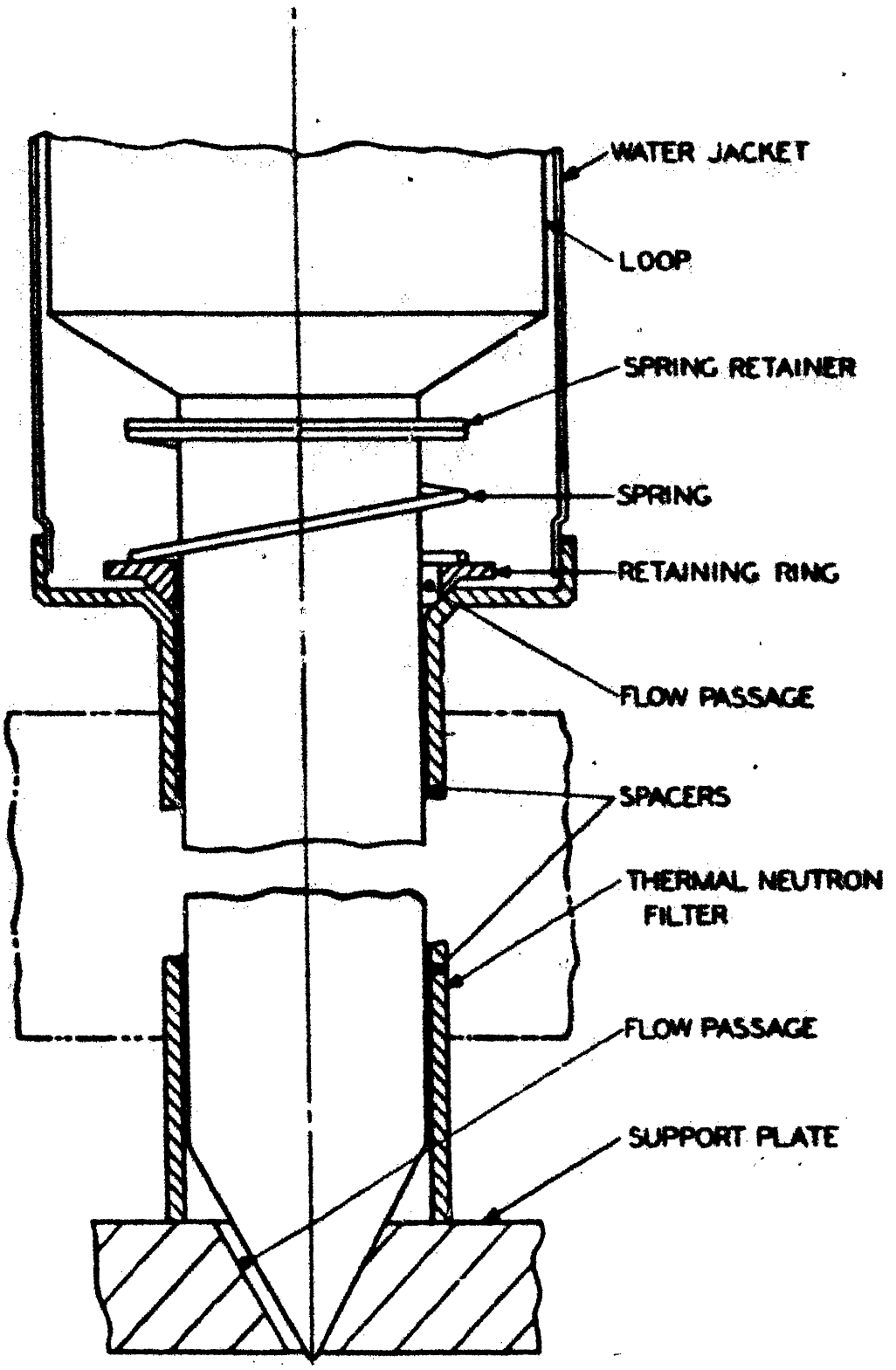

FIG. 5.1
THERMAL NEUTRON FILTER ASSEMBLY

this end of the filter. The retaining ring is attached to the spring to prevent loss of the ring.

5.22 Location of Filter

The filter shown in Figure 5.1 is located outside the loop. Locating the filter inside the loop was considered but rejected for the following reasons:

1. The heat generated in the filter must be removed through the loop heat exchanger. Because of the limited capacity of the heat exchanger, this additional heat load will reduce the allowable test specimen power.

2. The higher operating temperature will reduce the life of the filter.

3. Additional modifications to the loop are required.

4. The filter cannot be replaced easily.

5. Thermal transients may cause excessive stresses in the filter.

Locating the filter outside the loop eliminates these problems but introduces a new one. Since the filter and the outer wall of the loop must be cooled, ATR coolant must be allowed to flow between the loop and the filter. Introduction of this thin annulus of moderator between the filter and the test specimens produces considerable effect on the neutron spectrum that is incident on the test specimens. The water annulus must be of uniform width to prevent unacceptable maldistribution of the test specimen power densities. Uneven heat generation in the filter may cause the filter to bow and, thereby, reduce the annulus width. In addition, local reductions in the width of the annulus may affect the heat transfer coefficients and may cause hot spots. To maintain uniform annulus width, it may be necessary to attach the filter to either the loop or the extended core, or to insert spacers between the filter and the loop.

5.23 Choice of Filter Material

The reference filter is composed of an alloy of boron and austenitic stainless steel and has a B-10 concentration of 0.0052×10^{24} atoms per cubic centimeter of alloy. This concentration is equivalent to a loading of 1.2 w/o boron in a 93% enriched alloy of

boron and stainless steel. The filter alloy will be clad with stainless steel, or plated with some other suitable material to prevent excessive corrosion in water after an appreciable amount of burnup. If plating is used, careful selection and control of the method of plating will be required to insure a good bond between the filter alloy and the plated material. The fittings at the ends of the filter will be austenitic stainless steel.

Boron was selected for the following reasons:

1. The absorption cross-section of boron is inversely proportional to neutron energy, thereby fulfilling the functional requirement.

2. The cross-section curve does not have any resonances, precluding a possible source of difficulty and uncertainty in calculation.

3. Boron alloys have been fabricated and applied in a range of sizes, shapes, compositions, and isotopic enrichments, thus minimizing development and procurement problems.

The selection of the means of utilizing boron as a filter material was, in part, a process of elimination. All ceramics were rejected on the basis of possible void formation during operation: fused ceramics, because of cracking; and powdered ceramics, because of thermal- or vibration-initiated redistribution. From the several cermet and alloy materials considered, borated stainless steel was selected. Boron carbide-stainless steel cermets appear at least as good as borated stainless steel, but less information on B_4C-SS is available.

5.3 METALLURGICAL DESIGN BASIS

5.31 Allowable Stress

In the unirradiated condition the alloy of boron and stainless steel is sufficiently ductile to permit the use of normal forming and machining procedures.

After an appreciable amount of burnup takes place, the boron-stainless steel alloy becomes very brittle at irradiation temperatures of less than 450 F. Therefore, to preclude the possibility of cracking because of stresses during irradiation, the filter will be designed so that all deformation will be in the elastic range and so that the maximum allowable stress will be 25,000 psi. This amount

of stress is well within the allowable range as determined from post irradiation tensile tests on irradiated material of approximately the same composition as the filter.

5.32 Allowable Burnup

To establish the allowable burnup for the filter, all irradiation burnup data were converted to boron atoms burned per cubic centimeter of alloy. The conversion of boron atoms burned per cubic centimeter (helium atoms formed) of alloy is similar to the approach taken in APDA-133 [9]. Allowable burnup is assumed to be dependent on the gas pressure developed per unit volume of alloy. The allowable burnup at different alloy temperatures for 1 w/o boron in stainless steel is shown in Figure 5.2. It is considered that this curve may be used to establish the allowable burnup in the reference filter even though the boron concentration of the filter is 1.2 w/o.

The right-hand scale of Figure 5.2 is obtained by dividing the left-hand scale by the reference design B-10 concentration (52×10^{20} atoms per cubic centimeter of alloy). For the maximum filter temperature of 310 F, the maximum allowable burnup is 20%. (See Section 5.5 for determination of filter temperature). Since the left-hand scale is divided by the B-10 concentration to obtain the right-hand scale, reducing the B-10 concentration in the alloy will increase the allowable burnup per cent for the same allowable burnup in atoms per cubic centimeter. Thus, reducing the boron concentration by one-half doubles the allowable percentage of burnup.

The allowable burnup for temperatures less than 450 F was derived from irradiation data published in Nuclear Science and Engineering. [10]

Since irradiation data are not available for boron stainless steel (B-SS) alloys at temperatures greater than 450 F, it was necessary to obtain the data indirectly. The boron in B-SS alloys has negligible solid solubility in iron. Boron compounds are formed with other elements in stainless steel, and the result is that the alloy is essentially a cermet, although the particle size and distribution is not ideal. Assuming that this alloy does act as a cermet, it is possible to convert the high temperature data (above 800 F) for uranium oxide - stainless steel (UO_2-SS) dispersions presented in APDA-133 [9] to B-SS alloys. Since four times as many gas atoms are formed for each boron atom burned as are formed for each fission event, the average fissions per cubic centimeter curve derived from irradiation data of UO_2-SS was divided by four to arrive at about the same gas pressure per

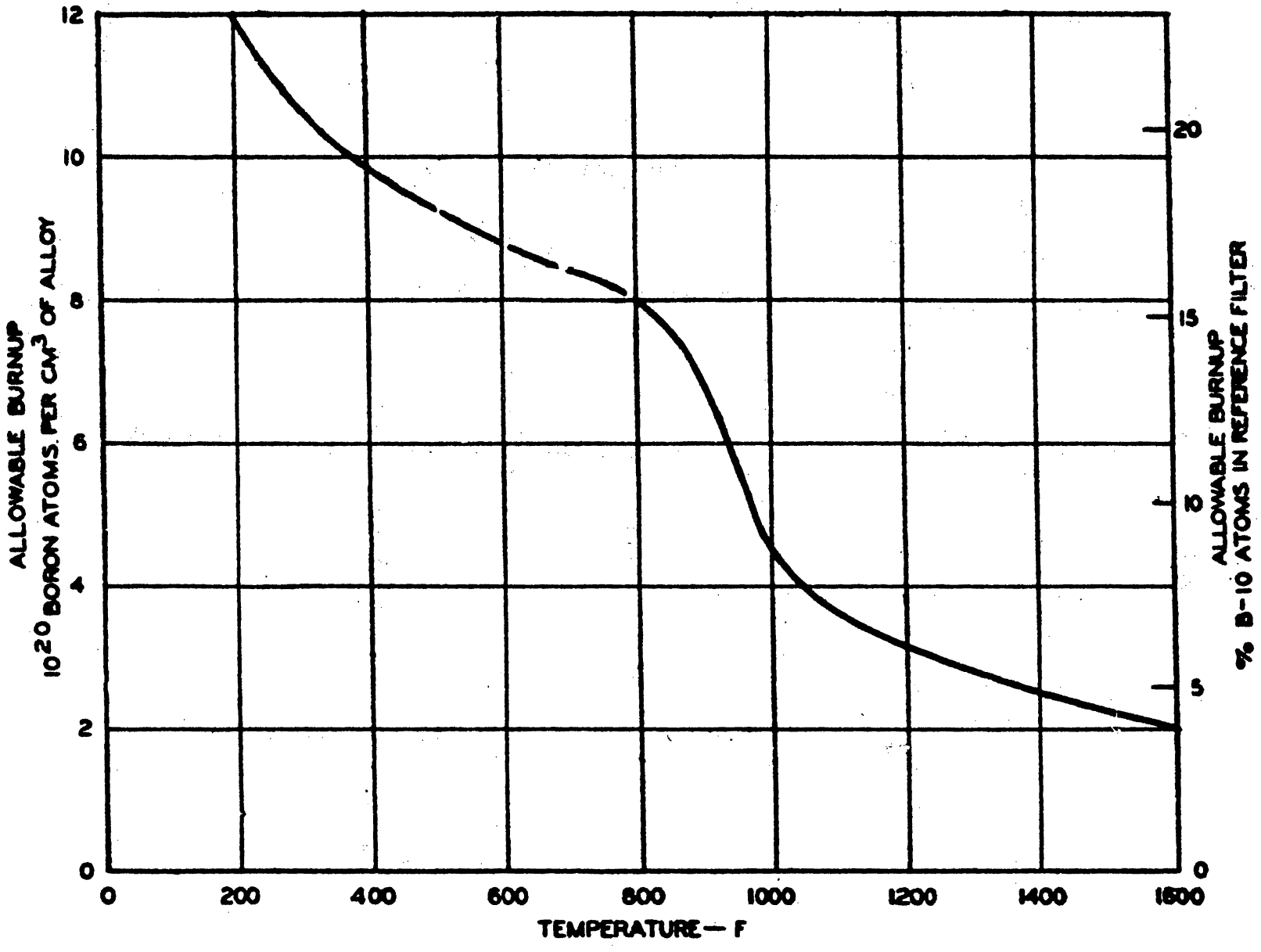

FIG. 5.2
BURNUP LIMITATIONS OF 10 W/O BORON STAINLESS STEEL ALLOY

unit volume. The allowable burnup between 450 F and 800 F was obtained by extrapolation of the curves from both sides of this region.

5.4 LIFE OF THERMAL NEUTRON FILTER

5.41 Design Limitations

The operating life of the thermal neutron filter must be determined in relation to the ATR core life to assure that the filter life does not restrict the normal operation of the whole ATR facility. The operating life of the thermal neutron filter is restricted either by irradiation damage to the B-SS filter material or by the change in flux (specimen power) and spectrum (power depression) caused by burnup of the B-10 atoms in the filter. The limitations on each of the above variables are shown in Table 5.1.

5.42 Effect of Irradiation Damage on Filter Life

The neutron heating and B-10 burnup characteristics of the filter as a function of B-10 concentration have been computed and are shown in Figure 5.3. The B-10 concentration is in units of atoms/cm^2 of filter surface. As stated in Section 4.6, the reference design model incorporates a 0.38-cm-thick (0.15-inch) stainless-steel cylindrical filter containing 0.0052×10^{24} atoms/cc of B-10. This is equivalent to 2.0×10^{21} atoms/cm^2 of filter surface. At this concentration the fractional destruction rate of B-10 in the filter is 0.66 per cent per day. Using the burnup data from Figure 5.3, the filter burnup was calculated as a function of time and is presented in Column 1 of Table 5.2. Sufficient cooling water is supplied to remove the neutron heating of the B-10 and the gamma heating of the stainless steel in the filter.

In Section 5.3 it was stated that the reference filter is limited to 20% burnup of the B-10 atoms because of irradiation damage considerations. Inspection of Table 5.2 indicates that a filter life of 32 days (2 ATR operating cycles) can be expected before this burnup is exceeded.

5.43 Effect of Filter Burnup on Test Specimen Life

The power, power depression, and burnup rate of the reference test specimen have been computed as a function of B-10 concentration and are presented in Figure 5.4. Starting with the reference B-10 concentration of 2.0×10^{21} atoms/cm^2, the sample power, power depression, and fuel burnup were cal-

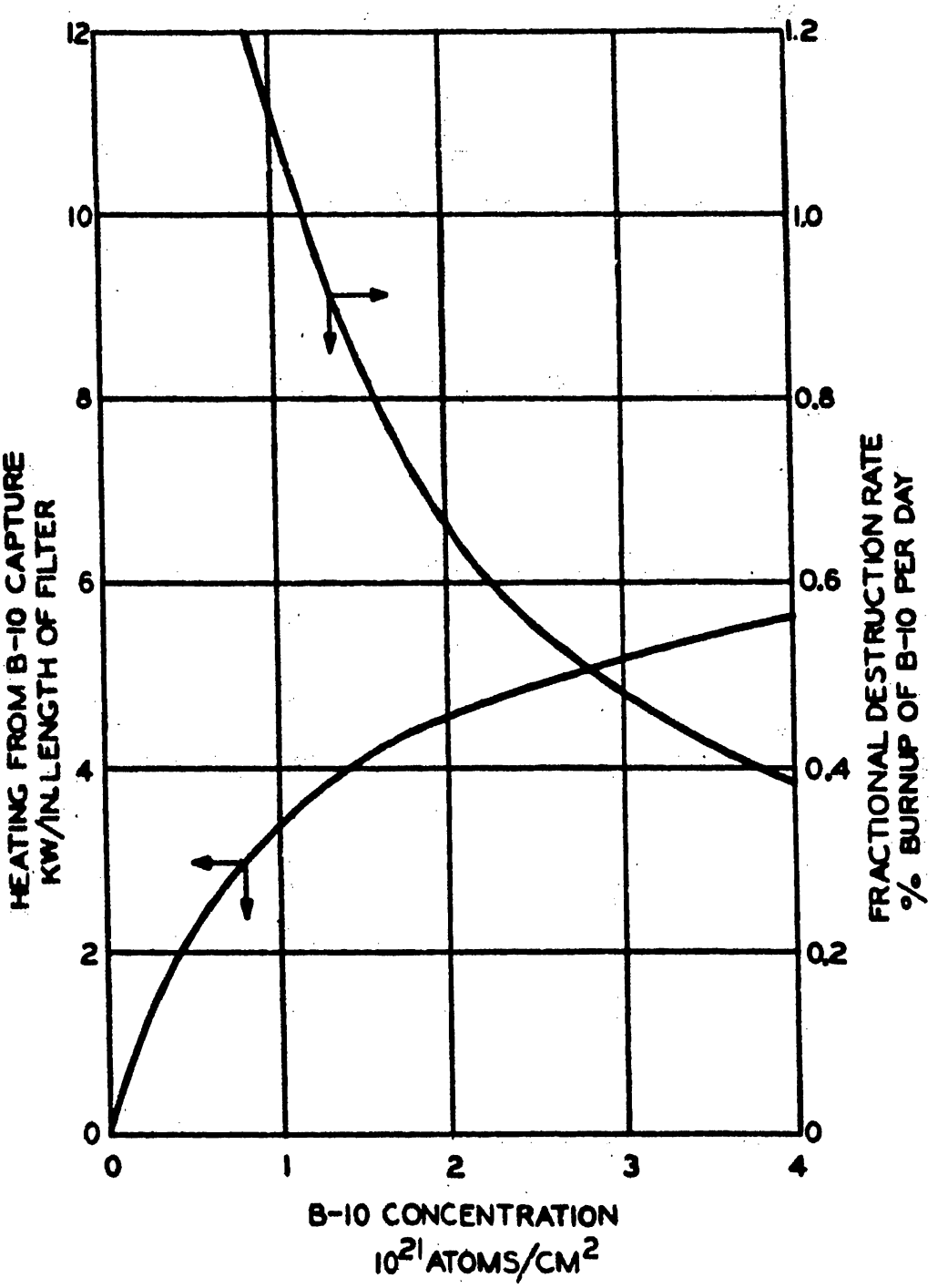

FIG. 5.3
HEATING AND BURNUP CHARACTERISTICS
OF THERMAL NEUTRON FILTER

TABLE 5.1 - FILTER DESIGN LIMITATIONS

Item	Design Limitation
Irradiation Damage to Reference Filter	20% B-10 Burnup
Specimen Power	±15%
Specimen Power Depression	1.5 Max/Min
Specimen Burnup for Loop Removal	2 a/o

TABLE 5.2 - FILTER LIFE

Time Days	Filter Burnup a/o B-10	Specimen Power Kw/in.	Power Depression Max/Min	Specimen Burnup a/o
0	0	1.65	1.31	0
20	12.5	1.72	1.37	.55
40	25	1.80	1.44	1.12
60	37.5	1.90	1.52	1.74
80	50	2.00	1.63	2.41

Initial Filter B-10 concentration, 2.0×10^{21} atoms/cm^2

PuO_2 Enrichment, 47.5%

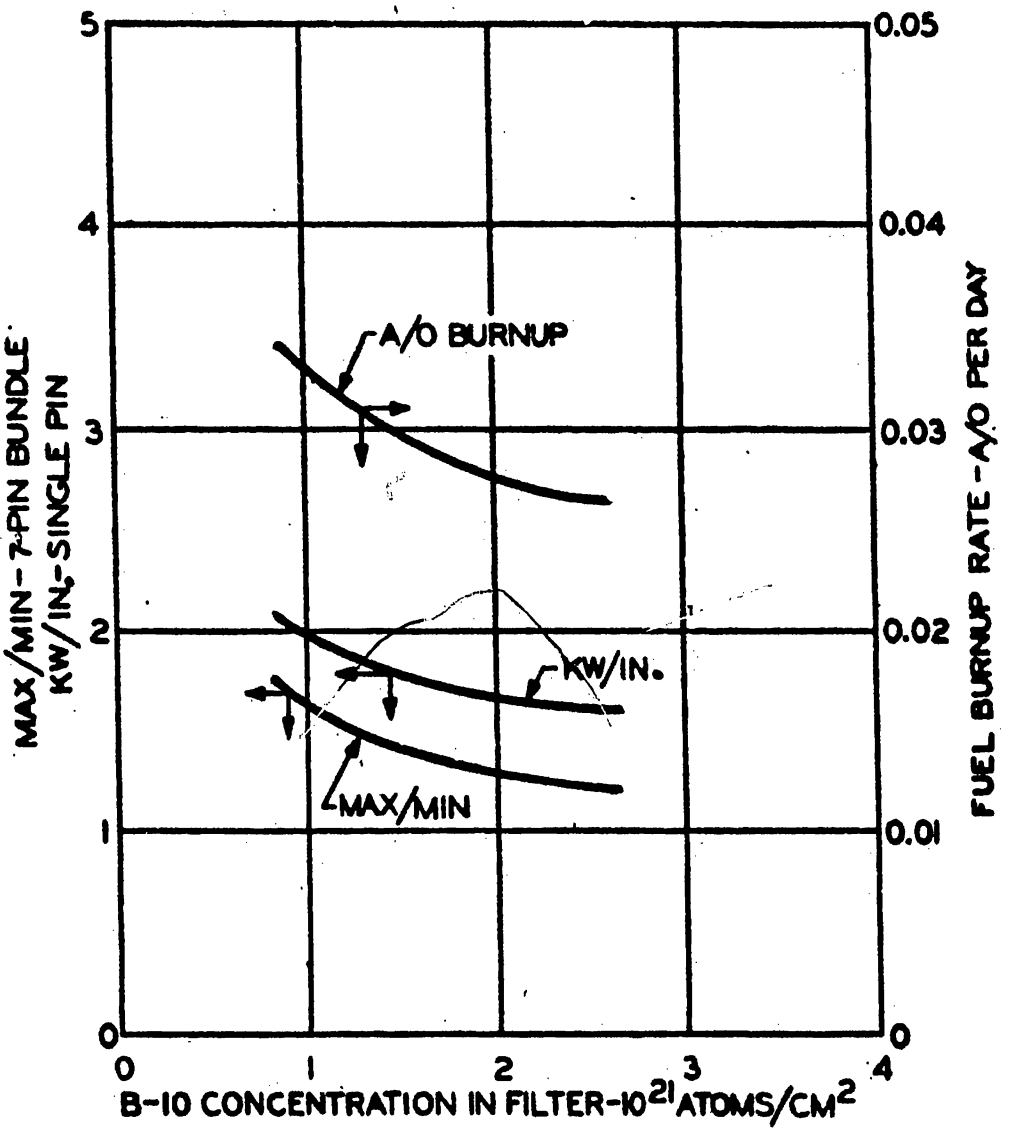

FIG. 5.4
HEATING AND BURNUP CHACTERISTICS
OF 7-PIN BUNDLE

culated as a function of time. The results of these calculations are presented in Table 5.2.

5.44 Allowable Filter Lifetime

A comparison of filter lifetime based on filter irradiation damage, specimen power, power depression, and specimen burnup is shown in Table 5.3. These data indicate that the filter life is adequate with respect to ATR operating cycle. However, the irradiation damage limits on the filter require that the loop be removed from the core (but not the reactor) and that the filter be replaced about twice as often as would be required because of test specimen limitations.

The allowable filter burnup can be increased if (1) the concentration of the B-10 (atoms/cc) is decreased and (2) the filter thickness is increased in order to keep the product (atoms/cm^2) constant. For example, if the filter thickness is increased to 0.64 cm (0.25 inches) and the amount of B-10 is decreased to 0.0031×10^{24} atoms/cc, the allowable burnup caused by irradiation damage would be increased to 33%. This percentage of burnup is equivalent to a filter lifetime of 53 days. This limitation on filter life is now about the same as the life limitation caused by the specimen power depression. Preliminary calculations show that the increased temperature and stresses in the filter, caused by increased gamma heating and a thicker filter, will still be within the design limitation. Temperatures and stresses are discussed in Section 5.5.

5.45 Alternate Filter Locations

Because the life of the filter is less than that of the extended core, and less than the fuel burnup required for inspection of test specimens, the reference filter will be installed separately from the loop and the extended core. The lifetime of the extended core region described in Section 6.0 is about 60 days. If the filter lifetime were about the same, the filter could be attached directly to the extended core section, and both could be removed at the same time. Further, if the filter life were about the same as the fuel burnup required for test specimen inspection, the filter could be attached directly to the in-pile loop. For all conditions, however, the filter design described in Section 5.2 is adequate since the filter can be changed independently of the extended core and in-pile loop.

TABLE 5.3 - COMPARISON OF FILTER AND CORE LIFE

Filter	Life (Days)	
Type of Filter	Thin	Thick
Irradiation Damage	32	53
Specimen Power	60	60
Power Depression	55	55
Specimen Burnup	68	68
Extended Core	~60	~60
ATR Core	~30	~30

Initial Filter B-10 concentration, 2.0×10^{21} atoms/cm^2

PuO_2 Enrichment, 47.5 per cent.

5.5 FILTER TEMPERATURES AND STRESSES

5.51 Power Generation

The reference filter power generation is about 300 kw. Assuming that two-thirds of the heat generated is removed from the outer surface of the filter, the maximum heat flux will be about 300,000 Btu/(hr) (sq ft) which is approximately one-half the average heat flux in the ATR core. The pressure drop across the ATR core is more than adequate to insure sufficient coolant flow to cool the reference design filter.

The boron concentration in the reference filter is 2.0×10^{21} B-10 atoms/cm^2. From Figure 5.3, it is seen that the maximum neutron-capture heating is about 4 1/2 kw/inch. From the data provided in IDO-16667[8], the maximum gamma heating is estimated to be 4 1/4 kw/inch. Figure 5.5 shows the computed curve of heat generation distribution in the filter wall at the location of maximum heating. In order to simplify calculations of temperatures and stresses, it was found desirable to approximate the actual heat generation by using two straight lines.

5.52 Temperatures

The basic differential equation for temperature is

$$\frac{d^2 T}{d R^2} + \frac{1}{R}\frac{dT}{dR} = -\frac{H(R)}{K}$$

where T = temperature

R = radius of filter

K = thermal conductivity

$H(R)$ = heat generation rate

Figure 5.6 shows the temperature profile for the reference design filter as calculated from the data of Figure 5.5. Exact determination of the temperature distribution is made difficult by both the nonuniformity of the neutron-capture heat generation and by the uncertainties in the values for gamma heating.

The profile is hardly affected by a change in surface temperature; thus, the temperature gradient will be independent of

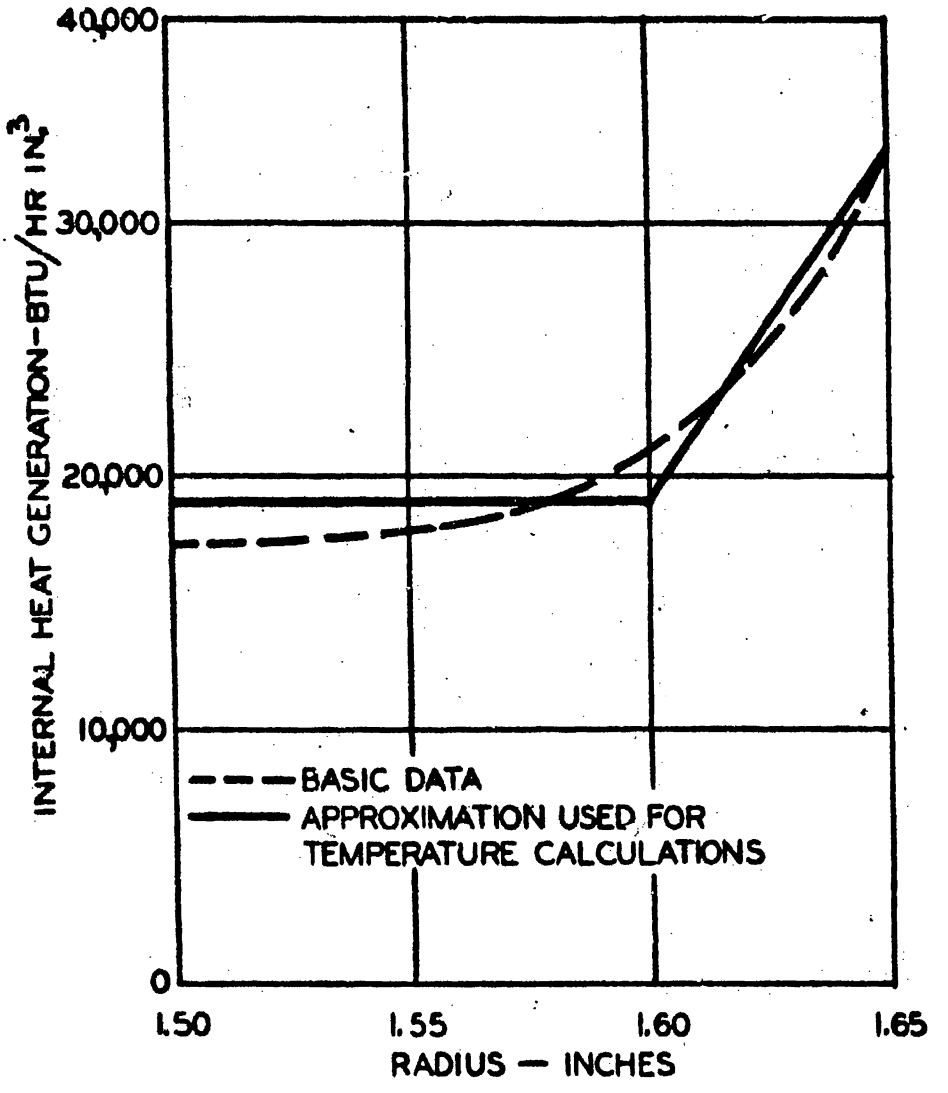

FIG. 5.5

INTERNAL HEAT GENERATION IN THERMAL NEUTRON FILTER

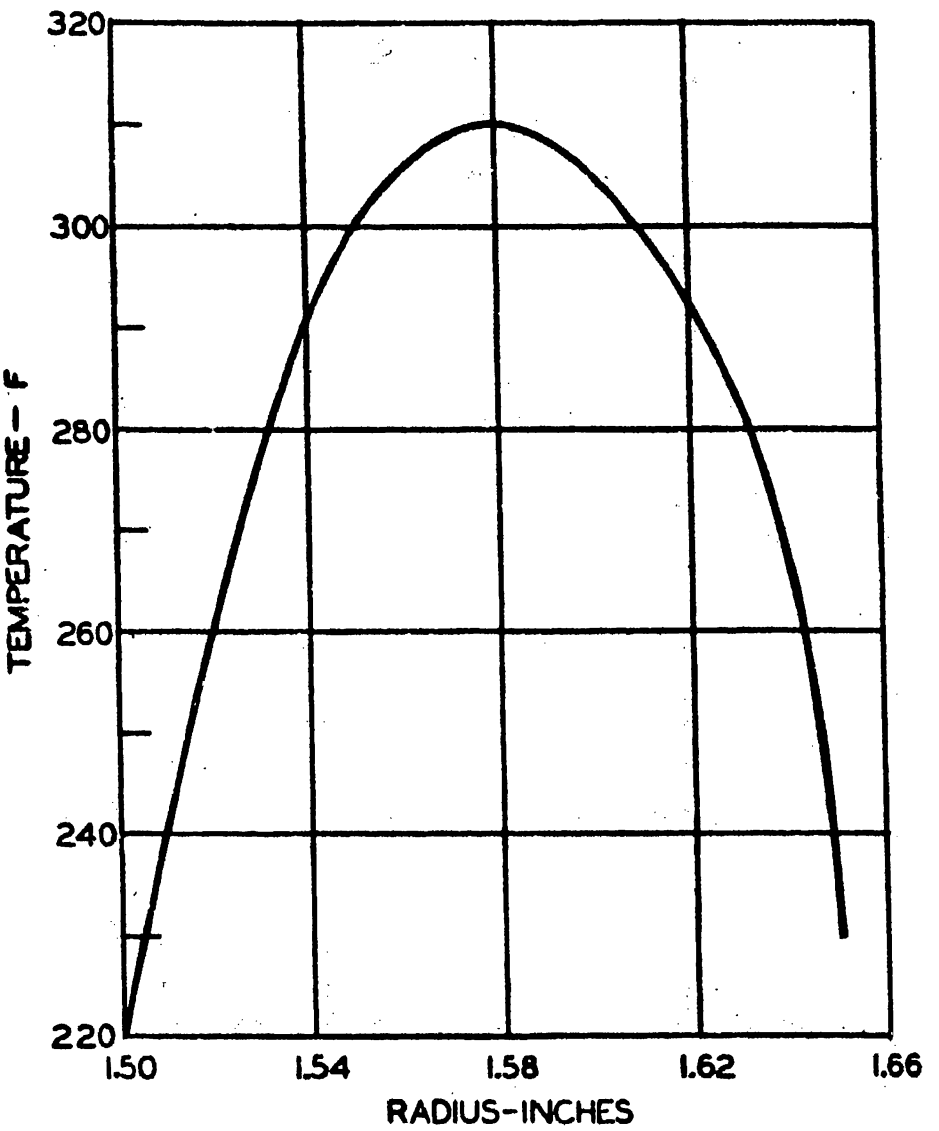

FIG. 5.6
TEMPERATURE PROFILE IN THERMAL NEUTRON FILTER.

the coolant velocity. The maximum temperature in the reference design filter will be approximately 310 F for the water flow rates listed in Table 0.1. Making the filter thicker will have little effect on the temperature gradient as long as the number of atoms of boron per square centimeter of surface is held constant (decreasing boron concentration). However, the difference between surface temperature and maximum temperature will increase in nearly the same ratio as the thickness.

5.53 Stresses

The thermal stresses in the filter are a result of the temperature gradients. The basic equations for the thermal stresses in a hollow cylinder as taken from "Theory of Elasticity" [11] are

$$\sigma_\theta = \frac{\alpha E}{1-\gamma}\,\frac{1}{R^2}\left[\frac{R^2+R_a^2}{R_b^2-R_a^2}\int_{R_a}^{R_b} TR\,dR - \int_{R_a}^{R} TR\,dR - TR^2\right]$$

$$\sigma_z = \frac{\alpha E}{1-\gamma}\left[\frac{2}{R_b^2-R_a^2}\int_{R_a}^{R_b} TR\,dR - T\right]$$

where σ_θ = tangential stress

σ_z = axial stress

α = coefficient of thermal expansion

E = modulus of elasticity

γ = Poisson's ration

R = cylinder radius

T = temperature

The thermal stresses in the reference filter, calculated from the temperature distribution in Figure 5.6, are shown in Figures 5.7 and 5.8. The tangential thermal stress reaches a peak

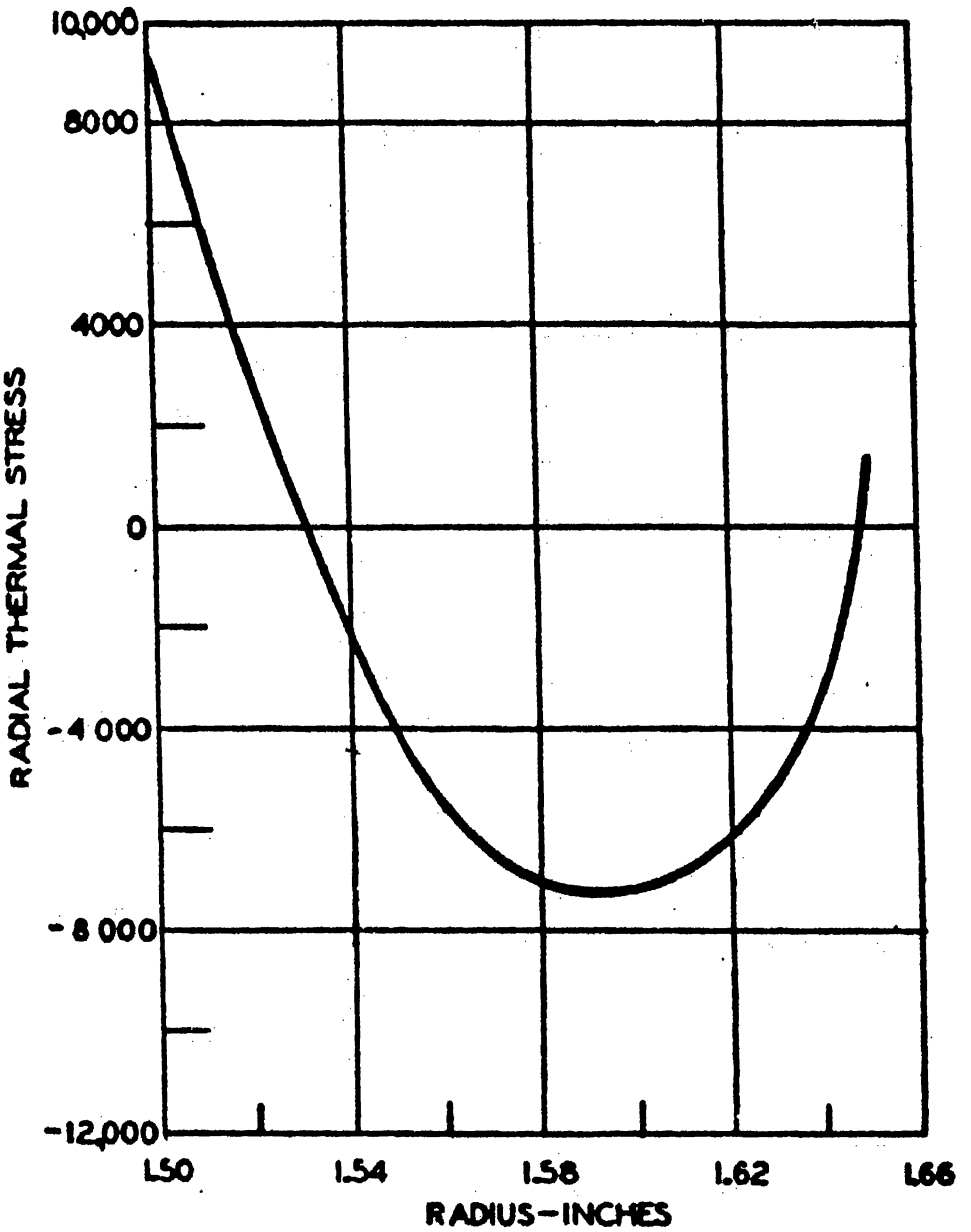

FIG. 5.7
TANGENTIAL THERMAL STRESS IN
THERMAL NEUTRON FILTER

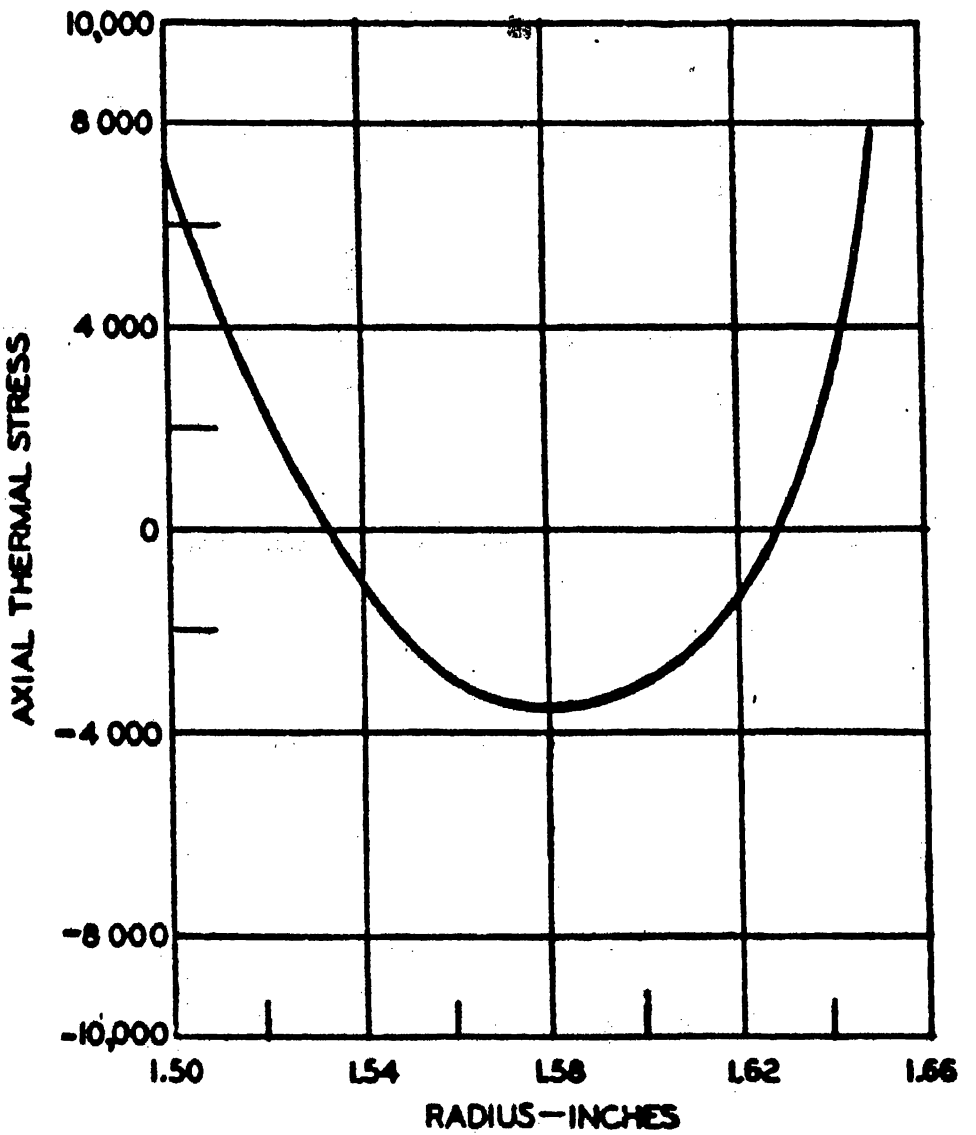

FIG. 5.8
AXIAL THERMAL STRESS IN
THERMAL NEUTRON FILTER

value of 9000 psi tension at the inner surface and 7000 psi compression near the center of the filter wall. The axial thermal stress peaks at 7000 psi tension and at 3500 psi compression at the same locations.

If it is assumed that the filter can be considered a thin cylinder, the thermal stress will be only a function of the difference between the surface temperature and maximum temperature. Thus, increasing the filter thickness will increase the thermal stress. As discussed in Section 5.52, the temperature difference will increase in nearly the same ratio as the thickness. Thus, increasing the thickness to 0.25 inch will increase the maximum thermal stress to approximately 15,000 psi, which is well within the design limit of 25,000 psi.

Since the coolant velocities in the flow channels on either side of the filter will differ, a lateral pressure will exist on the filter and induce stresses in the filter. Also, the force exerted by the spring on the top of the filter will induce stresses in the filter. Proper design will hold these stresses to small values, so that the combined thermal and mechanical stress will not exceed 25,000 psi.

6.0 EXTENDED CORE REGION

6.1 GENERAL

The most attractive method of achieving sufficient reactivity and maintaining suitable sample power for the desired irradiation tests is to extend the ATR core to the edge of the thermal neutron filter surrounding the experiment. To achieve this result, fuel elements that are geometrically similar to and metallurgically idential to ATR fuel elements are installed in the lobe flux trap region between the thermal neutron filter and the flux trap moderator column. The cross section of this region is shown in Figure 6.1. These fuel elements will have the same enriched uranium oxide aluminum cermet core, the same cladding, the same metal-to-water ratio, and the same percentage of burnable poison as the ATR core.

6.2 PHYSICAL DESCRIPTION OF EXTENDED CORE.

The extended core consists of eight circular segment fuel elements of the same nominal design as the ATR fuel element. The fuel elements consist of seven curved fuel plates mounted between two side plates to form a 45-degree segment of a right circular cylinder with an inside radius of 1.65 inches and an outside radius of 2.625 inches. The side plates are extended to form the bottom end box. The thickness, length, and spacing of the fuel plate are idential with those of the ATR fuel element. The fuel elements used in the extended core differ from the ATR fuel elements in that the comb used in the ATR fuel element is omitted. The longest horizontal span between the side plates of the extended core fuel element is less than the longest horizontal span between the side plate and comb of the ATR fuel element. Thus the comb may be safely omitted from the extended core fuel element.

6.3 EXTENDED CORE POWER GENERATION AND LIFE

The radial power density for the experimental lobe containing the fast fuel test loop, the thermal neutron filter (approximately 1 per cent B-10 by weight), and the extended core is shown in Figure 6.2. The axial power distribution is assumed to be identical in the ATR core and the extended core.

An examination of Figure 6.2 shows that

1. The average power density in the ATR core is twice the average power density in the extended core.

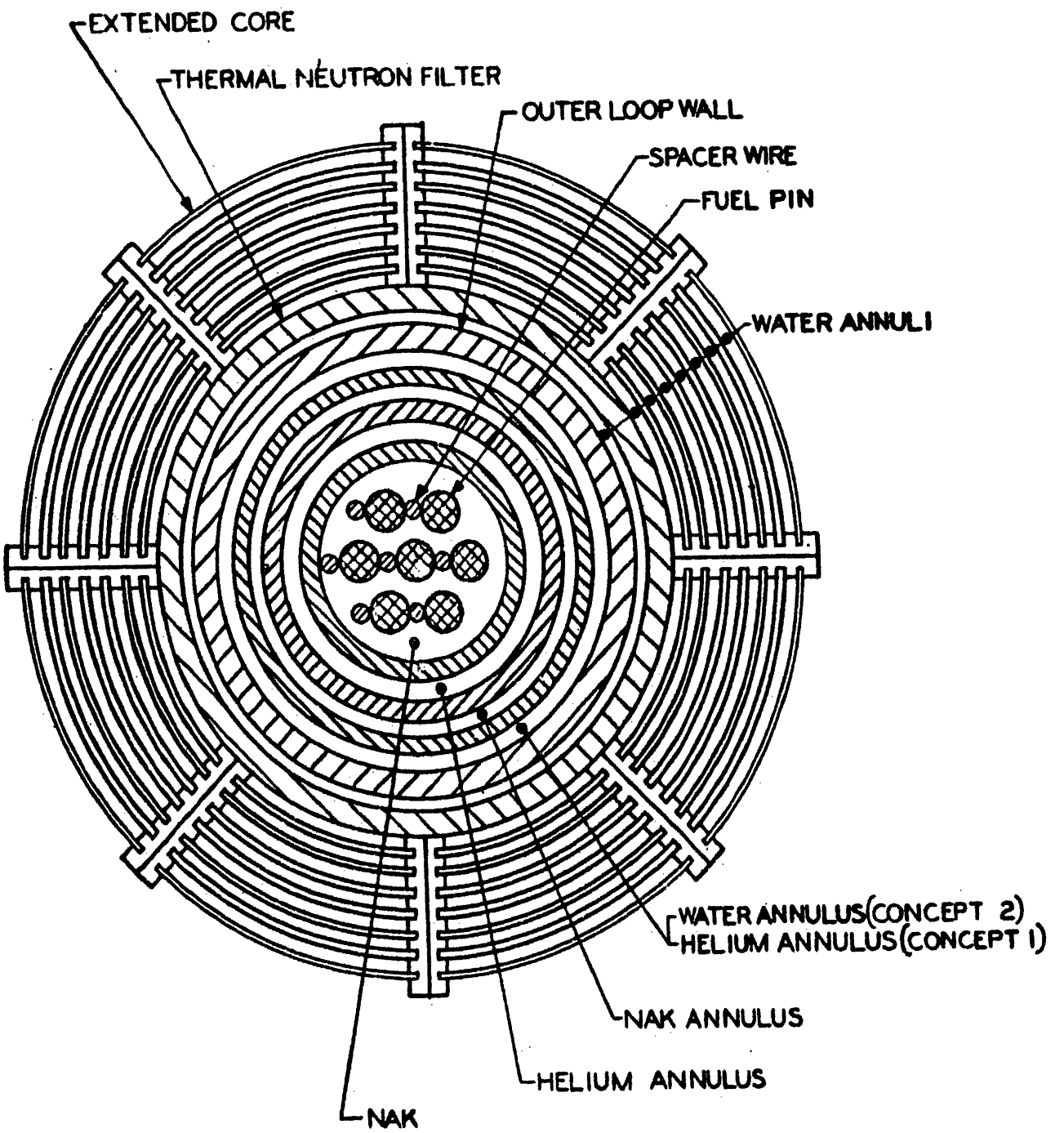

FIG. 6.1
CROSS SECTION
INPILE LOOP FACILITY

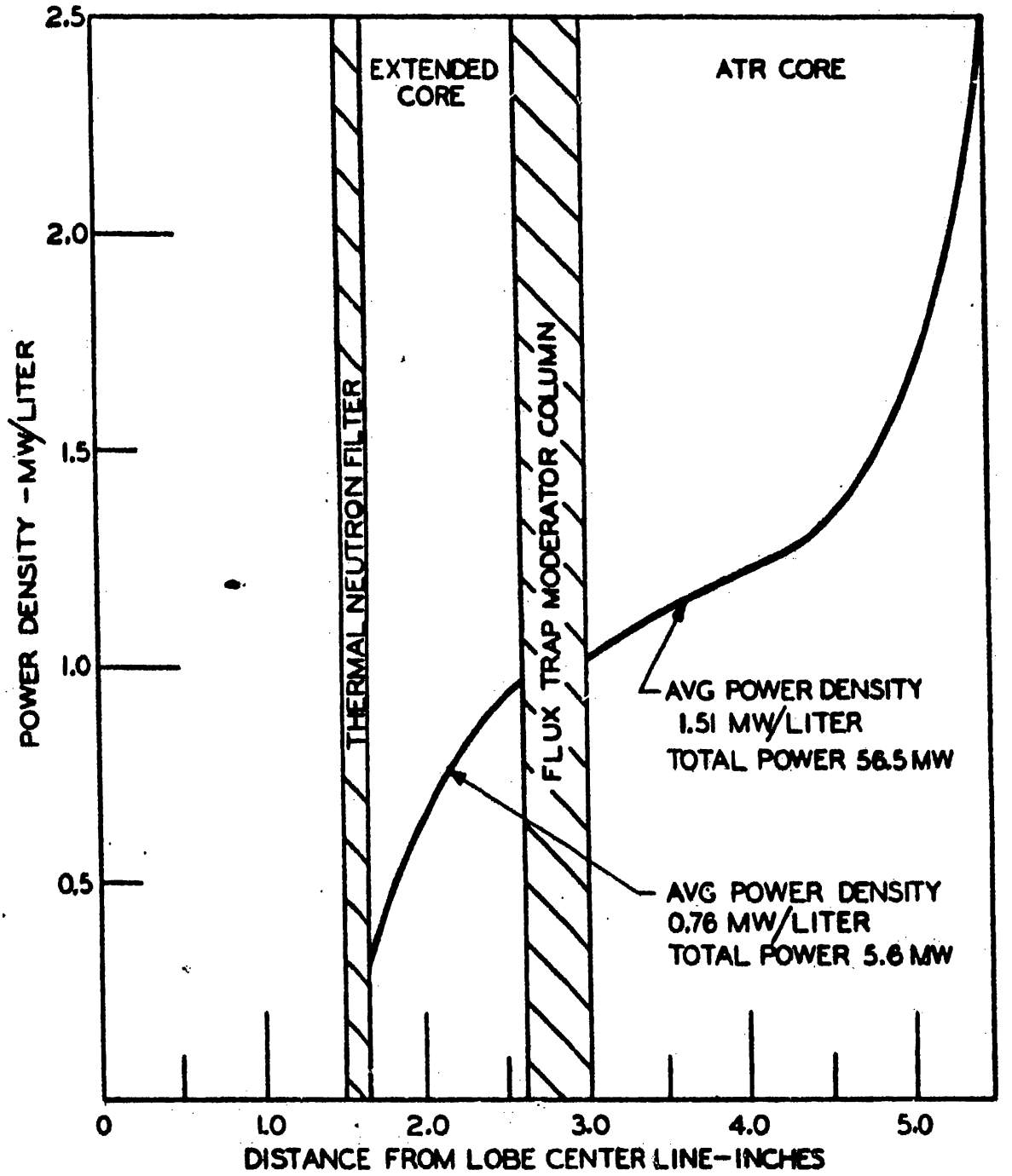

FIG. 6.2
RADIAL POWER DENSITY
AT CORE MIDPLANE

2. The maximum power density in the ATR core is 2-1/2 times the maximum power density in the extended core.

3. The maximum power density in the extended core is slightly less than the minimum power density in the ATR core.

Therefore, it is concluded that the extended core fuel element life will be twice the life of an ATR fuel element.

6.4 HYDRAULICS AND HEAT REMOVAL

The fuel element entrance and exit geometry, and the fuel plate spacing and length in the extended core and in the ATR core are identical. Since the equivalent diameter used for calculating the pressure loss for flow in annuli is only a function of the distance between cylinders, and since entrance and exit pressure losses are a function of geometry, the hydraulic characteristics of the extended core and the ATR core are identical for the in-pile test loop Concept No. 2 described in Section 3.32. Concept No. 1 described in Section 3.32 channels ATR cooling water through the loop water jacket and then through two annuli. These annuli are formed by the loop and the thermal neutron filter and by the thermal neutron filter and the innermost extended core fuel plate. Thus the hydraulic characteristics of this inner channel will differ slightly from the extended core.

Since it is desirable to keep the pressure drop of the water flowing through the water jacket equal to the pressure drop of the water flowing through the extended core, the water velocity in the channels on either side of the innermost fuel plate will differ slightly in Concept 1. This velocity difference will cause a lateral pressure to be exerted on the innermost fuel plate. The effect of this pressure on the fuel plate stresses will be investigated in the Title I work.

It has been indicated by the ATR designers that it is desirable to maintain the lobe pressure loss at one-half the core pressure loss or less. Therefore, the extended core and water jacket pressure losses have been set at 46 psi for both concepts. This gives a velocity of 30 feet per second in the extended core in both concepts and a velocity of 26 feet per second inside the innermost fuel plate in Concept 2.

Since the power densities and radii of the extended core are less than those of the ATR core, the heat fluxes, the fuel plate temperature gradients, and the fuel surface temperatures will be less than those of the ATR core. Comparison of Figure 6.2 with Table 8.7A, in IDO-16667, (8), shows that a coolant velocity of 30 feet per second in the extended

core will provide adequate cooling. Extrapolating from Figure 8.7A, indicates that a velocity of 26 feet per second in the channel between the innermost extended core fuel plate and the thermal neutron filter will provide adequate cooling for that fuel plate.

7.0 SHUTDOWN TEST SPECIMEN TEMPERATURE LIMITATIONS

7.1 ALLOWABLE POSTIRRADIATION TEMPERATURES

At any time after normal in-pile loop operation, temperature of the individual fuel elements resulting from decay heating of the fuel, must be limited to prevent postirradiation changes in the metallurgical properties of the fuel. If excessive temperatures were permitted to occur after irradiation, the resultant changes in the properties of the fuel element might be indistinguishable from the irradiation effects.

To estimate the maximum allowable temperature after shutdown for metallic, cermet, and ceramic fuel elements, data from postirradiation heating of the various elements were examined. This examination indicated that a surface temperature of 1000 F would be allowable for the metallic and cermet fuels and that a much higher temperature would be allowable for ceramic fuel. Above these temperatures, the creep properties of the materials begin to decrease, and swelling may occur because of fission gas pressure. The use of surface temperature instead of central temperature is permissable since the temperature drop in the individual fuel elements is very small after a decay time of one day.

Subsequent to irradiation of metallic fuel pins, it may be advisable to avoid phase transformations caused by high postirradiation temperatures. If this is a limitation, a maximum allowable shutdown temperature of 700 F would be specified for an alloy such as U-10 w/o Mo.

In summary, it has been estimated that maximum surface temperatures of 700 F or 1000 F can be tolerated for the metallic fuel systems and 1000 F for the cermet and ceramic fuel systems.

7.2 DECAY HEAT GENERATION

The decay heat generation from a test specimen bundle is a function of the following factors:

1. Residence time of the bundle in the reactor.
2. Operating power of the bundle.
3. Time since reactor shutdown (decay time).

Calculations of relative decay heat generation were made for several reactor residence times using the method employed by Perkins (12). The results of these calculations are shown in Figure 7.1.

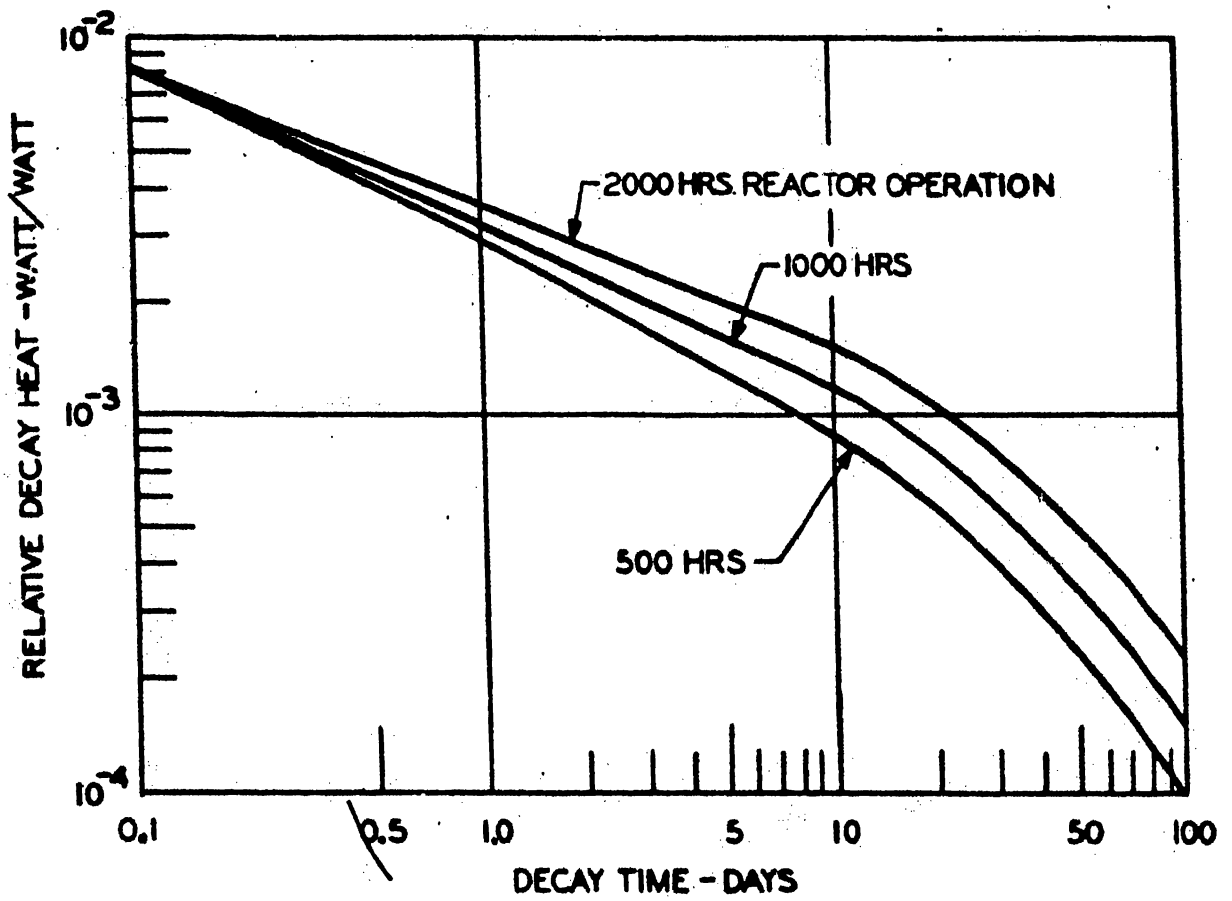

FIG. 7.1

DECAY HEAT OF 7-PIN TEST SPECIMEN

If the coolant pump and heat exchanger are operated after the reactor is shut down, the maximum fuel element surface temperature will be approximately 200 F irrespective of decay time. The most severe heat transfer conditions occur if the NaK coolant is drained from the fuel bundle and if stagnant helium surrounds the elements within the fuel bundle. Heat transfer calculations show that the fuel surface temperature will exceed 1000 F in less than one minute. For this reason, the fuel bundle must be immersed in NaK during all out-of-pile operations subsequent to irradiation.

If the coolant pump is shut down after the reactor is shut down, the surface temperature of the fuel bundle will rise from 200 F to an equilibrium temperature which is dependent on the decay heat generation and the thermal resistance characteristics of the loop walls and helium annuli. Heat transfer calculations have been made to determine the equilibrium fuel surface temperature after 2000 hours of reactor operation prior to shut down. Calculations were performed with the loop immersed in water (natural convection) and the loop in an air environment (forced convection). The results of these calculations are shown in Figure 7.2. The effect of radiation across the helium annuli was included in all calculations.

7.3 MINIMUM DECAY TIME

From the curves shown in Figure 7.2 it may be seen that once the reactor has been shut down the pumps and heat exchanger must operate for about 8 hours to insure that the maximum surface temperature of 1000 F is not exceeded for the cermet and ceramic fuel elements. An additional 16 hours' decay in water are needed before the loop may be removed from the water and exposed to air.

For metallic fuels (if it is necessary to avoid the phase transformation problem and restrict the temperature to 700 F) the pump and heat exchanger must be allowed to operate for about 1-1/2 days before shut down. An additional two days' decay in water is necessary before the loop may be removed from the water and exposed to air.

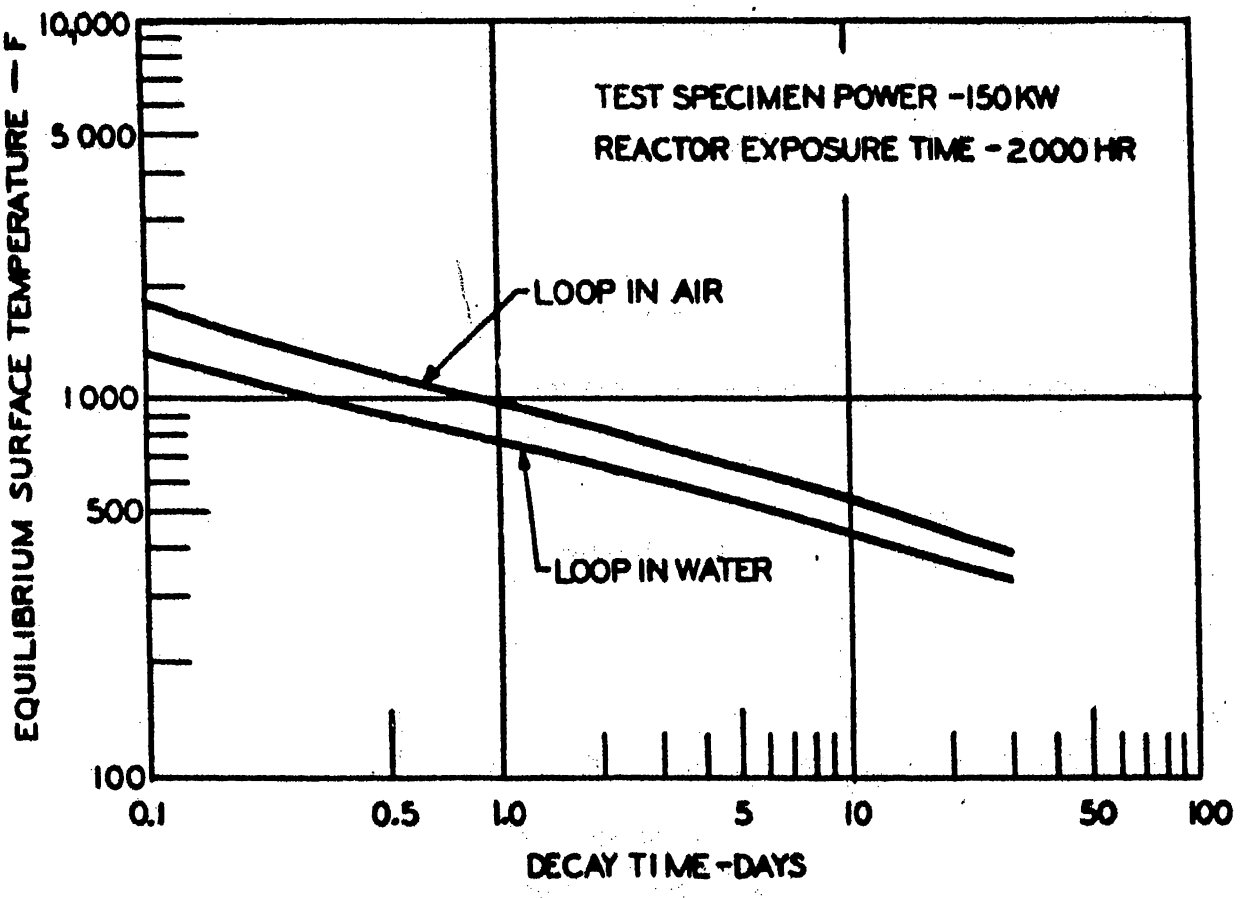

FIG. 7.2

SURFACE TEMPERATURE OF 7-PIN TEST SPECIMEN WITH PUMP AND HEAT EXCHANGER SHUTDOWN

8.0 LOOP HANDLING

8.1 GENERAL

Removal of the loop from the reactor vessel is necessary for inspection and evaluation of the fuel specimen at approximately 2-month intervals, and also for loop maintenance. Replacement of the thermal neutron filter and the extended core section will be required at approximately 2-month intervals, but this can be accomplished without removing the loop from the reactor vessel.

The most significant factors involved in handling of the loop are the size and weight of the loop, the radioactivity of loop components, the fuel specimen decay heat, the reactivity of the NaK with air and water, and the requirement to keep the loop in a position not more than 30 degrees from the vertical position. Calculations were made of the source strengths of the NaK contained within the loop, fuel, and stainless steel components. The results are shown in Table 8.1. All shielding requirements for loop handling and hot cell operations have been based on these calculations.

The decay heat problem presents several complications. As shown in Section 7.3, preliminary calculations of shutdown fuel specimen temperature indicate that it is marginal whether or not the fuel specimen can be adequately cooled unless the decay heat is removed by forced cooling for about one day after reactor shutdown. Therefore, the handling procedures described herein are based on keeping the loop in operation inside the reactor vessel for one day before loop transfer operations are attempted. This requirement may complicate reactor operating procedures; therefore, a more detailed study should be made of the decay heat problem in the Title I Design to ascertain whether forced cooling is required.

The size of the loop as finally designed will determine the method of removing the loop from the reactor. Removal and installation will be either through the drop tube into the canal or out through the vessel head into a loop transfer cask. Removal through the drop tube can be used for both loop concepts described in Section 3.32. Because of space limitations, removal through the vessel head can be used only in Loop Concept No. 2.

A detailed analysis of emergency conditions that might arise during loop transfer operations, and of the methods of coping with these situations, must be performed during the Title I Design.

TABLE 8.1 - SOURCE STRENGTHS OF LOOP COMPONENTS

Decay Time	NaK Gamma Curies	Fuel Specimen Gamma Curies	Stainless Steel Gamma Curies
0	1.21×10^{4}		
1 Hour	1.16×10^{4}		
2.4 Hours		1.63×10^{5}	1.25×10^{3}
1 Day	3.99×10^{3}	9.3×10^{4}	1.18×10^{3}
1 Week	5.14×10^{0}	5.33×10^{4}	
1 Month	5.61×10^{-2}	2.48×10^{4}	

---

1. The specific activity of the NaK at 0-time is 1.39 curies/cc. The specific activity of the Na-22 in the NaK at 0-time is 5×10^{-6} curies/cc. The soft gamma components of Na-24 and K-42 are readily absorbed and therefore were not used in calculating the shield thicknesses.

2. One gamma curie = 3.7×10^{10} gamma-photons/sec and is equal to the actual curie value divided by the number of gammas per disintegration.

3. A reactor exposure of 10,000 hours was used in the above calculations.

8.2 LOOP HANDLING FACILITIES

The major facilities and equipment needed for handling the loop are as follows:

1. Hot Cell - Description in Section 9.2.
2. Cranes - Description in Section 8.51.
3. Loop Thimble and Transfer Car - Description in Section 8.52.
4. Transfer Cask - Description in Section 8.53.
5. Special Tools for handling loop in the reactor or in the canal.
6. Utilities and services for the loop during transfer to the hot cell.

8.3 REFERENCE LOOP HANDLING PROCEDURE

The reference method of loop installation and removal presented herein is based on ATR Title I Drawing, ATR-1075-MTR-670-R-501. (13).

8.31 Removal Through the Drop Tube

The preparations required at the vessel top head and the vessel discharge chute are as follows:

1. The head shield ring and loop transfer shield plate are removed.
2. The cover plates are removed from the access ports in the vessel head that will be used for guiding the loop to the drop tube.
3. The drop tube cover is removed.
4. The loop thimble is positioned in the working canal beneath the drop tube.

Upon completion of the above preparations, the following procedure is used:

1. The loop leads to the junction at the top of the extension tube are disconnected.
2. The cable from the ATR 2-ton crane is attached to the loop extension tube. The loop seal is broken, and the

loop is raised up through seal until the bottom of the extension tube is several inches out of the vessel.

3. The removable support flange is attached to the main body of the loop, and the loop is lowered until the support flange rests on the vessel head. The position of the loop at this point is shown in Figure 8. 1.

4. The loop extension tube is disconnected and is raised sufficiently to permit access to the loop leads located at the top of the loop. The loop leads are disconnected and the extension tube is removed.

5. The cable from the ATR 2-ton crane is attached to the loop, the loop is raised slightly, and the loop support flange is removed.

6. With the use of special handling tools, which are inserted into the vessel through the access ports, and with the use of the crane, the loop is guided over to the drop tube. The loop is lowered through the drop tube into the loop thimble. The loop thimble is moved away from the drop tube into a vertical position in the working canal.

7. The drop tube cover, the vessel access port covers, the vessel shield ring, and the loop transfer shield plate all are replaced.

8. The crane over the canal area is attached to the loop thimble, and the thimble is placed in the thimble transfer cart. The transfer cart is moved with the building crane to the hot cell location.

8.32 Installation Through Drop Tube

The procedure for installing the loop through the drop tube is essentially the reverse of that given in the previous section for loop removal.

8.4 ALTERNATE LOOP HANDLING PROCEDURE

The alternate method of loop handling presented herein is based on ATR Title I Drawing ATR-1075-MTR-670-R-500 Revision O (14) and ATR Design Study S-R-64. (15).

8.41 Removal Through the Vessel Head

The preparations required at the vessel top head are as follows:

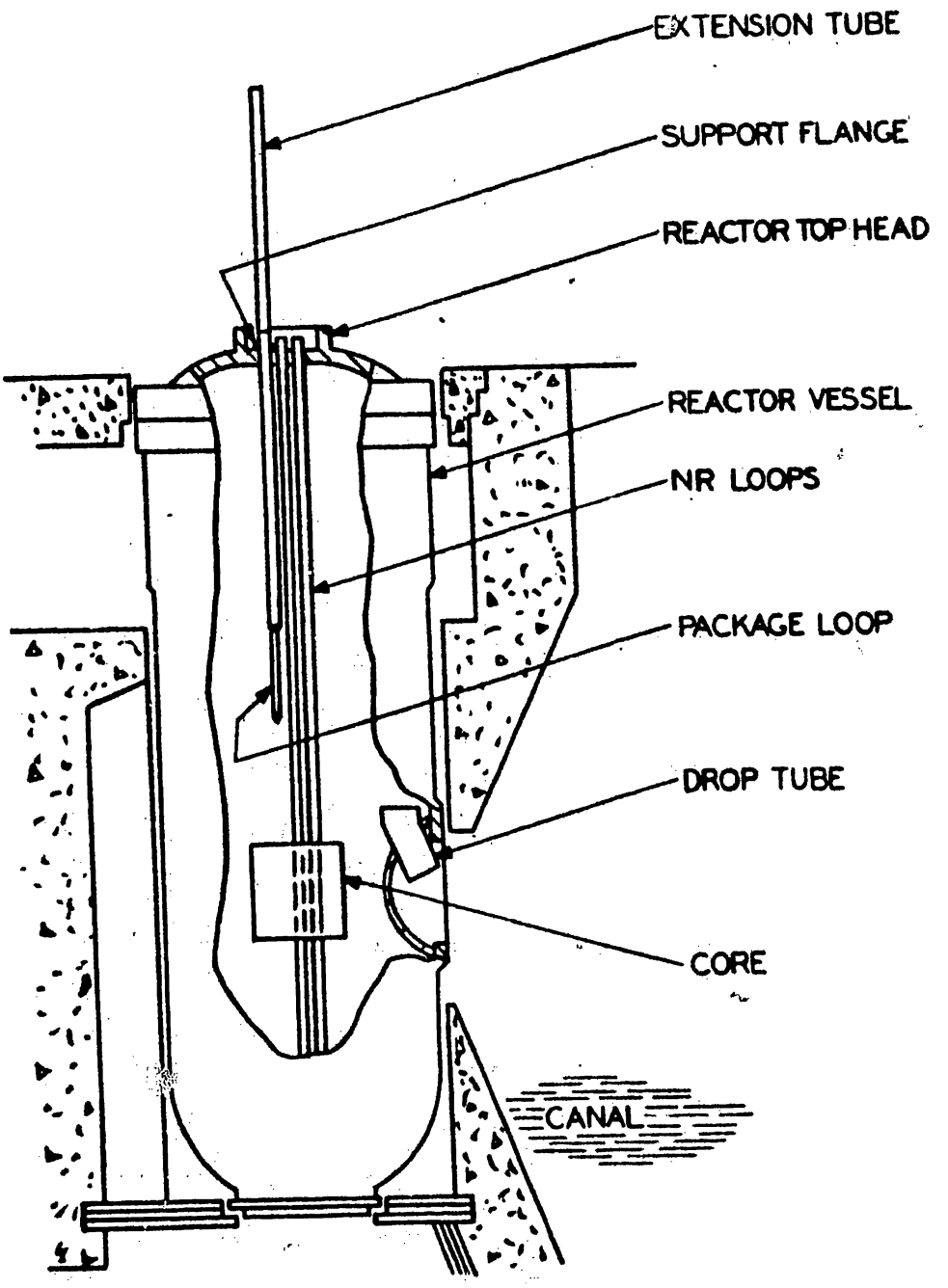

FIG. 8.1
LOOP REMOVAL PROCEDURE

1. The head shield ring and loop transfer shield plate are removed.

2. The cable from the ATR 2-ton crane is threaded through the cask adapter and through the appropriate hole in the loop transfer shield plate and is secured to the loop by attaching hooks to lifting attachments located on top of the loop extension tube.

3. The permanent loop lead connections are broken and capped.

4. The head shield ring and the loop transfer shield plate are reinstalled. The shield plate is indexed on the shield ring.

5. The cask adapter is seated and secured to the transfer shield plate.

In addition to the preparations at the top vessel head, the loop transfer cask must be prepared to receive the loop prior to its removal from the reactor. The preparations required are as follows:

1. The transfer cask, supported by the 40-ton ATR crane, is moved to a position adjacent to the reactor vessel head.

2. The loop supports in the transfer cask are moved to the retracted position.

3. The cask shielding valve is turned to the open position.

4. The cask crane hook is lowered so the hook extends out through the bottom of the cask.

Upon completion of the preparations at the vessel head and of the transfer cask, the loop is removed from the reactor by the following procedure:

1. The loop is raised by the ATR 2-ton crane until the bottom of the loop extension tube is several inches above the top of the cask adapter.

2. A removable support ring is attached to the main body of the loop just below the loop extension tube. The loop is lowered, permitting the support ring to rest on top of the cask adapter. The position of the loop and cask at this point is shown in Figure 8.2.

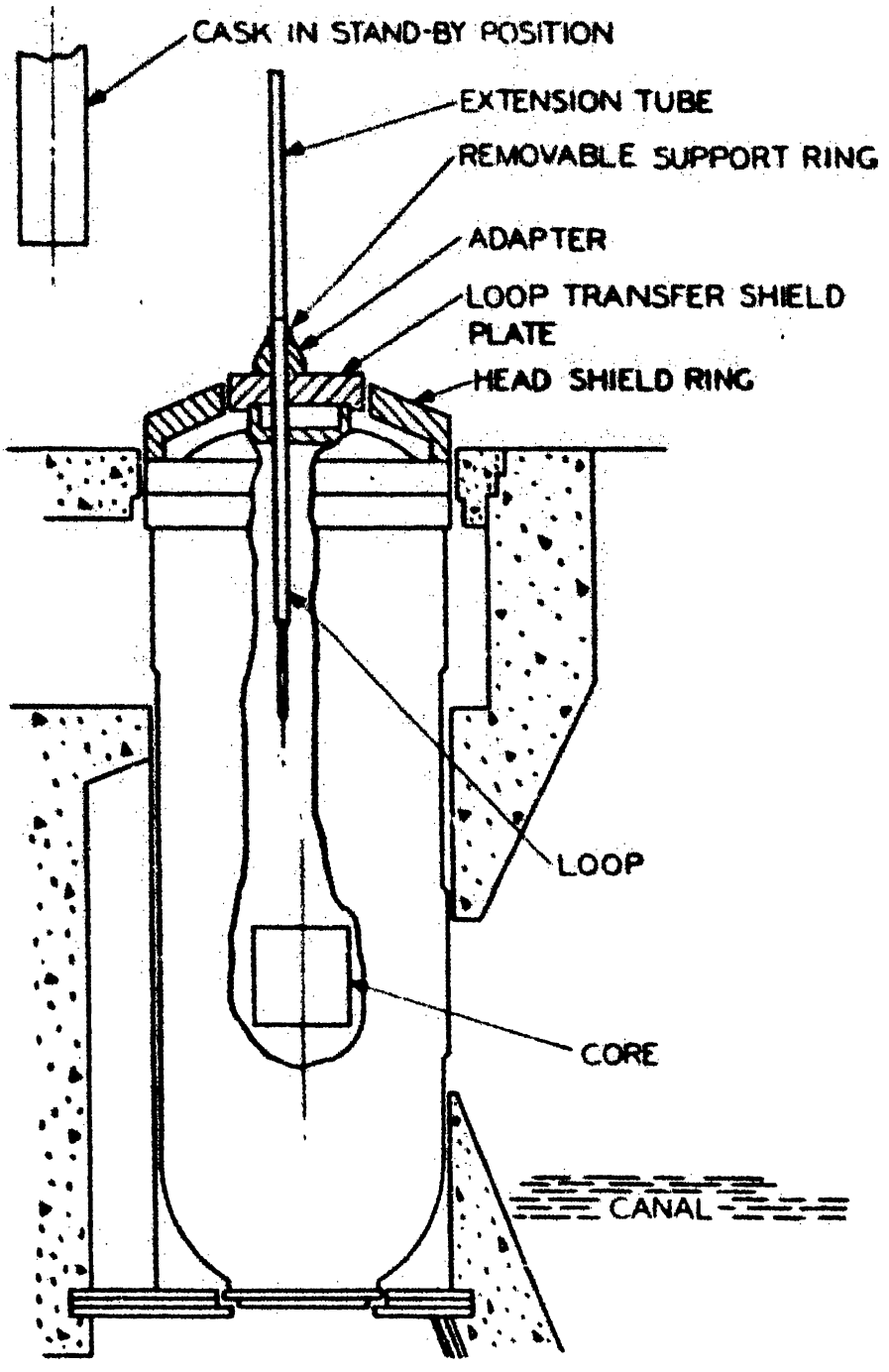

FIG. 8.2
LOOP REMOVAL PROCEDURE

3. The loop extension tube is disconnected from the main body of the loop. The tube is then raised about 1 foot to permit access to the loop leads located at the top of the loop. The leads are disconnected from the loop, and the loop extension tube is lifted out of the way with the 2-ton ATR crane.

4. The loop transfer cask is positioned so that it is directly above the loop and about 1 foot above the top of the cask adapter.

5. The cask crane hook is attached to the loop and the loop is raised sufficiently to permit removal of the support ring from the loop.

6. The cask is lowered onto the loop transfer shield plate with the cask adapter serving as a centering guide.

7. The cask crane raises the loop up into the cask. The arrangement of the loop and cask is shown in Figure 8.3.

8. The cask shield valve is turned to the close position and the loop supports are set to secure the loop.

9. The cask is raised off the cask adapter and the cask adapter then is removed from the shield plate. The cask is then ready to be transported to the hot cell.

8.42 Installation Through Vessel Head

The preparations required for installation of the loop are as follows:

1. The shield plug is removed from the appropriate hole in the loop transfer shield plate and the cask adapter is positioned and secured to the shield plate.

2. The transfer cask containing the loop is positioned on the cask adapter. The loop supports in the transfer cask are retracted, and the cask shield valve is opened.

3. The loop is lowered by the cask crane until the top of the loop is several inches above the top of the cask adapter.

4. The cask is raised by the ATR 40-ton crane until it is several inches off the cask adapter. The removable loop support flange is attached to the top of the loop; then the

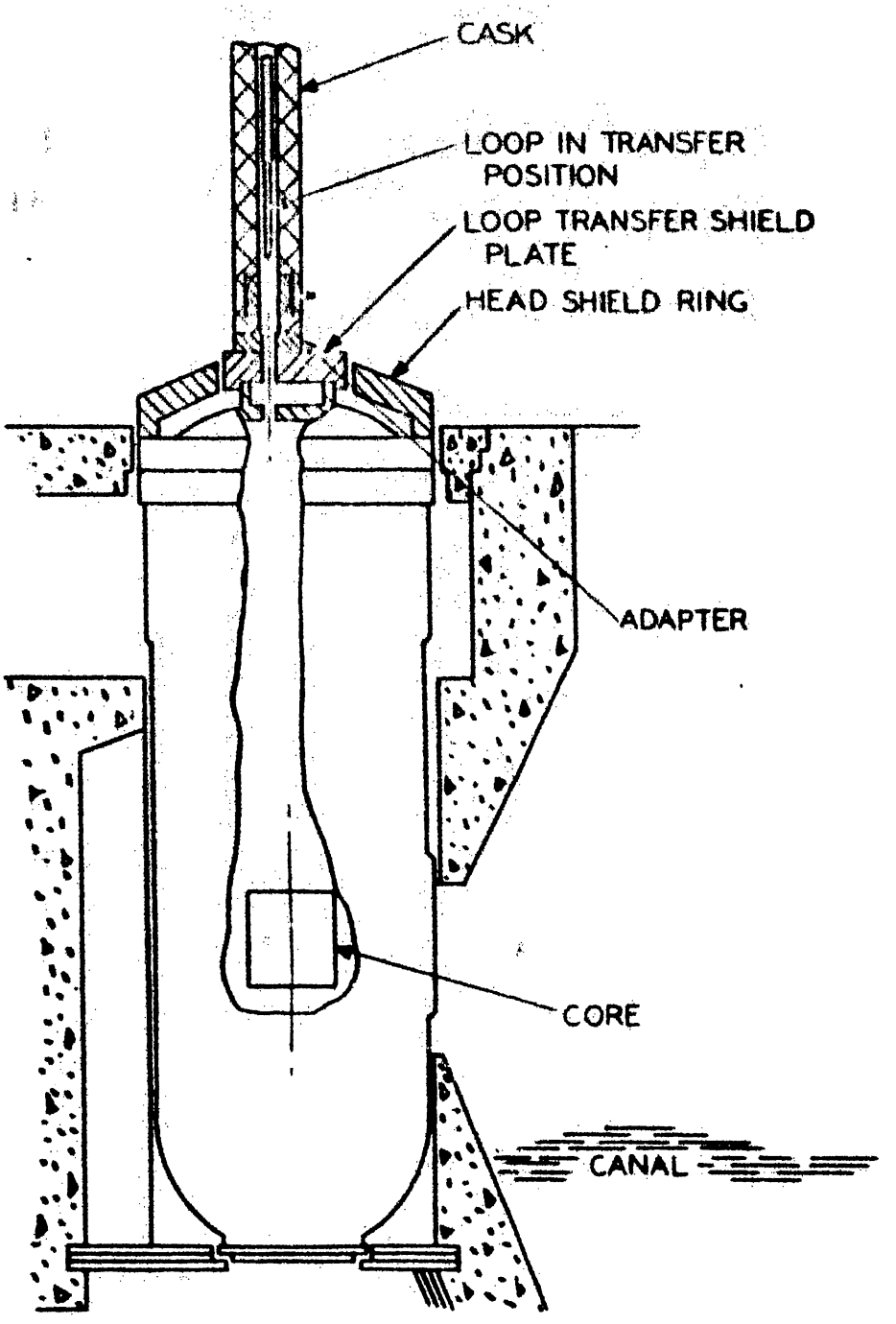

FIG. 8.3
LOOP REMOVAL PROCEDURE

loop is lowered by the cask crane until the support flange rests on the cask adapter.

5. The cask crane hook is disconnected from the loop and the cask is moved out of the way with the 40-ton ATR crane.

6. The loop extension tube is attached to the loop, then the loop is attached to the hooks of the 2-ton ATR crane.

7. The loop is raised slightly and the loop support flange is removed. Then the loop is lowered into the vessel until it rests on the ATR core support plate. The cable from the 2-ton ATR crane is disconnected from the crane hook.

8. The cask adapter is removed from the loop transfer shield plate, and the shield plate and shield ring are removed. The cable from the 2-ton ATR crane is slipped through the cask adapter and the shield plate as they are removed. Then the cable is disconnected from the loop.

9. The permanent loop lead connections are made up and the double O-ring seal between the loop and the vessel head is made up.

10. The vessel shield ring and the loop transfer shield plate are installed. The shield plug is replaced in the hole in the shield plate.

8.43 Transfer To and From Hot Cell

The principal requirement for the transfer of the loop is that at all times the loop must be kept within 30 degrees of the vertical position.

8.5 LOOP HANDLING EQUIPMENT

8.51 Reactor Building Crane Requirements

A 40-ton and a 2-ton crane with approximately 30 feet of headroom are required in the reactor building for handling the loop and the transfer cask. The cranes must be capable of being positioned directly over the loop test position. To prevent excessive pulling loads on the loop during its removal from the reactor, the 2-ton crane must be equipped with a suitable device such as a load cell or motor torque indicator.

To prevent dropping of the loop or cask, the cranes must be equipped with a fail-safe braking device or with a guaranteed power supply.

8.52 Loop Thimble and Thimble Transfer Cart

If the loop is removed from the reactor through the vessel drop tube, a thimble is required in the pool to receive the loop and then to support and protect it in the canal. The thimble is a stainless-steel or aluminum cylinder, approximately 8 inches in inside diameter by 14 feet in length and capped on one end. The walls and end cap are perforated to permit the canal water to cool the loop. Handling lugs mounted on the thimble wall are needed for lifting and for supporting in the transfer cart. For positioning the thimble underneath the drop tube, the concept shown on ATR Title I Drawing ATR-1075-MTR-670-R-501 Revision O (13) appears satisfactory.

The transfer cart is needed to transport the loop in a vertical position through the canal and to position the loop underneath the hot cell. A 6-foot depth of water above the top of the loop is required to keep the dose rate above the storage canal below 1.0 mrem/hr.

8.53 Loop Transfer Cask

If the loop is removed from the reactor through the reactor vessel head, a transfer cask is required to receive the loop. The basic design requirements of the loop transfer cask are adequate shielding and containment. A conceptual drawing of the cask is shown in Figure 8.4. Essentially, the cask consists of two concentric steel cylinders with a lead-filled annulus, fitted with a shielding plug in one end and a ball valve in the other end. The external cask dimensions are 32 inches in outside diameter by approximately 20 feet in over-all length, and the internal cavity dimensions are 10 inches in diameter by approximately 16 feet in length. The thickness of the walls and the end fittings is approximately 11 inches and is based on the calculated thickness of lead required to reduce the dose rate to 10 mrem/hr at a distance of 1 foot from the cask surface with the source strength shown in Table 8.1. The cask weights approximately 36 tons.

The cask requires a 1-ton capacity, motor-driven crane, located in the upper end of the cavity, which will be used for raising, lowering, and supporting the loop. Over-travel of the crane must be prevented, abnormal loads must be detected, and excess-

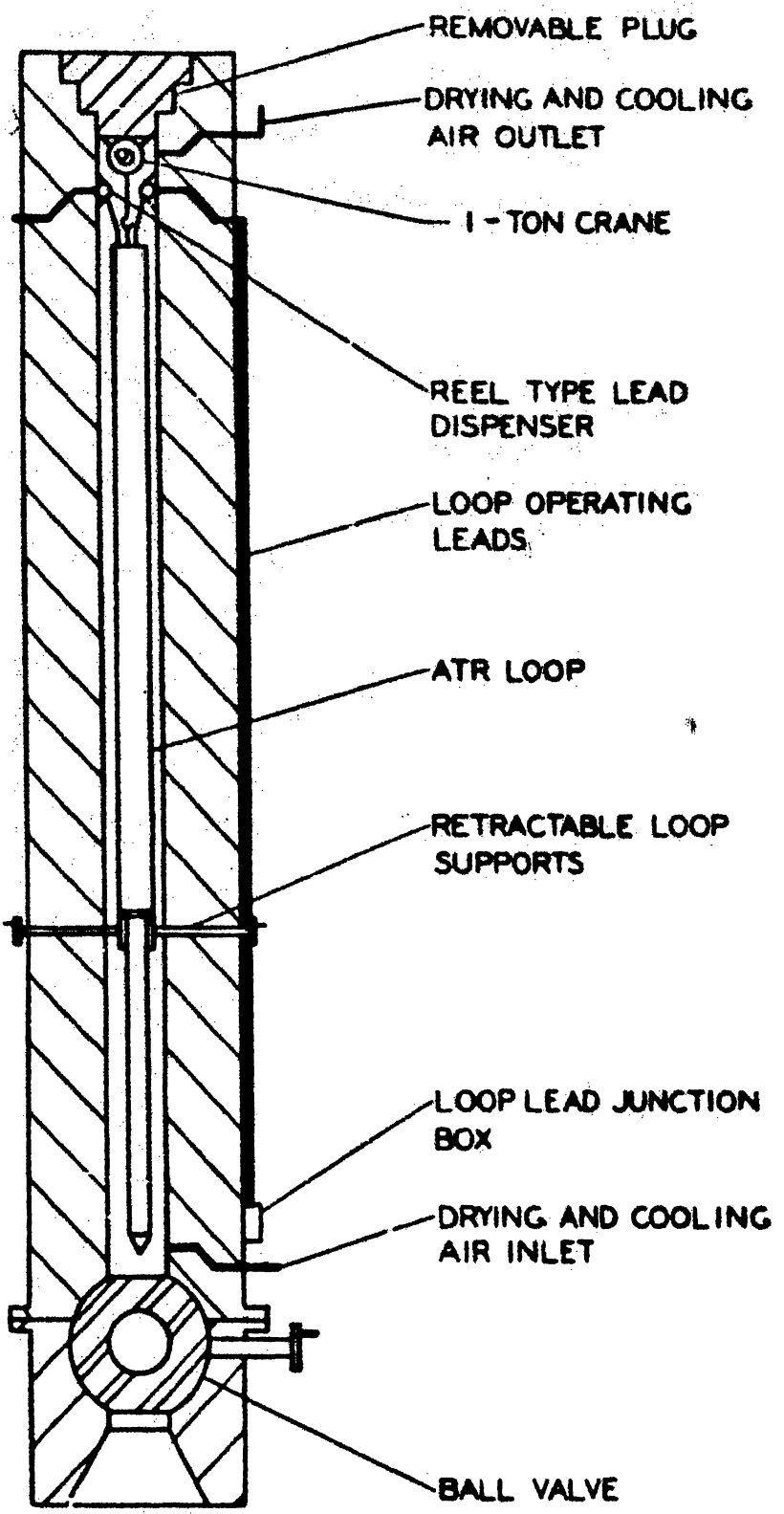

FIG. 8.4
LOOP TRANSFER CASK

ive loads prevented. Load cells, torque measurements, power cut-off, limit switches, etc., can be used to obtain needed control. The crane must be provided with a fail-safe device such as a magnetic-actuated brake which will prevent dropping of the loop in the event of loss of power to the crane drive.

Two motor-driven, reel-type lead dispensers are required to handle the utility and service leads for the loop if operation of the loop in the cask is required. The lead dispensers are located near the top of the cavity. Some means is required to control the reel-in of the leads so that they do not become too slack or too taut. This control could be accomplished by proper coupling of the crane and lead dispenser drives.

The ball valve, located in the lower end of the cask, is required to provide access to the cask cavity. This closure device must provide adequate shielding and pressure containment integrity, and must be removable for maintenance or replacement. The valve can be manually operated with a crank arrangement or it can be motor operated.

A removal plug in the top of the cask is required for access to the crane and the reel-type, utility-leads dispenser. The plug must be offset and gasketed to maintain shielding and containment integrity.

Positive supports are required inside the cask to restrain lateral movement of the loop. These supports must be retractable to provide sufficient clearance when the loop is raised or lowered in the cask. Penetration of the cask body by the support actuating mechanism must be offset and sealed to maintain the shielding and containment effectiveness.

A single-phase, 110-volt, a-c supply for the loop crane and lead dispenser reels is required. If operation of the loop in the cask is required, a 3-phase, 220 volt, a-c power supply for temporary operation of the loop pump will be required. A supply of coolant to the loop heat exchanger equivalent to 5 gpm of 100 F water will also be needed. A potentiometer or other device is needed to monitor the temperature of the loop coolant.

9.0 HOT CELL REQUIREMENTS AND PROCEDURES

9.1 GENERAL DESIGN REQUIREMENTS

A review of the available hot cell facilities at the NRTS indicates that these facilities are not suitable for the handling of the test loop because of limitations in cell height, shielding, openings, and atmosphere control.

This section of the report covers the requirements and description of a hot cell concept intended for the handling of the test loop. The basic function of the concept as presented herein is to provide a facility in which fuel specimens can be loaded into and/or removed from the test loop. This concept does not cover the methods and equipment concepts required for the postirradiation examination of fuel specimens, as discussed in Section 9.5. However, the hot cell concept does provide the basic requirements of space, shielding, cranes, manipulators, and environmental control to accommodate the postirradiation inspection equipment if desired.

The principal operations that the hot cell concept covers are as follows:

1. Cutting and disassembling the bottom closure section of the loop.
2. Containing and measuring the NaK drained from the loop during disassembly.
3. Removing the irradiated fuel specimen from the loop and transferring it into a storage container.
4. Inserting the fuel specimens into the loop.
5. Refilling the loop with the required quantity of NaK and helium gas.
6. Reassembling the bottom closure section of the loop.
7. Testing the reassembled loop.

To perform these operations, the hot cell design must provide the following requirements:

1. Sufficient head room for handling a full-length loop.

2. Sufficient space for performing the necessary operations.

3. Adequate radiation shielding and containment.

4. Adequate number and size of access ports for insertion and removal of loops, for transfer of working supplies, and for removal and installation of in-cell equipment.

5. Sufficient number and proper location of viewing windows and adequate lighting for visual observation of major operations.

6. Sufficient number and suitable types of cranes and manipulators to perform necessary operations.

7. Suitable tools and fixtures to perform necessary operations.

8. Supply of loop utilities.

9. Humidity- and temperature-controlled atmosphere. NaK and surfaces exposed to NaK must be covered with dry inert gas at all times.

9.2 DESCRIPTION OF HOT CELL

9.21 General

The principal structural features and the general equipment arrangement for the conceptual hot cell are shown in Figures 9.1 and 9.2. The hot cell is located over the storage canal. The loop, in the thimble, is positioned directly under the port in the cell floor. The hot cell crane raises the loop directly into the hot cell.

Figure 9.3 shows the hot cell modified to permit the loop to enter through an access port in the cell roof if the loop is transferred from the reactor by the transfer cask.

9.22 Cell Structure

The internal cell dimensions are 8 feet by 8 feet square by 25 feet high and are based on having two loops in the cell simultaneously. The thickness of the cell wall is 74 inches of concrete, 144 pounds per cubic foot density, and is based on a maximum dose rate of 0.25 mrem/hr at the external cell surface.

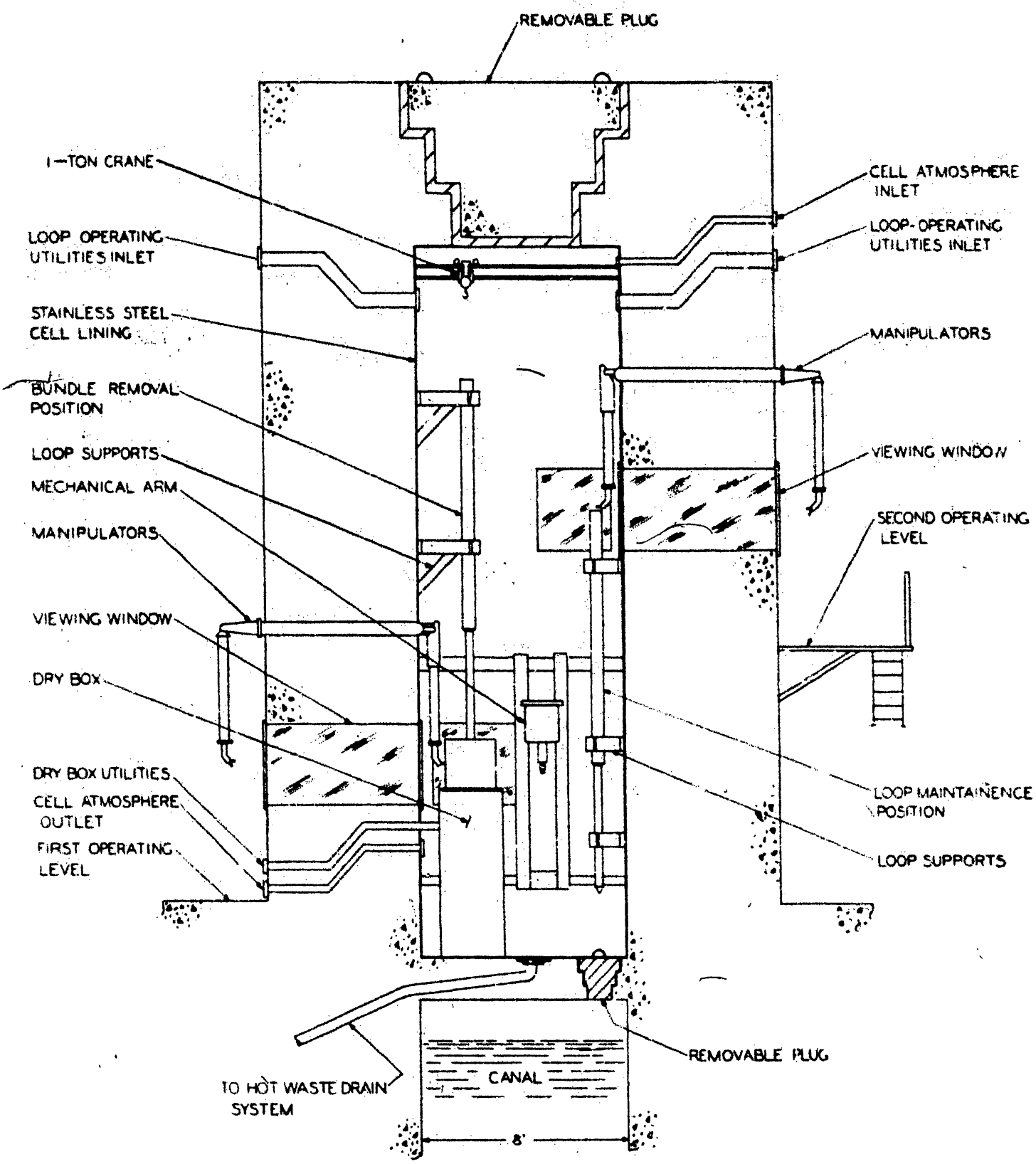

FIG. 9.1
HOT CELL ELEVATION

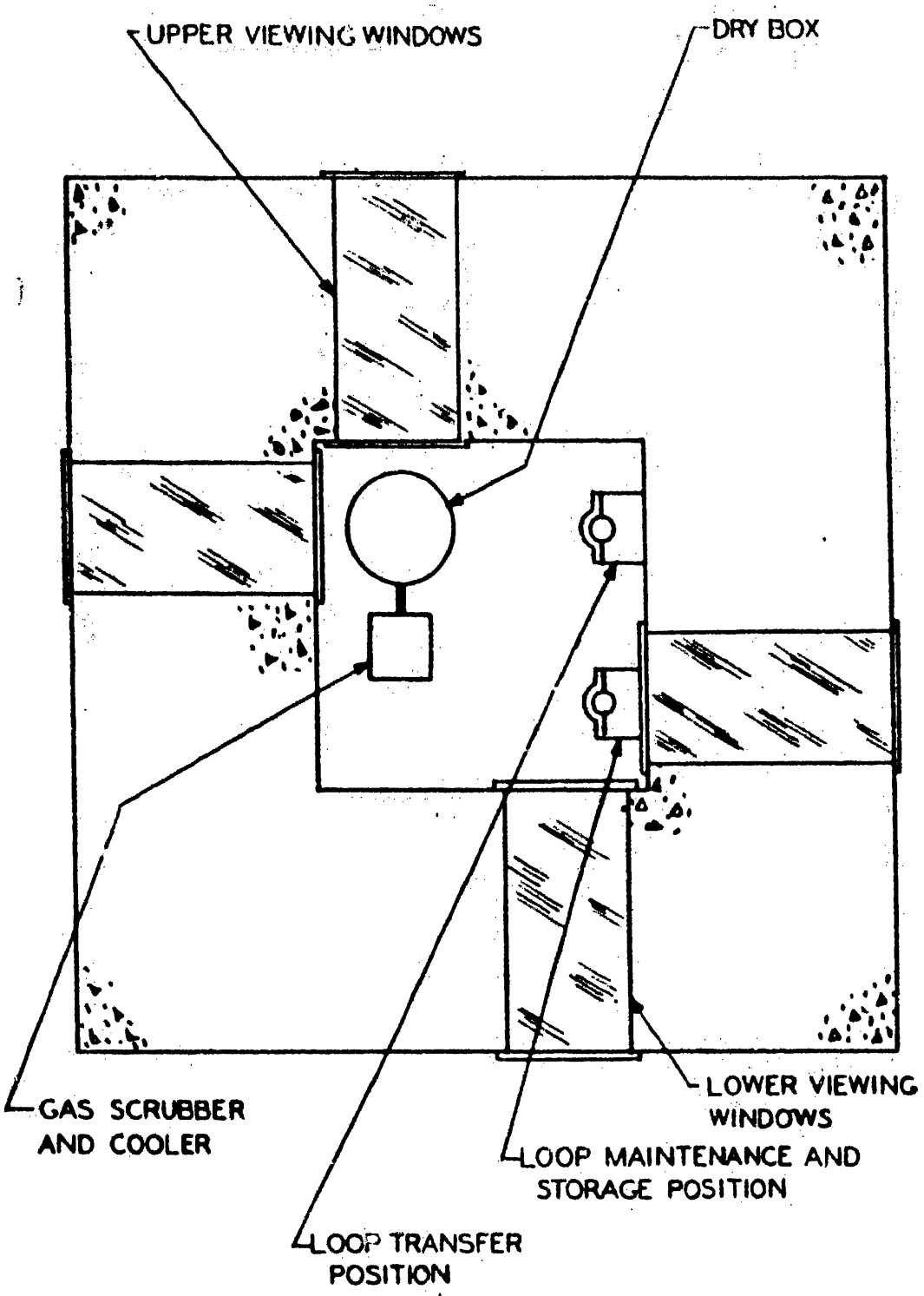

FIG. 9.2
HOT CELL
PLAN VIEW

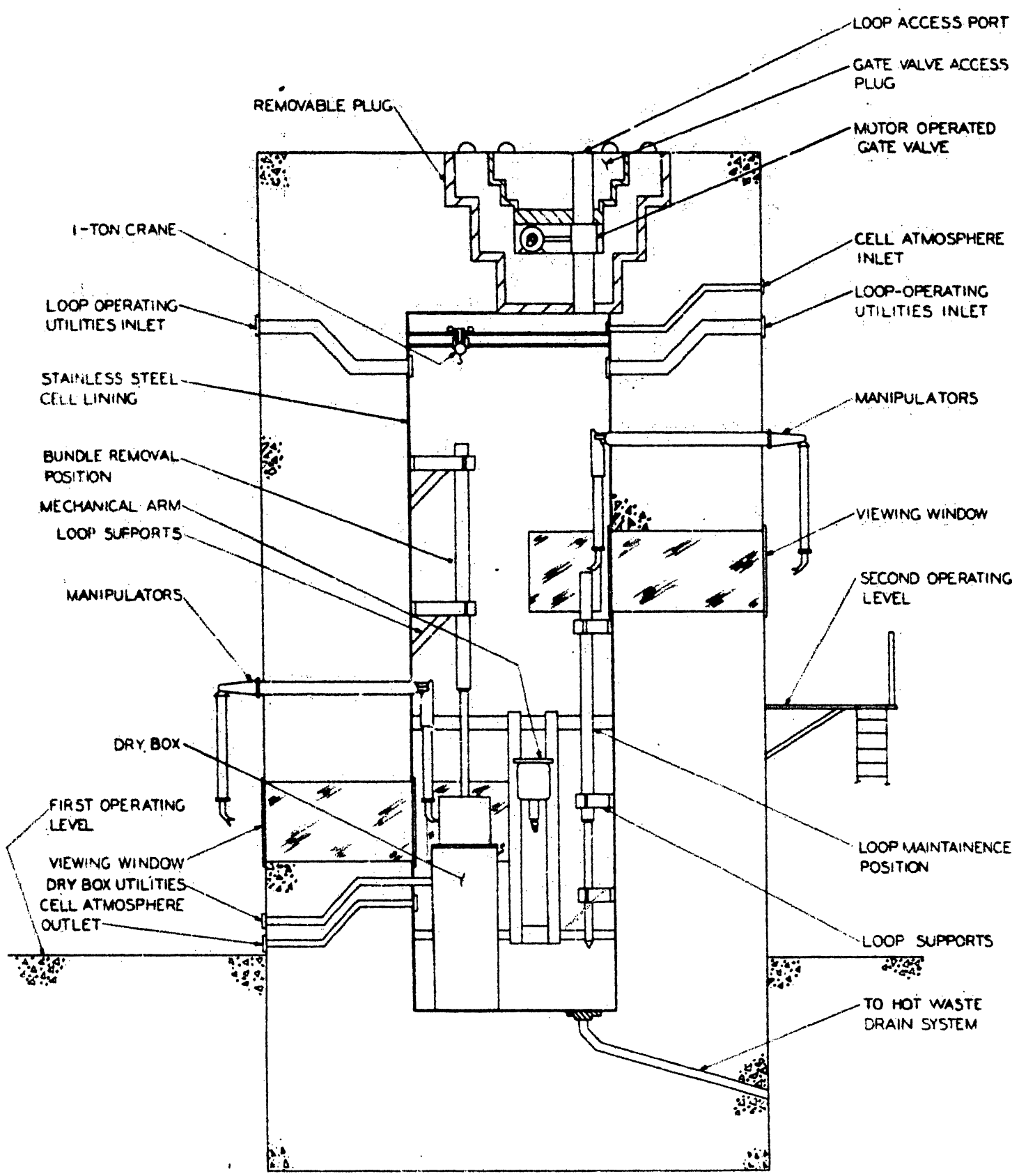

FIG. 9.3
HOT CELL ELEVATION
ALTERNATE CONCEPT

Preliminary calculations of the thickness of shielding materials for the hot cell required to reduce the dose rate to 0.25 mrem/hr at the surface are shown in Table 9.1.

There are numerous penetrations in the cell structure. There is a removable stepped plug, approximately 5 feet in diameter, in the cell roof to provide access to the cell crane, cell dry box, gas scrubber and cooler, and other large equipment. The loop access port is located in the cell floor. This port is approximately 10 inches in diameter and is fitted with a removable stepped plug. There are four penetrations for viewing windows. Two of the windows are approximately 36 inches by 36 inches and are located in adjacent walls at the level of the cell dry box. The other two windows are approximately 36 inches by 36 inches and are located in adjacent walls approximately at a level corresponding to the top of the loop. Other penetrations accommodate the two master-slave manipulators, the cell ventilation ducts, the cell utility lines, the loop utility lines, and the cell drain line. All penetrations must be designed so that the cell containment is not breached.

The cell interior is lined with stainless steel to provide leak-proof containment of the cell atmosphere and to simplify cell decontamination. Brackets welded to the steel liner serve to position and support the loops.

9.23 Cell Equipment

The main cell equipment items are the traveling crane, the master-slave manipulators, the mechanical arm, and the dry box. Minor equipment contained in the cell includes cell lighting fixtures, utility lines and fixtures, and a filter on the inlet to the exhaust ventilating duct.

The cell is equipped with a remotely operated 1-ton crane to be used for handling of the loops, the dry box, and other large equipment. The crane is located on tracks at the top of the cell and is capable of movements that cover essentially the entire cell area and all elevations within 1 1/2 feet of the cell roof. Suitable limit switches are required to prevent over-travel of the crane, and fail-safe protective devices are required to prevent dropping of equipment in the event of loss of power to the crane drive.

The cell is equipped with two sets of through-wall, master-slave manipulators and a single wall-mounted manipulator such as the General Mill Mechanical Arm. One set of

TABLE 9.1 - HOT CELL SHIELDING REQUIREMENTS

Time After Shutdown (days)	Number of Loops in Cell	Hot Cell Shield Thickness (Inches)		
		Lead	Concrete-Density of 144 lb/ft^3	Steel
0	1	13 1/4	68	22
5	1	12	62	20
0	2		74	
5	2		67	

master-slave manipulators is used primarily to assist in the dry box operations, and the other set is located to assist in the loop handling operations. The mechanical arm is mounted on a wall of the cell and is located to service the lower region of the cell.

An inert-atmosphere dry box is included in the cell for the unloading and loading of the loop. The dry box, a cylinder 2 1/2 feet in diameter and 8 feet long, is located on the cell floor in an upright position. A detailed description of the dry box is given in Section 9.3 (See also Figure 9.4)

Cell illumination, as required, can be supplied by sodium vapor lamps or other lighting units that may be readily replaced.

9.24 Cell Services

The services required for the hot cell include electric power for the loop and the cell equipment, instrument, air, process air, and water. These requirements are summarized as follows:

Electric power

480-volt, 3-phase, 50-ampere, 60-cycle, failure-free

Instrument Air

Pressure - 0 to 100 psig

Clean Process Air

Hot cell ventilation

Pressure - 1 to 5 inches of water less than the surrounding cell atmosphere.

Temperature - 75 to 85 F

Humidity - Essentially bone dry

Quantity - 800 SCFM

Helium

Quantity - 440 SCF per week, (2 cylinders/week)

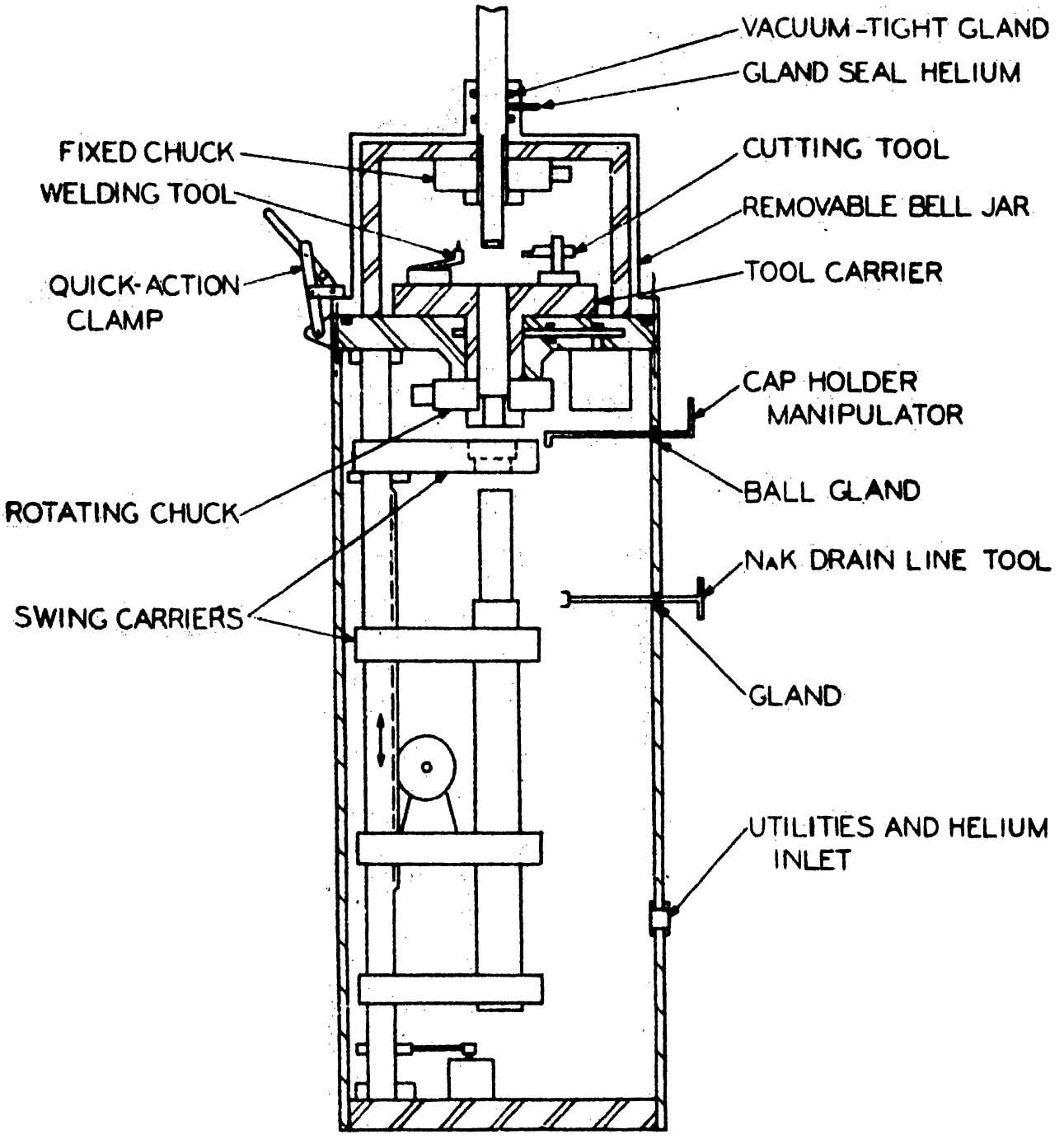

FIG. 9.4
DRY BOX

Dry box pressure - 3 inches of water less than cell pressure

Vacuum - as required for dry box evacuation in Section 9.3.

Water

Clean, filtered water supply

Pressure - 100 psi

Quantity - 50 gallons/month

Temperature - 85 F minimum

9.25 Cell Ventilation

The ventilation inlet and outlet ducts are located at the top and bottom of the cell, respectively. Clean, dry air, maintained at a temperature of 75 to 85 F, is supplied to the cell at a rate of one-half cell volume per minute. The cell is automatically maintained at an internal pressure that is from 1 to 5 inches of water pressure less than the external cell pressure. A replaceable absolute filter is placed at the inlet to the exhaust duct; the filter efficiency is checked continuously by monitoring the exhaust air down-stream of the filter.

9.3 LOOP INSTALLATION AND REMOVAL FROM HOT CELL

To transfer the loop into the hot cell from the storage canal, the loop is raised out of the canal and into the cell through a port in the floor of the cell. To transfer the loop into the hot cell from the transfer cask, the cask is positioned on top of the hot cell and the loop is lowered from the cask into the hot cell through the valved access port in the cell roof.

If necessary, loop operation can be maintained during these transfer operations by use of flexible leads. Once the loop is inside the cell it can be operated off the cell services, and the temporary leads can be disconnected and removed.

Within the hot cell, handling of the loop is accomplished by use of cranes, mechanical arms, and manipulators. The only complicated operations performed on the loop are the removal and reinstallation of the fuel bundle. These operations are carried out in the dry box and are discussed in the following section.

9.4 HOT CELL HANDLING PROCEDURES

9.41 Removable Loop Closure and Specimen Removal Container

A conceptual design of an irradiated-test-specimen removal container is shown in Figure 9.5. This device is used in conjunction with the removable loop closure shown in Figure 9.6 to permit removal of the fuel bundle in a NaK environment. This handling procedure is required as a result of decay heat calculations, which indicate that excessive fuel temperatures will occur if the NaK is drained before removing the fuel bundle from the loop. The decay heat problem is discussed in Section 7.0.

The irradiated-test-specimen removal container has external cooling fins to facilitate the removal of decay heat from the irradiated test specimens. The container contains a three-fingered extracting tool used to pull the irradiated test specimen out of the loop and into the container. The extracting tool is attached to the tool holder which is moved vertically in the container by three lead screws driven simultaneously by a planetary gear train. Double-gland seals with a NaK drain between the seals are used where the lead screws penetrate the bottom of the container. A removable upper cap is provided for maintenance of the internal parts of the container. The cap contains O-rings for sealing the container to the loop during test specimen removal operations. A container cover will be provided for attachment to the upper cap during container handling operations. Thermocouples will be installed in the container to measure the NaK temperature. A description of the removable loop closure shown in Figure 9.6 is given in Section 3.21.

9.42 Dry Box

Since it would be very difficult to clean the discharged loop if the NaK system were exposed to air, the environment in which the loop is unloaded and reloaded must be moisture-free and oxygen-free. To avoid the necessity of designing the entire hot cell for the high-purity inert atmosphere required, a smaller dry box is provided for use as a separate unit within the hot cell. A conceptual design of the dry box is shown in Figure 9.4. The dry box consists of a vacuum-and gas-tight chamber about 8 feet high and 2-1/2 feet in diameter. It contains all the machinery required for opening, unloading, recharging, and resealing the bottom end of the loop. Mechanical penetrations are kept to a minimum, and, wherever practical, electric motors are used for operations within the box.

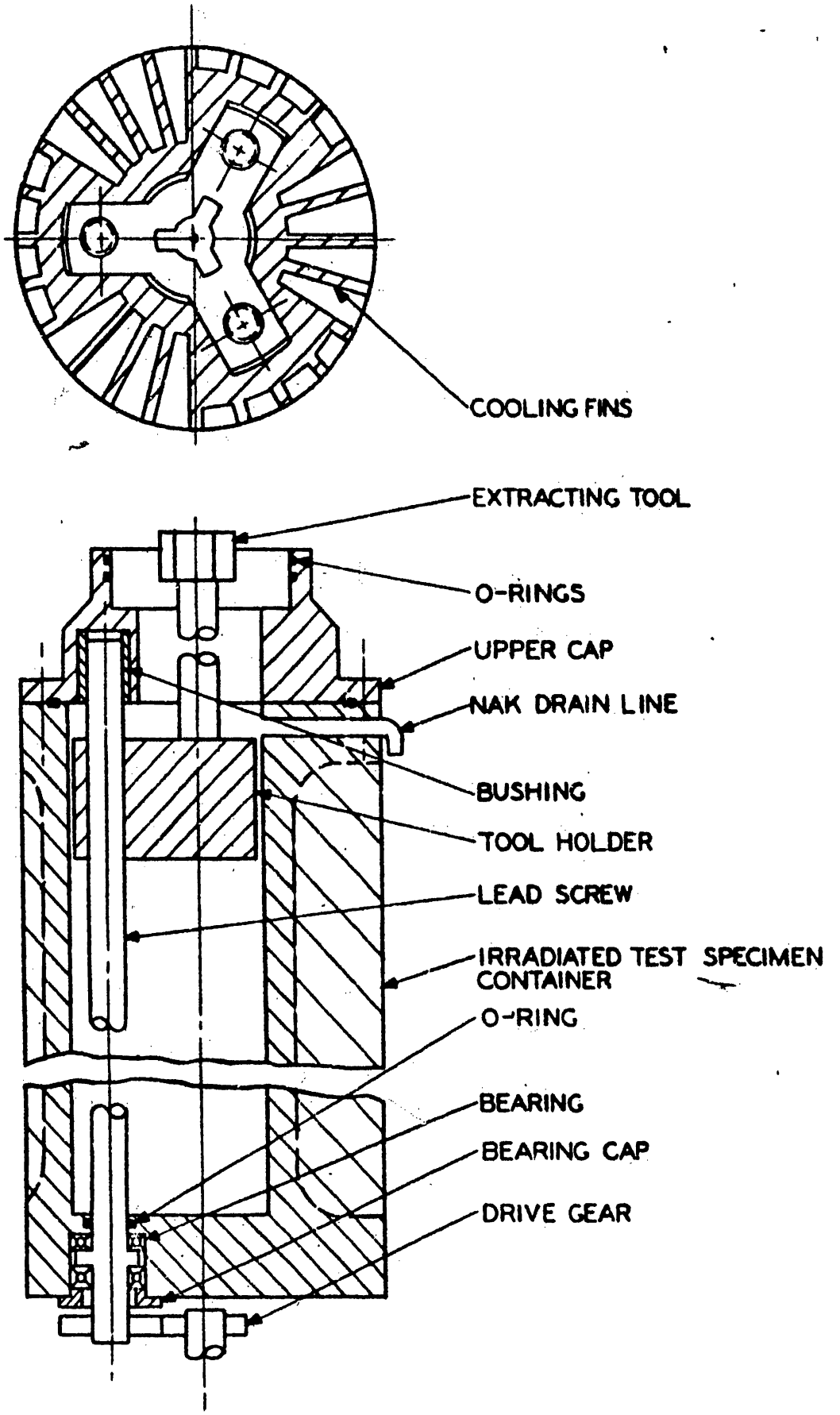

FIG: 9.5
TEST SPECIMEN REMOVAL CONTAINER

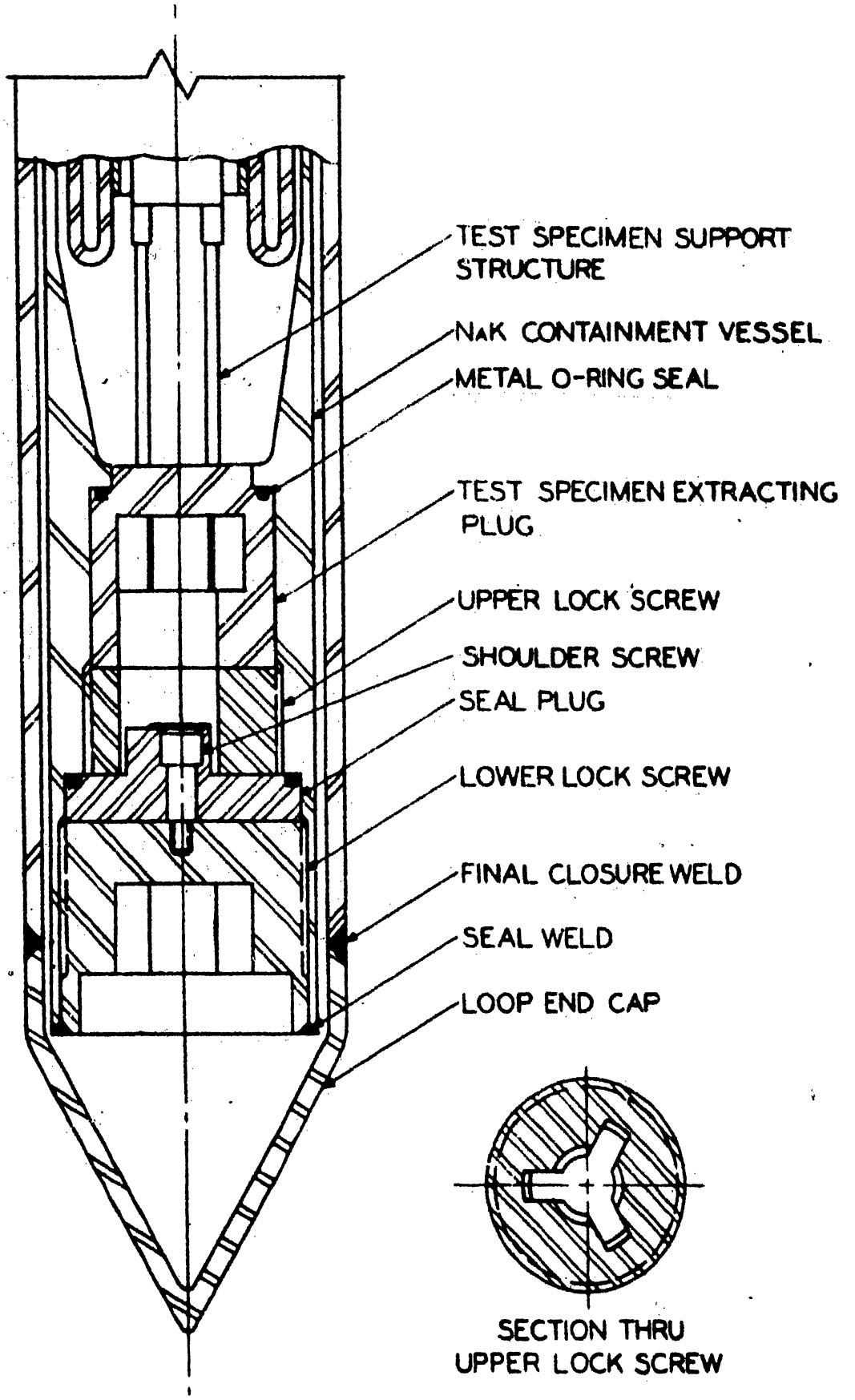

FIG. 9.6
REMOVABLE LOOP CLOSURE

The upper portion of the dry box consists of a bell jar which may be readily removed for access to the planetary tool carrier. A centering chuck, independent of the bell jar, is mounted above the tool carrier on a frame that is, in turn, rigidly attached to the carrier support table. Suitable remotely adjustable cutting and welding tools are mounted on the tool carrier, and a rotating chuck is attached to the lower end of the hollow tool carrier spindle. The tool carrier and rotating chuck assembly are driven by a variable-speed motor.

The lower portion of the dry box contains six swing carriers, arranged in two tiers of three so that the required containers and fittings may be aligned under the loop as needed. The three lower carriers handle the irradiated-test-specimen container, the new test specimen, and the radioactive-NaK container and scales. The three upper carriers handle the irradiated-test-specimen container cover, a chip cup for metal turnings from the cutting operations, and a radioactive-NaK container cap. Access to the lower chamber is required for installation and removal of the radioactive-NaK and irradiated test specimen containers and for maintenance of dry-box equipment. The dry box and the entire top portion is removed as a unit.

High-purity helium is used as the cover gas in the dry box. Purging and helium purity control in the dry box are accomplished by use of a high-vacuum pumping system coupled with a high-efficiency gas scrubber and cooler.

A detailed written procedure for handling the loop within the hot cell will be provided in the Title I design. The equipment will be tested in dry runs and installed in the dry box and the hot cell before the unloading operations start. The following procedure outline will serve as a guide for the design of the required equipment.

9.43 Dry Box Preparation

1. Carefully purge and install NaK in the irradiated-test-specimen container (Figure 9.5) to the level of the NaK drain line. Check NaK quantity by weighing the container before and after filling and noting the NaK temperature.

2. Install irradiated-test-specimen container in its swing carrier.

3. Weigh the radioactive-NaK container and place on the scales mounted in its swing carrier. Adjust swing carrier scales for zero reading with the container cap removed. Place the container cap in the proper upper swing carrier.

4. Place new test specimen in the new test specimen carrier.

5. Test operation of the lower dry box drives and manipulators.

6. Place chip cup in the proper upper swing carrier.

7. Install the tool carrier table and check out operation of all components.

8. Install the bell jar and place the plug in the opening through which loop will be introduced.

9. Evacuate dry box and test for leaks by noting loss of vacuum. If box will not hold high vacuum, it may be necessary to test with helium and a mass spectrometer to locate the leaks.

9.44 Loop Unloading Procedure

Flexible connections in the NaK and helium fill lines, and at the top of the loop will permit about a 2-foot vertical motion and a 3-foot lateral motion so the loop may be manipulated as required in the following steps. Prior to installation in the dry box, the flexible connections will be connected to the corresponding lines on the loop. The unloading procedure provides for continuous NaK immersion of the irradiated test specimen to prevent excessive fuel temperatures caused by decay heat.

1. Bleed helium from the outer annulus of the loop and take sample for analysis. Check the leak-detector indication for NaK in the loop end cap (Figure 9.6). The presence of NaK or fission-product gases in the helium buffer zone will dictate delay in opening the loop and the need for special precautions.

2. Remove the bell jar from the dry box and place centering fitting for loop end cap in rotating tool carrier.

3. Lower the loop into the fixed centering chuck until approximately in position for cutting-off the loop end cap above the weld.

4. Fit cutting tool and machine off the loop and cap.

5. Withdraw the loop from the chuck, and remove the cap and centering fitting from the cutting machine.

6. Seal the bell jar to the top of the dry box, introduce loop through the vacuum-tight glands, and secure in the fixed chuck.

7. Vent helium from the NaK system and take sample for analysis. (Special procedures may be required as dictated by the gas analysis.)

8. Start up the vacuum pump on the dry box, and make a leak test.

9. Reduce the dry box pressure to 0.1 micron of mercury to assure reasonable outgassing of internal parts.

10. Start up gas scrubber and introduce purified helium in the dry box. Maintain the dry box atmosphere about 3 inches water pressure negative to the hot cell.

11. Adjust the helium cover-gas pressure in the loop until it is less than the gas pressure in the dry box by an amount equivalent to the NaK head above the bottom of the loop. (This reduced pressure should prevent NaK leakage through faulty internal mechanical seals.)

12. Machine off the seal weld on the lower lock screw.

13. Engage lock-screw removal wrench on tool carrier, and remove lock screw.

14. Equalize gas pressure in irradiated-test-specimen container and dry box through vent in container cover. Note the NaK temperature in the container.

15. Lock the irradiated-test-specimen container in the swing carrier and clamp the container cover in the rotating chuck. Rotate chuck to remove cap. Lower irradiated-test-specimen container and place cap in proper upper swing carrier.

16. Align the irradiated-test-specimen container, and elevate through the too-carrier spindle until the extracting tool is engaged with the upper lock screw. (The lower end of the loop should now be sealed to the spent fuel container as shown in Figure 9.7.)

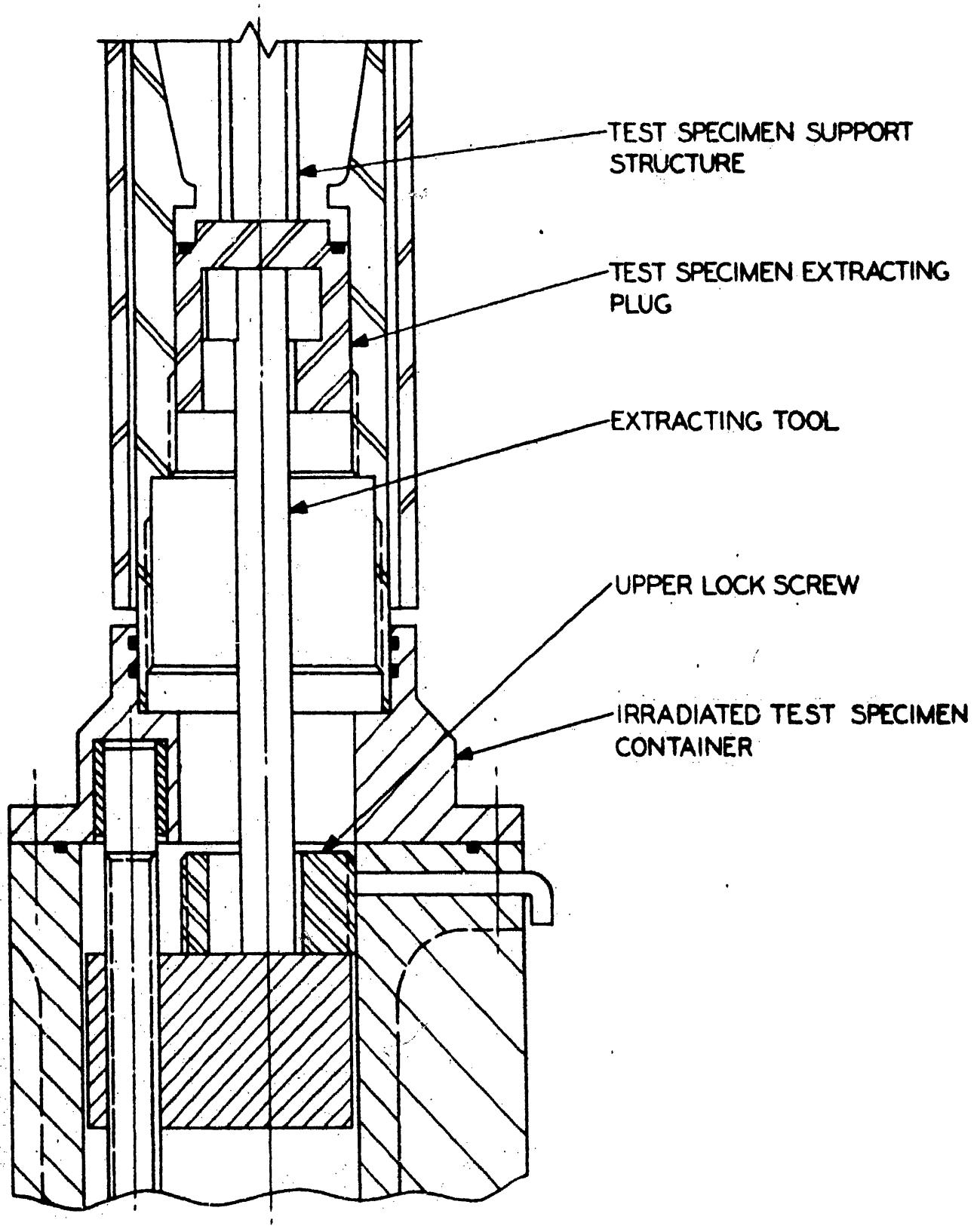

FIG. 9.7
TEST SPECIMEN REMOVAL

17. Clamp container into the rotating chuck.

18. Using NaK drain line, pressurize irradiated-test-specimen container with helium and test for leaks. If satisfactory, reduce to pressure in dry box and close off drain line.

19. Slowly rotate the irradiated-test-specimen container until the upper lock screw is free. Count the revolutions to determine when the screw is free. If the irradiated-test-specimen is free in the loop, the test specimen extracting plug will follow the lock nut and engage the extracting tool.

20. Loosen the specimen container in the rotating chuck, elevate the container, and rotate in small increments until a lock between the extracting tool and the test specimen extracting plug is assured.

21. Actuate the extracting tool screw drive and withdraw the test specimen into the container (see Figure 9.7). The number of revolutions of the screw drive established by counter, the load on the tool carrier motor, and a gamma ray counter in the lower dry box chamber should indicate when the fuel is fully withdrawn.

22. When the test specimen extracting plug is loosened in step 19 or 20, NaK from the loop will flow down around the extracting tool to fill the void above the NaK installed in the irradiated-specimen container. The displaced gas should bubble up into the loop. Thus, when the test specimen is fully extracted, the quantity of NaK above the container drain line elevation will equal the quantity installed in the loop plus an amount equivalent to the increase in volume of the NaK installed in the irradiated-specimen container produced by thermal expansion, the amount displaced from the container by the test specimens, and the NaK lost by leakage through the mechanical seals. Read the temperature of the NaK in the irradiated specimen container.

23. Place the empty radioactive-NaK container next to the irradiated-test-specimen container and position the NaK drain line over the empty NaK container.

24. Open the NaK drain-line cock and equalize the dry box and loop cover-helium pressures.

25. When the NaK stops flowing, purge with helium from the loop to dry box. (Carefully note the increase in weight of the NaK container and the NaK temperature in the irradiated-test-specimen container.)

26. Release the irradiated-test-specimen container from the rotating chuck and withdraw about two inches below the bottom of the loop. Flush helium from the loop into the dry box until NaK stops dripping.

27. Withdraw the irradiated-test-specimen container into the lower dry box chamber. Swing the irradiated-test-specimen container cover into position and tighten with rotating chuck.

28. Center the radioactive-NaK cover in the rotating chuck and install on the NaK container.

9.45 Installation of Fuel Bundle Into Bottom of Loop

1. Align new test-specimen carrier and install test specimen in loop, using rack and pinion drive on swing carrier. (The carrier consists of a guide tube with a rack and pinion operated elevator.)

2. The new upper lock screw is installed on the swing-carrier tool at the time the fuel bundle is placed on the carrier. When this screw contacts the threads in the loop, clamp the carrier tool in the rotating chuck and tighten the screw. (Note the motor load.)

3. Pressurize the loop NaK space with helium and test for leakage by loss of pressure method.

4. Remove loop from dry box and set dry-box bell jar to one side.

5. Clean the lower lock screw threads with alcohol and dry with acetone.

6. Replace the loop in the fixed centering chuck and install new seal plug and lower lock screw. (Note the motor load.)

7. Set up welding jig and seal weld the lower lock screw to NaK containment vessel.

8. Check weld integrity. (Investigation of an X-ray inspection system using the gamma rays from the shell is suggested.)

9. Install new loop end cap.

10. Set up welding jig and weld.

11. Fill helium buffer space in loop and test outer weld with mass spectrometer leak detector.

The loop is now ready for refilling with NaK and recharging with the desired helium pressures for operation. The procedure for initial filling may be followed.

After the loop is resealed and ready for transfer to the reactor, the dry box tool carrier table is removed and the irradiated fuel and irradiated NaK containers are discharged from the dry box. Prior to transfer out of the hot cell, a safety cup is sealed to the bottom of the irradiated fuel container to cover the gear drive and screw shaft and seals.

9.46 NaK Filling Procedure

The filling equipment has been used by Pratt & Whitney Aircraft for the filling of the PW-19 experiment in the ETR. With minor modifications, the existing equipment can be used for filling the fast reactor fuel test loop. In writing the detailed filling instructions for this loop filling instruction, CNLM-1192, ("Filling Instructions for the Pratt & Whitney Forced Convection Liquid-Metal In-Pile Loop Experiment, PW-19") may be used as a guide.

The amount of NaK required to be charged into the loop is critical. Since it is expected that some NaK will be entrapped and retained in the loop, the amount of NaK drained from the loop when removing the test specimen will have been carefully measured for replacement. After the required amount of purified NaK is inserted in the loop NaK container and the liquid-metal transfer is completed, the fill tube is capped at the top connection and checked for leaks. The liquid-metal and helium systems will then be pressurized through the helium fill tubes, and inspected after sealing by a mass spectrometer leak check. If a weld seal is used, a liquid penetrant inspection will become an additional requirement.

Since the loop will be in the hot cell during filling, the fill stand will be connected to linkages on the hot cell, which are

in turn connected to the loop. Permanent through-cell NaK-fill lines will be installed in two locations for the reference hot cell and at one location for the alternate hot cell. Flexible leads with suitable leak tight fittings will be attached to the NaK-fill line and helium-fill line and the top loop connections will be equipped with suitable back-pressure valves to prevent back-leakage of helium and/or NaK respectively when the flexible cell leads are disconnected. After the filling process is performed and the NaK line pressurized to assure complete line drainage, the flexible NaK-fill and helium lines will be removed at the top loop connections, capped, and leak checked. The other connections can be removed later as desired or convenient.

Protective clothing and face shields will be provided for personnel handling NaK. Adequate safety regulations for the handling of NaK will also be provided. To protect against fires, steel pans of ample capacity to contain all of the NaK in the filling system will be placed under the loop and the fill system. These pans will be filled with Ansul Chemical Company's Met-L-X to a depth of 3 inches. Adequate Met-L-X fire extinguishers will also be provided.

9.5 EXAMINATION REQUIREMENTS OF ATR FAST LOOP FUEL SAMPLES

Upon removal of a fuel bundle from the loop, it will be necessary to do the tests shown in Table 9.2 on ceramic, cermet, or metallic fast reactor fuels. These are certainly not the only tests which might be required by various experimenters but are considered to be typical of the ones that would be required by APDA if they were irradiating fuel bundles.

If the fuel is manufactured with plutonium, it may be necessary to do the post-irradiation examinations in a hot cell equipped for alpha activity or in a hot cell with a glove box facility for limiting the spread of plutonium.

TABLE 9.2 - FAST REACTOR FUEL EXAMINATION REQUIREMENTS

Work to be Done	Fuel Type		
	Ceramic	Cermet	Metallic
Before Removal of Fuel from Bundle			
1. Macro and Visual Inspection (up to 30X)	x	x	x
2. Measurement of Fuel Spacing	x	x	x
After Removal of Fuel From Bundle - Nondestructive Testing			
1. Macro Inspection (up to 30X)	x	x	x
2. Macro Photography	x	x	x
3. Fuel Outside Dimensions	x	x	x
4. Density and/or Weight	x	x	x
5. Gamma Scan for Relative Activity and Fuel Redistribution	x	x	x
6. Electrical Resistivity	-	x	x[1]
7. Leak Detection	x	x	x
8. Measurement of Meat by NDT (if possible)	x	-	x[2]
9. Fission Gas Release and Reseal of Tubes	x	-	x[2]
10. Auxiliary Dosimetry Elements	x	x	x
After Completion of Irradiation Studies - Destructive Testing			
1. Fuel Clad Stripping	x	-	x[2]
2. Metallography	x	x	x
3. Fuel Density	x	x	x[2]
4. Radiochemical Burnup	x	x	x
5. Strength Properties	-	x	x

[1] Clad integral with fuel.

[2] Sodium bonded elements.

10.0 ACKNOWLEDGMENTS

A. P. D. A. wishes to thank the following persons for their invaluable assistance in the preparation of this report:

Dr. G. W. Wensch and Dr. I. Zartman of the AEC, Division of Reactor Development, for their support and technical guidance on liquid-metal-cooled in-pile loops; Mr. A. J. Parks and Mr. R. V. Steel of Pratt & Whitney Aircraft Co., for their help in obtaining design information on the P&W in-pile loop; Mr. R. H. Gordon and Dr. A. W. Flynn of EBASCO, Mr. A. H. Lazar of Babcock & Wilcox Co., and Mr. J. B. Legerski of the AEC, Idaho Operations Office, for their review and comments during the conceptual design effort.

APPENDIX A - PHYSICS

A1. Basic Feasibility Computational Model

To determine basic feasibility, a nominal and perhaps somewhat schematic model of the test lobe has been considered, however, the model chosen maintains all the characteristics of the actual lobe that significantly effect the neutron physics of the system. The most obvious simplification is the use of one dimensional cylindrical geometry to mock up the rather complex geometry of the actual lobe. A picture of the actual shape of the lobe is given in Figure 4.1. The specifications for the reference design model are given in Section A3.

Outer radii defining the regions of the cylindrical model used here are given in Table A1. The radii used for the various regions given in Table A1 were obtained in the following manner:

Region 1 - A test sample radius was chosen that would both accommodate large fuel pin bundles and fit comfortably within the flux trap defined in Figure 3.3A of Reference (8).

Region 2 - The test wall thickness was fixed at a value appropriate for the pressures and temperatures expected in the test sample. Test wall coolant is included in this region.

Region 3 - The thermal neutron filter was arbitrarily chosen to be 1/8-inch thick for the initial physics computations.

Regions 4, 5 - Radii defining the core were taken directly from Reference (21). For simplification, all space between the core and filter is considered the flux trap.

Region 6 - The outer radius defining the aluminum A 1 wall was chosen to give a wall thickness of 0.090 inch.

Region 7 - Outer radius of the reflector was taken from Reference (21).

Region 8 - Since the physics computation is quite insensitive to shield thickness, the outer radius of the shield was chosen quite arbitrarily.

TABLE A1 - REGION RADII FOR BASIC FEASIBILITY MODEL (CYLINDRICAL GEOMETRY)

Region Number	Region Name	Outer Radius (cm)
1	Test Sample	1.905
2	Test Wall	3.811
3	Filter	4.128
4	Flux Trap	7.62
5	Core	13.97
6	Aluminum Wall	14.20
7	Reflector	31.12
8	Shield	61.12

A summary of region compositions is given in Table A2. Values for the reactor proper are basically those given for the ATR in References (8) and (21). Values for the test sample, test wall, filter, and flux trap (Regions 1 through 4) are discussed below.

Test Sample - A nominal test sample of 19 fuel pins was chosen. To insure maximum power the pins were assumed to consist of high density PuO_2. The effects of dilution are discussed in Section 4.42. The effect of cladding is neglected. A pin diameter of 0.212 inches was chosen; this represents a typical value for oxide-type pins. The remaining volume is occupied by liquid sodium of 2 density of 0.819 gm/cm^3. The test sample region compositions result from homogenization of the above components. The total test fuel volume resulting from the above dimensions represents a near maximum for this test loop. However, any results concerning feasibility from the point of view of pin power and power depressions across the loop will also hold or be conservative when applied to smaller test fuel volumes with equal or lower fuel concentrations.

Test Wall - A natural choice for the test wall composition is stainless steel. For physics computations, stainless steel will be mocked up with iron. The test wall region is composed of 0.3125 v/o liquid sodium for cooling purposes. Density of the sodium is taken to be 0.86 gm/cm^3.

Filter - Boron is chosen as the filter material. It effectively shields thermal neutrons and offers some shielding to neutrons whose energies correspond to those of the high cross-section resonance regions of the test specimen. Further, boron cross-sections over a wide energy region and the physical characteristics of boron compounds are known quite well.

Several boron concentrations are analyzed in order to provide a range of power levels and power depressions. The specific concentrations chosen are given with the results in Table 4.1 of the main body of the report.

TABLE A2 - REGION COMPOSITIONS BY ELEMENT FOR BASIC FEASIBILITY STUDY

Region Number	Region Name	Element	Elemental Number Density (atoms/cm^3 x 10^{-24})
1	Test Sample	Pu-239	0.008607
		O	0.017214
		Na	0.01338
2	Test Wall	Fe	0.05842
		Na	0.007038
3	Filter	B	Variable
4	Flux Trap	Al	0.0543
		H	0.00654
		O	0.00327
5	Core	U-235	0.0003223
		U-238	0.00002426
		Al	0.0266
		H	0.03652
		O	0.01826
		Fe	0.0005222
		B	0.00002713
6	Aluminum Wall	Al	0.0603
7	Reflector	Be	0.1108
		H	0.00654
		O	0.00327
8	Shield	Fe	0.0316
		H	0.0410
		O	0.0205

Axial buckling = 0.000533 cm^{-2}

Flux Trap - The flux trap as envisioned by those interested in thermal flux loop testing consists mainly of moderating material. However, for the case at hand, moderating material in the flux trap medium must be kept at a minimum to allow the passage of fast neutrons to the test sample. Aluminum was chosen as the chief material for this region; 10 v/o water was allowed for cooling purposes. Water density corresponds to a temperature of 158 F.

The physics analysis has been based chiefly on 16-group diffusion theory in one-dimensional cylindrical geometry as solved by the digital computer code AIM-VI. The code is an extension of AIM-V, which is described in "AIM-VI-A Multigroup, One-Dimensional Equation Code."(16). A single pin analysis not employing diffusion theory is discussed in Section 4.32. Also, the uncertainties involved in the use of diffusion theory to predict neutron transmission through the highly absorbing neutron filter are discussed in Section A.51.

A2. Cross Sections

The chief source of the multigroup cross sections including fission spectrum is the 16-group library 3W-383 compiled by Atomics International and currently used with the digital code AIM-VI. Energy definition of the groups is given in Table A3. Exceptions to the source mentioned above are discussed below by element.

Pu-239

There is no Pu-239 in the 16-group library mentioned above. The 16-group values for Pu-239 that have been used are nominally those given on page 623 of "Computational Survey of Idealized Fast Breeder Reactors." (17). However, the fission and capture cross section in the region of resolved resonances must be discussed further. The flux spectrum transmitted through the low-energy neutron filter is such that this resonance region accounts for a large fraction of the absorption rate in the sample. Precise determinations of the group cross sections involved (Groups 9 through 12, 14, 15) require a rather complex computation utilizing specific knowledge of operating temperature, sample size and composition, and composition of coolant. Therefore, for the purpose of establishing feasibility of the filter concept, cross-section limits have been established that bracket the true group values. Analyses will be performed using both the upper and lower limit to the cross section in the resonance region.

An obvious upper limit will be the capture and fission cross sections that correspond to infinite dilution. These are the values given

TABLE A3 - SIXTEEN-GROUP SPECIFICATIONS

Group	Energy Range	Lethargy Range	Δ u
1	3 - 10 mev	0 - 1.204	1.204
2	1.4 - 3	1.204 - 1.966	0.762
3	0.9 - 1.4	1.966 - 2.408	0.442
4	0.4 - 0.9	2.408 - 3.219	0.811
5	0.1 - 0.4	3.219 - 4.605	1.386
6	17 - 100 kev	4.605 - 6.377	1.772
7	3 - 17	6.377 - 8.112	1.735
8	0.55 - 3	8.112 - 9.808	1.696
9	100 - 550 ev	9.808 -11.513	1.705
10	30 - 100	11.513 -12.717	1.204
11	10 - 30	12.717 -13.816	1.099
12	3 - 10	13.816 -15.020	1.204
13	1 - 3	15.020 -16.119	1.099
14	0.4 - 1	16.119 -17.035	0.916
15	0.1 - 0.4	17.035 -18.421	1.386
16	Thermal (.025)	18.421 - arbitrary	arbitrary

on page 623 of Reference (17). A lower limit has been established with the aid of Figures 3 and 4 of Reference (17). Here, group cross sections are plotted as a function of the effective total scattering cross section per absorber atom for a homogeneous mixture. An effective value of scattering per atom that takes into account the heterogeneity of the system is estimated for the system of PuO_2 pins in sodium. (See page 175 of "Neutron Self Shielding." (18)). The resulting value is 10 barns per atom. Since the effects of Doppler broadening have thus far been omitted, the group cross sections in the resonance region corresponding to a scattering cross section of 10 barns per atom represent a lower limit. Specific values were obtained from Figures 3 and 4 of Reference (17) mentioned above. The resulting upper and lower limit group cross section in the resonance region are summarized in Table A4.

Since it is expected that high operating temperatures will be attained in the test samples, Doppler broadening may be expected to significantly increase the true cross sections above the lower limit values given in Table A4. However, the resulting true values will be biased toward the lower cross section limits (with the possible exception of Group 9) unless the moderation of the test sample region is significantly increased.

An accurate value of thermal cross section (Group 16) is rather difficult to obtain because of the complex nature of the thermal flux spectrum in the test sample. However, contribution to total sample power from this group is almost negligible so that the analysis is quite insensitive to the thermal cross section values chosen. A nominal value was obtained by assuming the thermal spectrum to be a Maxwellian distribution corresponding to the core temperature (158 F). The resulting capture and fission cross-section values are used in conjunction with the lower limit resonance values and are given in Table A4. Thermal cross section values used in conjunction with the upper limit cross sections in the resonance region were taken directly from page 623 of Reference (17). These values are repeated in Table A4.

U-235

Cross-section values for U-235 are those of the 16-group library mentioned earlier with the following exceptions: capture and fission cross sections in Groups 11 and 12 are altered to take into account the effect of finite dilution in the core; the thermal values (Group 16) of capture and fission are adjusted to correspond to a Maxwellian distribution of thermal neutron flux for the core operating temperature. Alterations in the resonance region utilize Figures 1 and 2 of Reference (17). The revised values are given in Table A4.

Since an analysis of uranium oxide as the sample material is included, the U-235 cross sections in the region of resolved resonances

TABLE A4 - SUMMARY OF REVISED MULTIGROUP CROSS SECTIONS

Pu-239

Group	$\nu\sigma_f$ (maximum) (barns)	σ_a (maximum) (barns)	$\nu\sigma_f$ (minimum) (barns)	σ_a (minimum) (barns)
9	47.19	25.1	40.04	21
10	120.12	83.0	22.88	12
11	223.08	133.0	48.62	25
12	68.64	43.0	20.02	10
14	397.54	224.0	228.8	124
15	3492.06	2013.0	2173.6	1220
16	2016.3	980.0	1898.0	905

U-235

Group	$\nu\sigma_f$ (barns)	σ_a (barns)
11	112.7	74
12	84.6	53
16	1140.0	549

Hydrogen

Group	σ_t (barns)
16	29.33

Boron

Group	σ_a (barns)
16	618

U-238
(for sample dilution study only)

Group	σ_a (barns)
8	2
9	4
10	10
11	6
12	10

U-235
(for cases involving UO_2 samples only)

Group	$\nu\sigma_f$ (barns)	σ_a (barns)
10	82.81	51.8
11	41.65	26.0
12	30.01	24.5
13	44.35	23.1
16	1140.0	549.0

must be altered to correspond to the dilution of the sample. The method of alteration is identical to that used for the lower limit values of Pu-239. Specific values were obtained from Figures 1 and 2 of Reference (17) for a dilution of 10 barns per atom. These revised values are given in Table A4. For the sake of simplicity, the above revisions in U-235 resonance cross sections were also used in the core for the cases involving UO_2 samples. The resulting values of effective multiplication have been corrected to take into account the accompanying reduction in U-235 absorption. The effect on other quantities is negligible since the fractional changes in absorption rates involved is not great.

U-238

Since the core is highly enriched, results are not sensitive to reasonable variations in U-238 cross section. Therefore, for the basic feasibility study, the library values mentioned above were used without alteration. However, an investigation was made of the effect of diluting the PuO_2 sample with depleted UO_2. Absorption cross sections in the resolved resonance regions of U-238 now become important. The corresponding group values were obtained in the same manner as the lower limit group values in the resonance region for Pu-239. However, to be conservative, the effective scattering per atom was increased to 30 barns per atom. Based on the computational model given in "The Quantitative Evaluation of Resonance Integrals." (19) for the volume component of the U-238 resonance integral, the maximum increase possible because of Doppler broadening at 3000 F for the resonances of interest is a factor of 1.5. The resulting U-238 absorption cross sections were doubled so as to adequately allow for Doppler broadening since such broadening has a deleterious effect on power depression. The resulting values are given in Table A4.

Boron

Cross section values for boron are those of the 16-group library mentioned earlier with the exception of the thermal absorption cross section. This cross section has been adjusted to correspond to a Maxwellian thermal flux distribution at 158 F. The resulting value is given in Table A4.

Hydrogen

Cross-section values for hydrogen are those of the 16-group library mentioned earlier with the exception of the thermal value for the transport cross section. The microscopic transport cross section is adjusted so that when used in conjunction with water at a density of 1 gm/cm^3, the diffusion coefficient for water becomes 1.60 cm. The resulting value of the transport cross section is given in Table A4.

A2.1 Pu-239 Cross Section Options

To ensure the bracketing of the true group cross section values in the regions of resolved resonances, two sets of Pu-239 cross sections have been used in the basic feasibility analysis. It is desirable to establish a single reference case and, hence, a choice as to which of the two options is better will be made. It should be mentioned at the outset, however, that basic feasibility criteria may be met with either option with a realizable filter. * Admittedly, design problems would increase were the high option the correct value, since any increase in boron increases design problems.

If the sample region were part of a normal core with a slowing down source, the low limit cross sections that correspond to very undilute material with a Doppler broadening correction would be appropriate. In the case at hand however, the problem is partially like a transmission problem with a given incident flux spectrum and negligible diffusion and slowing down. Hence, if treated entirely as a transmission problem, at the outside edge of the sample region the appropriate cross section would be the actual Doppler broadened Breit-Wigner shape. However, at a distance of several mean free paths inside the pin, a small fraction of the pin diameter, self-shielding in the energy regions of the resolved resonances would quickly reduce the effective cross sections.

Neither of the foregoing extremes are the case. However, it is felt that there is sufficient scattering (approximately 10 barns per plutonium atom due to oxygen alone) to warrant the conventional treatment and justify choice of the lower cross section limit. However, an estimate of the effect of pure transmission on power depression through a single pin is obtained by comparing exponential attenuation with the high limit cross section to that obtained using the low limit value. The distances over which the foregoing comparisons are made are taken as 3 mean free paths for the Group 15 absorption cross section. It can be shown that by far the greatest power depression near the outside of the sample is due to the component in Group 15. The result is that a pure transmission model would increase the power depression by approximately 10%. Though the effect is not desirable, it is by no means disastrous. Further, since the assumptions implicit in the analysis above are quite conservative, the 10% value may be considered maximum.

The reference case for basic feasibility therefore has been chosen among those corresponding to the minimum Pu-239 cross section values. Also, the design values are based on analysis that utilize the minimum values.

* * The B-10 concentrations used in Cases 3 and 5 approximately correspond to 2 and 1 w/o, respectively, of fully enriched boron in stainless steel for the geometry used.

A3. Physics Specifications for Reference Design

Physics computations for the conceptual design of the fast test loop are based upon a one-dimensional cylindrical model similar to that used for the basic feasibility study (See Section A1) but incorporating the following revisions. The sample loop inside diameter (accommodating seven fuel pins of diameter 0.236 inches) is reduced; tube wall composition is altered slightly; the 1/16-inch water gap interior to the filter has been included for cooling purposes; filter is taken as boron steel with thickness increased to 0.15 inches; the flux trap has been replaced by an extended core identical in composition to the nominal core; the inner aluminum wall of the core has been included as a separate region. Various sample enrichments of both PuO_2 are considered in the analysis.

A summary of region concentrations and outer radii for each region used in the conceptual design physics computation is given in Tables A5 and A6.

A4. Effect of a Cadmium Filter on the Pu-239 Resonance at 0.297 ev

A brief analysis of the variation of power spectrum across the plutonium sample reveals that a major portion of the power depression is due to the plutonium cross-section resonance at 0.297 ev, which occurs in energy Group 15 of the 16-group set. An estimate of its effect is obtained by deleting the fifteenth group component from the flux incident on the sample and comparing the resulting power depression with that obtained in the normal manner. This comparison has been performed for Case 5 (the reference case) and Case 7 (the case in which the 1/16-inch water annulus is included). The results are included in Table A7.

Upon examination of Table A7 it is immediately obvious that the Group 15 flux component is a major cause of the power depression in the plutonium sample. Further, it can be seen that its power contribution is insignificant only at the sample edge by comparison of the fractional contribution of the flux component at the edge of the sample to the fractional contribution averaged over the entire sample.

If the flux in the vicinity of the 0.297 ev resonance could be removed without appreciably altering the higher energy flux, the sample power depressions would be greatly reduced. The inclusion of cadmium in the filter offers an interesting possibility for such flux removal. At the energy of the plutonium resonance peak (.297 ev), cadmium and B-10 have approximately the same cross section. However, between 0.297 ev and the Group 15 lower energy boundary, the cadmium cross section is significantly greater than that of B-10. Contrarily, above 0.297 ev the reverse is true for most of the energy range of interest. Therefore, it may be possible to add to a B-10 filter, for example, twice as much

TABLE A5 - REGION CONCENTRATIONS AND OUTER RADII FOR PHYSICS MODEL OF FAST LOOP REFERENCE DESIGN (CYLINDRICAL GEOMETRY)

Region Name	Outer Radius (cm)	Element	Elemental Number Density (atoms/cm^3 x 10^{-24})
Test Sample	1.08	See Table A6 for fuel concentrations.	
		Fe	0.0203
		Na	0.00484
Test Wall	3.65	Fe	0.0483
		Na	0.00473
Cooling Annulus	3.81	H	0.0654
		O	0.0327
Filter	4.19	B-10	0.00523
		Fe	0.08212
Extended Core	6.67	U-235	0.0003223
		U-238	0.00002426
		Al	0.0266
		H	0.03652
		O	0.01826
		Fe	0.0005222
		B	0.00002713
Aluminum Wall	7.62	Al	0.0603
Core	13.97	U-235	0.0003223
		U-238	0.00002426
		Al	0.0266
		H	0.03652
		O	0.01826
		Fe	0.0005222
		B	0.00002713
Aluminum Wall	14.20	Al	0.0603
Reflector	31.12	Be	0.1108
		H	0.00654
		O	0.00327
Shield	61.12	Fe	0.0316
		H	0.0410
		O	0.0205

Axial buckling = 0.000533 cm^{-2}

TABLE A6 - SAMPLE FUEL CONCENTRATIONS
FOR PHYSICS MODEL OF FAST LOOP CONCEPTUAL DESIGN
(atoms/cm^3 x 10^{-24})

	Sample Fuel			
Case	Pu-239	U-235	U-238	Oxygen
12	0.01212 (100%)	0	0	0.02424
13	0.00909 (75%)	0	0.00303	0.02424
14	0.00303 (25%)	0	0.00909	0.02424
15	0	0.01212 (100%)	0	0.02424
16	0	0.00909 (75%)	0.00303	0.02424
17	0	0.00303 (25%)	0.00909	0.02424

TABLE A7 - EFFECT OF 0.297 ev Pu-239 RESONANCE (GROUP 15) ON SAMPLE POWER DEPRESSION

Case	Normal Power Depression	Power Depression Group 15 Deleted	Edge Power From Group 15 (%)	Average Power From Group 15 (%)
5	1.29	1.15	11	1.5
7	1.43	1.22	15	2.2

cadmium, on a number density basis, as B-10. Hence, the power contribution of the 0.297-ev plutonium resonance would be significantly reduced, while the effect on the higher energy contributions would be relatively small.

The optimum combination of cadmium and B-10 is not clear at this point. The analysis in the vicinity of the 0.297-ev plutonium resonance would be quite complex due to the sharp energy dependence of the cross sections involved. However, it is expected that a definite improvement in power depression for plutonium samples could be achieved through the use of a combination of B-10 and cadmium in the filter. An upper limit to the improvement in power depression that could be expected may be obtained from Table A7, where power depressions omitting the contribution of Group 15 are tabulated. It is interesting to note that the corresponding reduction in total sample power caused by the deletion of the Group 15 contribution is relatively small.

A5. Review of Computational Uncertainties

Various characteristics of the proposed fast lobe design make rigorous physics computations in certain areas rather difficult. Hence, more approximate methods have been used where it was felt a more rigorous approach would be too time consuming and hence beyond the scope of this preliminary conceptual design report. Therefore, the uncertainties inplicit in the more approximate methods are discussed in the following paragraphs.

A5.1 Diffusion Theory

Multigroup diffusion theory has been the basis for the bulk of the physics analysis discussed herein. Small, highly absorbing regions, such as the neutron filter, severely test the applicability of diffusion theory. In the case of the filter, however, the resulting inaccuracies in pin power for a given filter may be compensated for by some flexibility in the choice of filter size and poison concentration.

A comparison has been made of the flux depression based on straight-line transmission, over an interval equal to the filter thickness, to diffusion theory results at energies where transmission phenomena should predominate. Results indicate that diffusion theory underestimates flux depression through the filter. An upper limit to flux depression is obtained by assuming exponential attenuation through a distance equal to twice that of the filter thickness (mean chord length for equivalent slab). Comparison of the resulting expontial flux depression to depression predicted by diffusion theory over the energy groups where

diffusion theory is questionable will lead to an estimate of the power uncertainty in the sample. The resulting uncertainty in sample power for a given eiltor is ± 25% for the reference case.

No attempt has been made to estimate uncertainty in predicted lobe reactivity values obtained from the diffusion theory model.

A5.2 Cross Sections

A large fraction of sample power and the power depression are caused chiefly by the large resonances in the fuel sample (Pu-239) at low energies. The corresponding effective group cross sections are quite sensitive to the fine structure of the flux spectrum. Due to the nonuniform geometry and severe anistropy of the indicent fluxes, these effective cross sections are difficult to obtain. Here, a philosophy of extremes is employed where upper and lower limits that bracket the true cross section values are used. Since acceptable results are obtained with either set, basic feasibility of the concept is not imperiled by these sample cross-section uncertainties. A plot of sample power as a function of sample power depression for both Pu-239 cross-section extremes used is given in Figure A1. For power depressions of interest (1.5) the curves are fairly insensitive to resonance cross-section choice. A proper choice is nevertheless important. The basis for such a choice and the method for obtaining maximum and minimum limits together with an estimate of the effect of a cross-section error is given in Section A2.1.

A5.3 Power Depression Through Single Pin

Both cross section uncertainties as discussed above and non-symmetric geometry make analysis of power depression through a single pin rather difficult. Again, a philosophy of extremes is employed so as to bracket the true value. Basis for these extremes are given in Sections 4.31 and 4.32.

A5.4 One-Dimensional Model

Mocking up the actual ATR lobe in one-dimensional cylindrical geometry obviously introduces error into the computational results. The expected asymmetry of the thermal neutron flux is not expected to be large based on the results of "Thermal Flux Profile." (20). The higher energy fluxes may show a greater asymmetry but the asymmetry is not expected to affect feasibility. A prediction of the effects of the nonsymmetric geometry involved may be made within the limits of diffusion theory by employing the two-dimensional PDQ code. A

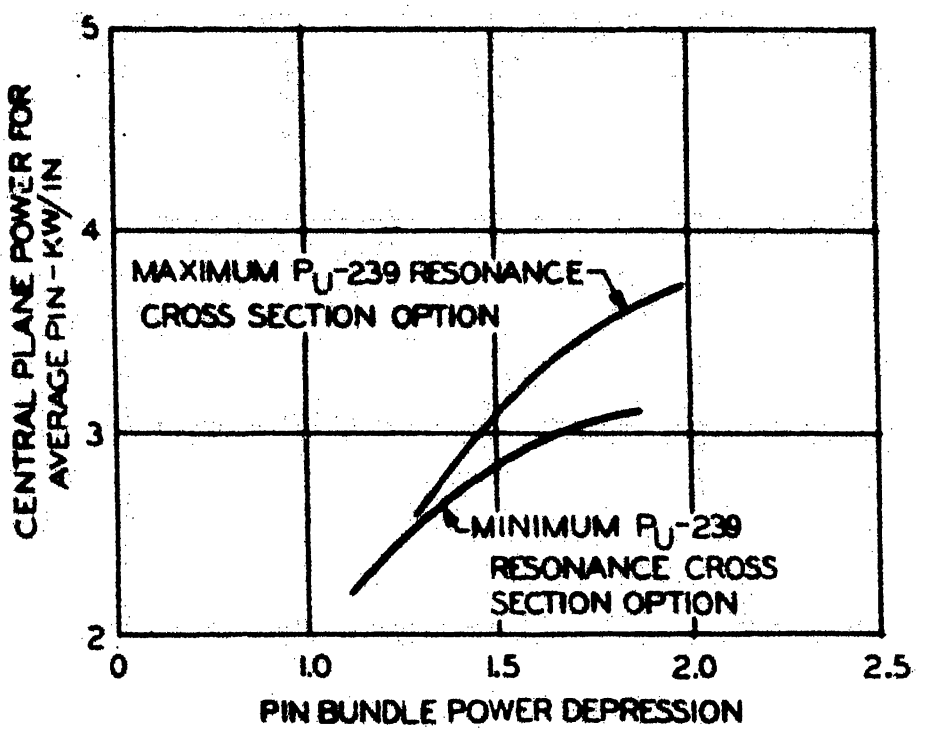

FIG. A.1
EFFECT OF RESONANCE CROSS SECTION ON SPECIMEN PERFORMANCE

judicious selection of energy groups (maximum of four allowed) should allow one to estimate the flux patterns over the energy ranges of importance.

Any absolute determination of reactivity must also incorporate a two-dimensional analysis. However, all reactivity analyses of this study have been on a relative basis using a standard value. It is not expected that the use of cylindrical geometry will introduce significant error in the determination of these relative values. The limitations of diffusion theory is a greater source of uncertainty at this point.

A5.5 Reduction of Uncertainty

Uncertainty analysis in this report has been brief. However, based on the results obtained where the philosophy of extremes has been employed and based on the rather wide range of design alternatives available, neither the basic feasibility nor the practicability of a working design for the fast test loop is imperiled by the uncertainties involved.

Obviously, before a final design can be accomplished, the uncertainty in some of the design variables must be decreased. A parameter study incorporating one velocity transport theory would aid in the establishing more precisely the necessary boron thickness. A multigroup transport analysis of the proposed design would be quite valuable in further reducing uncertainty and in revealing the directional aspects of the neutron fluxes involved. However, the need of a critical experiment employing the filter concept cannot be overstated. Reactivity and fission distribution measurements can remove many of the uncertainties involved in the filter concept analysis.

APPENDIX B

RECOMMENDED TITLE I DESIGN STUDIES

B1. LOOP HEAT TRANSFER STUDY

A comprehensive study of the heat transfer system will be required in the Title I effort to determine the optimum heat transfer system and the optimum operating conditions for the in-pile loop. Some of the mechanisms of heat transfer were deliberately neglected in the conceptual design to give the most conservative heat exchanger capability. Thus, it is expected that the capacity of the heat exchanger will be greater than that shown in Figures 3.13 and 3.14. The comprehensive study will determine the NaK flow rate to be used. It appears that a portion of the NaK flow must be allowed to bypass the test specimen if the desired temperatures into and out of the test specimen are to be held and the maximum allowable primary coolant temperature is not to be exceeded. The study also may indicate that air is preferable to either helium or water. The use of gas for the secondary coolant increases the temperature control and reduces the minimum test specimen power but exacts a penalty in the form of reduced capacity, increased circulation costs, and the inability to remove the loop through the top head of the ATR pressure vessel. The use of water increases the heat transfer capability of the unit for given temperatures but also limits the amount of control of loop temperatures that may be attained without boiling in the secondary coolant channel.

The heat transfer from the outer cylinder of the loop and the thermal neutron filter to the ATR primary coolant in the in-core region must be checked in the Title I effort to be certain that the stresses due to temperature gradients are not excessive. The work performed in the conceptual design indicates that no serious problems are involved.

B2. LOOP STRESS ANALYSIS

A comprehensive stress analysis will be required in the Title I work. Much of the work done by Pratt & Whitney should be applicable to the proposed modifications to the Pratt & Whitney loops. It is expected that the major stress components will be due to temperature effects, as the internal helium pressures can be chosen to minimize the stress components due to pressure. Some difficulty may be experienced in balancing these pressures in Concept 1 because the preliminary calculation of the secondary coolant pressure drop through the loop is approximately 300 psi for an inlet pressure of 600 psig.

Since the major stresses will be thermal, the stress analysis will require a comprehensive heat transfer analysis. The spiraled pump discharge tubes must be checked to be certain they will accommodate the differential expansion between the hot and cold legs of the NaK circuit. The preliminary work indicates they will be sufficiently flexible for this service. In Concept 2, a temperature difference of 1000 F exists between the primary and secondary coolants where the primary coolant enters the heat exchanger. This temperature difference is divided between two stainless-steel walls and two film resistances. Thus, the maximum strain across any one wall is less than 0.004 inch/inch and is acceptable. The acceptable strain of 0.004 inch/inch is based on a conservative extrapolation of strain-fatigue data for Type 304 stainless steel[22] The discontinuity stresses at junctions between adjacent parts, as well as the stresses due to the axial and radial temperature, must be accounted for. Thus, a strain fatigue criterion similar to a modified Goodman Diagram must be established, based on metal temperatures and expected number of cycles. The combined heat transfer analysis and stress analysis may require revision of the NaK temperatures listed in the Summary (Table of Design and Performance Objectives).

B3. LOOP THERMOCOUPLE LOCATIONS

With one exception, the number of thermocouples and the method of installation will be identical to the original P&W design. The location and number of thermocouples is given in Report CNLM-1194[1] and in the P&W drawings listed in Appendix C. Because the fuel bundle is designed to be removable, it may not be possible to install a thermocouple on the fuel specimen. Therefore, this problem should be studied during the Title I effort. If it is impossible to install a thermocouple on the fuel specimen, the temperature of the fuel can be estimated by thermocouples installed in the NaK stream above and below the test specimen. In addition, provision should be made for either replacing or doubling the number of thermocouples used to monitor critical operating conditions that may affect reactor safety, e.g., the NaK outlet temperature from the test specimen.

B4. THERMAL NEUTRON FILTER

A comprehensive physics study will be required in the Title I effort in order to specify the final design of the thermal neutron filter. The study should include the following:

1. Determining the composition-dependent multigroup cross sections in the plutonium resonance region.

2. Programing and running a transport analysis of neutron transmission through the boron-loaded filter.

3. Studying the methods of adjusting initial lobe reactivity and time-reactivity variation. The fuel concentration and burnable poison content of the extended core should be investigated.

4. Establishing the preliminary design characteristics of the filter and running a two-dimensional computer program to determine the interaction of the fast reactor fuel testing lobe with the remainder of the reactor system.

5. Planning the critical experiment.

A study of thermal neutron filter lifetime in relation to fuel specimen lifetime (burnup, power, power depression) and extended core lifetime should be made. If the filter lifetime is limiting, an investigation of thicker filters with lower boron concentration should be made. The effect of lobe reactivity as a function of time should be investigated also.

After establishing the design characteristics of the neutron filter, a fabrication development program should be undertaken. In all probability the reference filter will be a vendor supplied item. In addition, a radiation testing program should be undertaken which should include the following items:

1. Out-of-pile testing.
2. In-pile testing.
3. Post irradiation testing.

B5. DECAY HEAT PROBLEM

Comprehensive decay heat calculations and heat transfer studies should be undertaken to determine the required time after reactor shutdown before the loop heat exchanger and motor can be shutdown. The calculations performed in the conceptual design study were conservative, since natural convection of the NaK in the loop was not considered.

B6. TEST SPECIMEN REMOVAL SYSTEM

During the Title I effort it will be necessary to make working models of the removable loop closure (Section 3.21) and the test specimen removal container (Section 9.41). Since the success of the entire remote loading and unloading operation depends on the proper function of these components, a complete functional mock-up must be fabricated and operated. The requirements of the mock-up are as follows:

a. A simulated loop

   (1) NaK capacity equivalent to actual loop but no pumps or heat transfer requirements.
   (2) Simulated fuel bundle.
   (3) Loop closure.
   (4) Simplified NaK fill system.

b. Test specimen removal container.
c. Simulated radioactive-NaK container.
d. Suitable glove-type dry box and handling jigs.

The functional mockup will be used for automatic cutting and welding studies, testing and examination of welds, and remote-operated loading and unloading studies.

B7. DRY BOX

The dry box is a specialized machine, custom designed to perform the task outlined in the minimum space required and with as simple an operating procedure as possible.

Features requiring special attention are outlined below:

a. The Dry Box

As far as possible construction should be of flame- and caustic-resistant transparent material that will not appreciably darken under gamma irradiation. The shape may be either cylindrical or rectangular. A survey for the best material of construction will be required, and realistic specifications, perhaps short of the ideal, may be necessary.

b. The Dry Box Atmosphere Control System

This system must be capable of producing and maintaining a helium atmosphere in the dry box such that the loop Nak or sodium will remain bright and uncontaminated. Also, there must be suitable circulation and cooling of the gas atmosphere to remove the heat generated in the removed fuel bundle without causing excessive temperatures in the dry box or the fuel bundle. For safety, cooling water should be at subatmospheric pressure as in the plutonium facility at ANL.

An experimental model of the gas scrubber may be required. Major components are

(1) Vacuum roughing pump.
(2) Vacuum oil diffusion pump.
(3) Liquid nitrogen cold trap.
(4) Gas scrubbing tower.
(5) Gas circulating pump (for helium).
(6) Gas cooling heat exchanger.
(7) Gas purity monitoring equipment.
(8) Gas temperature monitoring and control.
(9) Gas sampling connections for activity monitoring.

c. Lower Portion of Dry Box

Figure 9.4 does not indicate a means of access to the lower chamber of the dry box nor the exact nature of the six carriers mentioned in Section 9.42. The components of the lower dry box are as follows:

(1) Carrier for the specimen removal container.

(a) Capable of horizontal and vertical motion.
(b) Such that the container may be locked so that it cannot rotate or,
(c) Supported so that it may rotate freely as required.

(2) Carrier for the irradiated NaK container.

This carrier should incorporate a weighing device for measuring the quantity of NaK introduced. Horizontal and vertical mobility are required for removal and installation of the cover. The exact method of transferring Nak from the specimen removal container to the irradiated NaK container must be considered in the carrier design.

(3) Carrier for the new test specimen.

(a) Capable of horizontal and vertical alignment
(b) Such that the fuel bundle may be elevated all the way into the loop
(c) Provision for clamping and rotating the support to secure the lock screw as outlined in item 2 section 9.45.

(4) The cap holders noted in section 9.42.

These must be capable of horizontal motion to align the caps and provide a means for a gripping and releasing. Also they must be free to elevate with the lower carriers.

(5) The mechanical components for the manipulation of the carriers.

These components will probably require custom design and manufacture. Suitable vacuum-tight electrical and mechanical seals may be found on the market.

d. Tool Carrier and Machinery Table

This item will have to be custom designed but conventional components may be selected for chucks and tool holders. Items requiring special attention are

(1) Tool carrier rotating assembly and drive.
(2) Remote operation of chucks and tool holders.
(3) Method for measuring torque applied by motor drives, as will be required in remote operations. Suggested method is motor current.
(4) Alignment and inspection equipment required to set up and monitor work.

e. Loop Entry Vacuum and Gas Tight Gland

(1) A double seal is suggested with a vacuum and/or gas intermediate annulus.
(2) Design of a mating surface on the loop may be required.
(3) One alternate scheme for this might be to have a fixed, as opposed to sliding, seal on the loop and to provide for large elevation adjustment in the dry box.

APPENDIX C

PRATT & WHITNEY REPORTS AND DRAWINGS

C1 REPORTS

Report Number	Title
TIM 602 Part II	Forced Convection Liquid Metal In-Pile Loop Hazards Evaluation (CONFIDENTIAL)
IDO-16545	PW-19 Hazards Survey (SECRET)
TIM 318 Supplement B	Plastic Strain Fatigue Test
TIM 476	Forced Convection Liquid Metal In-Pile Loop Pump Performance Characteristics
TIM 479	Forced Convection Liquid Metal In-Pile Loop Lower End Temperature Distribution and Heat Transfer Calculation
TIM 480	Forced Convection Liquid Metal In-Pile Loop Upper End Heat Transfer Analysis
TIM 483	Forced Convection Liquid Metal In-Pile Loop Liquid Metal Pressure Drop Calculation
TIM 499	Forced Convection Liquid Metal In-Pile Loop Liquid Metal Volume Calculation
TIM 552	Forced Convection Liquid Metal In-Pile Loop Hydrodynamic Test of the Liquid Metal Circuit
TIM 557	ETR In-Pile Loop Stress Analysis
TIM 557 Supplement A	ETR Mark II In-Pile Loop Stress Analysis
TIM 575	Forced Convection Liquid Metal In-Pile Loop Helium Pressure Calculations
TIM 575 Supplement 1	Forced Convection Liquid Metal In-Pile Loop Helium Pressure Calculations
TIM 602 Part I	Forced Convection Liquid Metal In-Pile Loop Hazards Evaluation

Report Number	Title
CNLM-1192	Filling Instructions for the Pratt & Whitney Forced Convection Liquid Metal In-Pile Loop Experiment
CNLM-1194	Experimental Operating Instructions for the Pratt & Whitney Forced Convection Liquid Metal In-Pile Loop Experiment

C2 DRAWINGS

Drawing No.	Title
T-1000384	Pin - Support Arm Connecting Link
T-1000385	Support Assembly - ETR In-pile Loop
T-1000419	Lock - In-Pile Loop Housing
T-1000421	Tube - 0.840 OD x 0.625 ID x 9.030 Long
T-1000422	Tube - 1.310 OD x 1.045 ID x 6.000 Long
T-1000424	Support - ETR In-pile Loop
T-1000426	Tee - Air Manifold Tube
T-1000435	Coupling - 1.000 Diameter Tube
T-1000437	Support - Thermocouple Tubes
T-1009394	Cap - In-pile Loop
T-1009396	Jacket - Intermediate Inner, Water
T-1009405	Connector - Water Jacket
T-1009406	Tube - Water Jacket
T-1009409	Reducer - Inner Water Jacket Tubes
T-1009410	Jacket - Inner Upper, Water
T-1009412	Jacket - Liquid Metal Outer
T-1009414	Reducer - Liquid Metal - Upper Outer Jacket
T-1009415	Jacket - Outer Upper, Liquid Metal
T-1009416	Jacket - Upper Inner, Liquid Metal
T-1009418	Jacket - Lower Inner, Liquid Metal
T-1009419	Spacer - Outer Lower, Liquid Metal Jacket
T-1009420	Cap - Lower Liquid Metal Jacket, Inner
T-1009424	Spacer - Upper Water Jacket
T-1009425	Support - Spacer - Upper Water Jacket
T-1009493	Deflector - Water

Drawing No.	Title
T-1009591	Reducer - Liquid Metal
T-1009592	Cap - Liquid Metal
T-1009593	Tube - Liquid Metal
T-1009594	Tube - Liquid Metal Fill
T-1009596	Reducer - Inner Helium Jacket
T-1009597	Reducer - Outer Helium Jacket
T-1009598	Jacket - Air
T-1009601	Header - Motor Housing Case
T-1009603	Jacket - Helium
T-1009608	Tube - Helium Fill
T-1009631	Block - Transition
T-1009633	Housing - Motor Case
T-1009637	Ring - Retaining, External Steel
T-1009644	Wire - Insulated
T-1009645	Strap - Thermocouple Tube Support
T-1010202	Probe - Liquid Metal Detector
T-1010203	Insulator - Liquid Metal Detector Probe
T-1010262	Motor - Pump Drive
T-1010263	Impeller - Liquid Metal Pump
T-1010273	Impeller Option - Liquid Metal Pump, Assembly of (Instl Control No.)
T-1010741	Wrench Assembly - Socket
T-1010751	Lifting Tool Assembly - Water Jacket
T-1010760	Hook Assembly - In-pile Loop Lifting
T-1010767	Lifting Assembly - In-pile Loop Dumping
T-1010769	Plug Assembly - Air Tube
T-1010775	Reducer Assembly - Air Tube
T-1010783	Lifting Rod Assembly

Drawing No.	Title
T-1010786	Eye - Lifting Rod
T-1010787	Retriever Assembly
T-1010798	Cable Assembly - Lifting
T-1010800	Cable Assembly - Lifting
T-1010804	Wrench Assembly - Socket
T-1011114	Coffin - In-pile Loop, Assembly
T-1011150	Support - Upper Platform, Assembly of
T-1011396	Support - Motor
T-1011397	Lug - Motor Support
T-1011398	Screw - Set Special
T-1011730	Jacket - Inner Liquid Metal, Lower
T-1011822	Support - Coffin Accessories, Assembly of
T-1011859	Cradle - In-pile Loop Liner, Assembly of
T-1011977	Impeller - Liquid Metal Pump, Assembly of
T-1012078	Coffin Liner - Cradle Base Support, Assembly of
T-1012218	Tube - 1.000 OD x 0.049 Wall x 6.905 Long
T-1012220	Union, Reducing - 1.000 Dia x 0.750 Diameter Tube (Spec Control Dwg)
T-1012308	Water Jacket, Assembly of
T-1012315	Pin - Dowel - 0.0625 Dia x 0.810 Long
T-1012535	Bolt - 0.250-20 x 0.750 Long, Drilled Hex Head
T-1012849	Jacket - Inner Liquid Metal, Upper
T-1013220	Gasket - Coffin Cover
T-1013282	In-pile Loop Assembly (ETR)
T-1013290	Cradle - Assembly of
T-1013483	Support - Thermocouple
T-1013485	Connector - Electrical (Spec Control Dwg)

Drawing No.	Title
T-1013486	Connector - Electrical (Spec Control Dwg)
T-1013487	Support - Motor Lead
T-1013491	Tube - 0.250 OD x 0.035 Wall - 54.000 Long, Helium Fill
T-1013493	Plug - Helium Cap
T-1013494	Support - Thermocouple
T-1013495	Support - Thermocouple
T-1013499	Support - Motor Lead Connector
T-1013501	Cover - Motor Lead Connector
T-1013504	Header - In-pile Tubes
T-1013506	Plug - Helium Cap
T-1013511	Lead - 3 - Wire Complete, 0.3125 Diameter
T-1013678	Tube - Thermocouple Leads, Assembly of
T-1013685	Reducer - In-pile Loop
T-1013686	Tube - Air
T-1013782	Thermo Well
T-1013852	Support - Thermocouple
T-1013853	Tube - 1.000 Diameter x 0.049 Wall x 12.780 Long
T-1014054	Tube - 1.000 Diameter x 0.049 Wall x 12.150 Long
T-1014118	Helium Chamber Cover - Assembly of
T-1014119	Block - Transition, Assembly of
T-1014120	Housing - Impeller, Assembly of
T-1014132	Reducer - Liquid Metal Upper Inner Jacket
T-1014867	Support - Tube, Assembly of
T-1015173	Lock - Test Element Beams
T-1015178	Housing - Test Elements
T-1015179	Cap - Liquid Metal Jacket, Inner
T-1015180	Cap - Lower Liquid Metal Jacket, Outer

Drawing No.	Title
T-1015181	Housing - Test Elements, Assembly of
T-1015182 SH2	In-pile Loop, Assembly of
TLH-100422	Guillotine - ETR In-pile Loop
TLJ-100293	In-pile Loop ETR - Assembly of
TLK-100428 SH1	Accessories Coffin - In-pile Loop
CB-101171	Cover (Split) - High-Temp Properties Rig
CC-101059	Stabilizer (Upper) - In-pile Liquid Metal Prep. Stand
CC-101313	Chamber - Thermo Leak Check
CC-101494	Support - Loop
CD-101027	Stand - for Removable Fill Dolly Frame
CD-100690	Instrumentation Diagram, In-pile Loop
CD-100788	Schematic Diagram, In-pile Loop, Annunciators
CD-100789	Electrical Schematic, In-pile Loop, Alarm, and Alarm Test Circuits
CD-100792	Pneumatic and Piping Schematic, In-pile Loop
CD-100795	Electrical Schematic, In-pile Loop Reactor Control
CD-101144	Electrical Schematic, In-pile Loop, Pump Motor Drive No. 1
CD-101145	Electrical Schematic, In-pile Loop, Pump Motor Drive No. 2
CD-101146	Electrical, Pneumatic, and Piping, Parts List, In-pile Loop
CLD-10126-3-5	Electrical and Piping Schematic - Liquid Metal Fill Dolly
CLD-10129-3	Electrical Schematic, In-pile Loop, Power
CLD-10129-4	Layout and Location, In-pile Loop, Control Panel
CLR-10126-1	Layout - In-pile Liquid Metal Fill Dolly
CLR-10129-9	Stand - Loop Prep. Demountable and Portable
CR-100920	Frame - In-pile Liquid Metal Fill Dolly

APPENDIX D

LIST OF REFERENCES

1. "Experimental Operating Instructions for the Pratt & Whitney Forced Convection Liquid Metal Inpile Loop Experiment (PW-19)," Report No. CNLM-1194, Pratt & Whitney Aircraft, 1959.

2. Lubarsky, B. and Kaufman, S. J., NACA TN-3336, Washington D. C., 1955.

3. Stoever, Chem. and Met. Engineering, May 1944.

4. Sieder, E. M. and Tate, G. E., Ind. Eng. Chem., 28, 1429-1436, 1936.

5. Johnson, C. W., and Dreisbach, R., "Forced Convection Liquid Metal Inpile Loop Liquid Metal Pressure Drop Calculations," Report No. TIM 483, Pratt & Whitney Aircraft, 1958.

6. "Hydraulic Flow Calculations for MTR - ETR Experiments," Report No. IDO-16368.

7. "Flow of Fluids, "Technical Paper No. 410, Crane Company, Chicago, Illinois, 1957.

8. DeBoisblanc, D. R. et al, "The Advanced Test Reactor-ATR Final Conceptual Design," Report No. IDO-16667, Phillips Petroleum Company, Atomic Energy Division, September 20, 1960.

9. "Fast Reactor Core Design Parameter Study," Atomic Power Development Associates, Report No. APDA-133, March, 1960.

10. "Symposium on Reactor Control Materials," Nuclear Science and Engineering, Vol 4 No. 3, September 1958.

11. Timoshenko, S. and Goodier, J. N., Theory of Elasticity, McGraw-Hill, 2nd Edition 1961.

12. Perkins, J. F., "Energy Release from the Decay of Fission Products," Nuclear Science and Engineering, Vol. 3, June 1958.

13. "Capsule Experiment Handling Arrangement," Drawing No. ATR-1075-MTR-670-R-501, Rev. O, Babcock and Wilcox Company, Atomic Energy Division, April 1961.

14. "Top Head Arrangement," Drawing No. ATR-1075-MTR-670-R-500, Rev. O, Babcock and Wilcox Company, Atomic Energy Division, May 1961.

15. Sandrock, R., "ATR Top Head Study", Study S-R-64, Babcock and Wilcox Company, Atomic Energy Division, May 22, 1961.

16. Flatt, H.P. and Baller, D.C., "AIM VI - A Multigroup, One-Dimensional Diffusion Equation Code," NAA-SR-4694, March 1, 1960.

17. Roach, W.H., "Computational Survey of Idealized Fast Breeder Reactors," Nuclear Science and Engineering, Vol. 8, No. 6, December 1960

18. Zweifel, P.F., "Neutron Self Shielding," Nucleonics, Vol. 18, No. 11, November 1960.

19. "The Quantitative Evaluation of Resonance Integrals," Proceedings of the Second International Conference, Geneva, Vol. 16, September, 1958.

20. "Thermal Flux Profile," Drawings No. 2060-R and 2065-R, Babcock and Wilcox Company, Atomic Energy Division, February 1961.

21. Luckow, W.K., "Single-Lobe Be-Reflected Reference Core," Internal Letter of Babcock and Wilcox Company, Atomic Energy Division, January 5, 1961.

22. "High-Temperature-Strain Fatigue Testing With A Modified Direct-Stress Fatigue Machine," Atomics International, Report No. NAA-SR-4051, October 1959.